GEOLOGICA ULTRAIECTINA

Mededelingen van het
Instituut voor Aardwetenschappen der
Rijksuniversiteit te Utrecht

No. 29

EVOLUTION OF PASSIVE CONTINENTAL MARGINS AND INITIATION OF SUBDUCTION ZONES

SIERD CLOETINGH

EVOLUTION OF PASSIVE CONTINENTAL MARGINS AND INITIATION OF SUBDUCTION ZONES

PROEFSCHRIFT

TER VERKRIJGING VAN DE GRAAD VAN DOCTOR IN DE WISKUNDE EN NATUURWETENSCHAPPEN AAN DE RIJKSUNIVERSITEIT TE UTRECHT, OP GEZAG VAN DE RECTOR MAGNIFICUS PROF. DR. O. J. DE JONG, VOLGENS BESLUIT VAN HET COLLEGE VAN DECANEN IN HET OPENBAAR TE VERDEDIGEN OP MAANDAG 6 DECEMBER 1982 DES NAMIDDAGS TE 4.15 UUR

DOOR

SIERD AUKE PIETER LEONARD CLOETINGH

GEBOREN OP 20 AUGUSTUS 1950 TE GRONINGEN

PROMOTOR: PROF. DR. N. J. VLAAR

Aan mijn vader

The research described in this thesis was carried out at the Department of Theoretical Geophysics, Institute of Earth Sciences, State University of Utrecht, Utrecht, The Netherlands

CONTENTS

VOORWOORD (PREFACE) 7

SAMENVATTING (SUMMARY IN DUTCH) 9

CHAPTER 1 - INTRODUCTION AND SUMMARY 11

CHAPTER 2 - DEFORMATION OF OCEANIC LITHOSPHERE 15
2.1 Gravitational stability of oceanic lithosphere 15
2.2 Forces acting on the lithosphere with implications for the stress distribution 17
2.3 Lithospheric bending and rheology 28
2.3.1 Bending of a uniform elastic plate with a hydrostatic restoring force 28
2.3.2 Bending of an elastic-perfectly plastic plate 35
2.3.3 The depth-dependent rheology 38

CHAPTER 3 - ANALYSIS OF THE STATE OF STRESS AT PASSIVE MARGINS 48
3.1 One dimensional bending of an infinite uniform elastic thin plate due to an instantaneously applied triangular sediment wedge: analytical solutions 49
3.2 Numerical models of the state of stress at passive margins 53
3.2.1 Description of the models 53
3.2.2 Results 59
3.2.3 Investigation of the assumption of instantaneously applied loads 66
3.3 Evaluation and discussion 69
3.3.1 Geological inferences 69
3.3.2 Alternative scenarios 70

REFERENCES 72

APPENDIX - THE FINITE ELEMENT ANALYSIS 81

SUPPLEMENT - SUPPORTING PAPERS 91

1. State of stress at passive margins and initiation of subduction zones 93
2. Evolution of passive continental margins and initiation of subduction zones 107

CURRICULUM VITAE 111

VOORWOORD

Veel dank ben ik verschuldigd aan allen die aan de totstandkoming van dit proefschrift hebben bijgedragen.

In het bijzonder dank ik mijn promotor, Prof.Dr.N.J.Vlaar, voor de suggestie van het onderwerp, voor zijn bijdragen tot mijn wetenschappelijke vorming en voor zijn constructieve benadering van mijn werk.

De intensieve en plezierige samenwerking met Rinus Wortel is de afgelopen jaren voor mij van grote betekenis geweest. Voor zijn vele suggesties bij de uitvoering van mijn promotie-onderzoek ben ik hem zeer erkentelijk. Ook mijn overige collegas op de afdeling Theoretische Geofysica dank ik voor de prettige werksfeer. Guust Nolet toonde een vaak actieve belangstelling voor de resultaten van dit onderzoek.

Gerald Wisse dank ik voor zijn ondersteuning bij de uitvoering van de eindige elementen berekeningen. Vooral zijn praktische benadering daarbij heb ik zeer op prijs gesteld. De directies van de rekencentra van de T.H.Delft en van de R.U.Utrecht ben ik erkentelijk voor de door hen geschapen budgetaire faciliteiten die de uitvoering van de modelberekeningen mogelijk hebben gemaakt.

De teken- en foto-afdeling van het Instituut voor Aardwetenschappen heeft op voortreffelijke wijze de figuren verzorgd. John Cornwell gaf nuttige wenken met betrekking tot de Engelse tekst.

Dé Pattynama en Vinod Kanhai hebben met veel inzet en geduld het manuscript getypt.

SAMENVATTING

Ondanks de vooruitgang die de laatste jaren is geboekt bij de bestudering van de dynamische aspecten van de plaattektoniek, heeft het tot dusverre ontbroken aan een goed inzicht in het proces dat ten grondslag ligt aan de initiatie van subductie. Aangezien initiatie van subductie een essentieel element vormt van de dynamica van de lithosfeer, is dit een van de kernproblemen van de geodynamica geworden.

De doelstelling van dit proefschrift is te komen tot een systematisch onderzoek van de mechanische condities waaronder de initiatie van een subductiezone kan plaats vinden. Met name concentreren we ons daarbij op de vraag of de spanningen, die bij *passieve* continentranden in de lithosfeer worden opgebouwd, voldoende groot zijn om passieve continentale marges te transformeren tot *actieve* continentale marges.

Na een inleidend hoofdstuk wordt in *hoofdstuk 2* nader ingegaan op een aantal aspecten van de deformatie van oceanische lithosfeer. De nadruk ligt in dit hoofdstuk op de thermische en mechanische eigenschappen van oceanische lithosfeer en op de krachten die op de lithosfeer aangrijpen. Eerder onderzoek van Vlaar en Wortel heeft aangetoond dat de ouderdom van oceanische lithosfeer een fundamentele grootheid is voor studies van de dynamica van de lithosfeer. Hoofdstuk 2 laat zien dat ook de sterkte van oceanische lithosfeer een functie is van de ouderdom. Aangetoond wordt, dat in het algemeen de op de lithosfeer aangrijpende krachten niet voldoende groot zijn om de lithosfeer op te breken. De aanwezigheid van dikke sedimentpakketten aan passieve marges kan echter, door de daardoor geinduceerde doorbuiging van de lithosfeer, leiden tot een relatief hoog spanningsniveau.

In *hoofdstuk 3* wordt de spanningstoestand aan passieve marges in detail onderzocht. Op grond van de gecombineerde aanwezigheid van een gecompliceerd stelsel van krachten en lateraal variërende, diepte-afhankelijke rheologische eigenschappen aan passieve marges, wordt bij dit onderzoek een belangrijke plaats gegeven aan de eindige elementen methode. De spanningstoestand wordt onderzocht in verschillende stadia van de evolutie van passieve marges. De modelberekeningen tonen aan dat ten gevolge van de voortgaande accumulatie van sedimenten, het spanningsniveau met de ouderdom van de marge toeneemt. In het algemeen echter blijven de geinduceerde spanningen op een te laag niveau om te kunnen

resulteren in een opbreken van de lithosfeer, dit temeer omdat de sterkte van de lithosfeer eveneens met de ouderdom toeneemt.

Wanneer echter jonge lithosfeer (ouderdom tot 20 miljoen jaar) wordt belast met een dik sedimentpakket van ca. 10 km, kunnen de geinduceerde spanningen toereikend zijn om de lithosfeer op te breken en subductie te initiëren. Dit proces kan een effectief mechanisme zijn voor de sluiting van kleine oceanische bekkens. De sluiting van kleine bekkens speelt een belangrijke rol bij het proces van gebergtevorming. Studies van gebergteketens, variërend in ouderdom van het Precambrium tot aan de recente Alpiene plooiingsfase, tonen op grote schaal deformatie aan van passieve marges van kleine oceanische bekkens.

De *appendix* geeft een overzicht van een aantal specifieke aspecten van de eindige elementen methode, die voor dit werk, maar ook voor andere gebieden van de geodynamica, van bijzonder belang zijn. Het *supplement* bevat twee overdrukken van publicaties die betrekking hebben op het onderwerp van dit proefschrift.

Samenvattend kan gesteld worden dat de numerieke modelberekeningen van de evolutie van passieve continentale marges een beter inzicht hebben verschaft in de rol die passieve marges kunnen spelen bij het proces van initiatie van subductie. Een verbetering van het inzicht in de tektonische evolutie van passieve continentale marges kan van belang zijn voor de exploratie van olie- en gasvoorkomens. Daarnaast geeft dit onderzoek een aangrijpingspunt bij verdere studie van het vraagstuk van de gebergtevorming.

CHAPTER 1

INTRODUCTION AND SUMMARY

The initiation of subduction is a key element in plate tectonic schemes for the evolution of the Earth's lithosphere. Nevertheless, up to present, the underlying mechanism has not been very well understood (e.g. Dickinson and Seely, 1979; Hager, 1980; Kanamori, 1980). The insight into the initiation of subduction process has lagged far behind the progress made in the last few years in the study of other aspects of plate tectonics, making this topic an outstanding problem in geodynamics (Dziewonski and Boschi, 1980; Flinn, 1982). Vlaar and Wortel (Vlaar, 1975; Vlaar and Wortel, 1976; Wortel, 1980) have shown that a fundamental parameter in lithospheric studies is provided by the age of the oceanic lithosphere. It was, therefore, decided to investigate whether the age-dependence of lithospheric properties might provide a clue to better understanding of the initiation of the subduction process (Cloetingh et al., 1981).

It is the aim of this thesis to give a systematic investigation into the mechanical conditions under which the initiation of a subduction zone can take place.

The lithosphere has considerable strength (Kirby, 1980) and is capable of supporting stresses of the order of several kilobars on geological timescales (Watts et al., 1980). It follows that this analysis deals basically with the assessment of the possibilities for plate rupture. In general, tectonic forces acting on the lithosphere (Forsyth and Uyeda, 1975) do not generate stresses of several kilobars. Thus, special circumstances with a local concentration of forces, in an optimal combination with a suitable rheological structure, are required to induce lithospheric failure.

It is, therefore, plausible that initiation of subduction takes place preferentially at pre-existing weakness zones or in regions where the lithosphere is stressed by forces arising from mechanisms not associated with these tectonic forces. Passive continental margins are characterized by a lateral contrast between oceanic and continental lithosphere, and are downflexed (Fig.1.1) under the influence of the thick sedimentary deposits usually present at passive margins (e.g.Watkins and Drake, 1982).

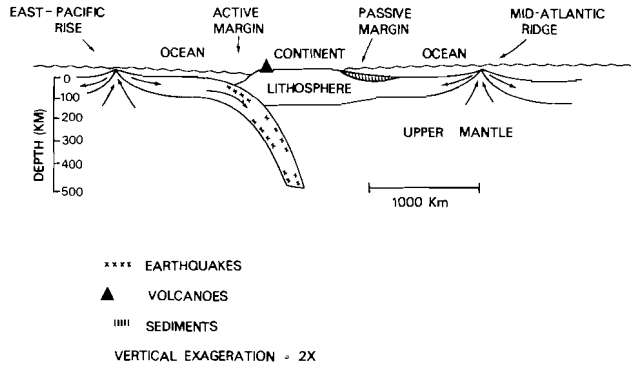

Fig.1.1 - Cross section through the lithosphere taken from the East-Pacific rise to the Mid-Atlantic ridge. The directions of the spreading of oceanic lithosphere are shown by arrows. Some characteristic features of active and passive continental margins are indicated in the figure.

According to recent estimates (Southam and Hay, 1981), approximately one third of all Phanerozoic sediments are located in passive continental margins formed by the break-up of Pangea (180-200 m.y. ago). Since that event, the total length of segments of passive margins has been increasing with time to the present length of approximately 70.000 km (Southam and Hay, 1981). Reconstructions of sedimentary sequences incorporated in orogenic belts (Stoneley, 1969) yield estimates for maximum thicknesses comparable with those encountered at passive margins. These observations, together with geological arguments put forward by others (Dietz, 1963; Dewey, 1969; Speed and Sleep, 1982), make passive margins obvious potential sites for initiation of subduction.

The present work, therefore, focuses on the state of stress at passive margins, to investigate whether the stresses generated at passive margins are sufficiently high to induce lithospheric failure and initiation of subduction. For such an analysis, insight in and knowledge of the deformation of oceanic lithosphere is essential. Before proceeding to the stress analysis given in chapter 3, it is, therefore, appropriate to review in chapter 2 features pertinent to the deformation of oceanic lithosphere, with emphasis on the gravitational stability of oceanic lithosphere, the forces acting on the lithosphere, and the important subject of lithospheric bending and the rheology of the oceanic lithosphere. It is there demonstrated that the governing properties are a function of the age of the lithosphere involved, a consideration that has not been taken into account in earlier work dealing with the state of stress at passive margins (Walcott, 1972; Bott and Dean, 1972; Turcotte et al., 1977a). The combination of a complicated set of forces, variable geometry and depth-dependent rheological properties reported in chapter 2, motivated the use of the finite element method for the stress analysis. This technique was chosen, especially because of its capability of dealing with non-linear modelling. Chapter 3 contains an extensive account of a model study of the state of stress at passive margins during various stages of its evolution. Quantitative models of the evolution of passive margins are increasing in importance in evaluating petroleum potential (Watkins and Drake, 1982; Emery, 1980) and the significance of the transition from passive to active margins for hydrocarbon exploration has recently come

to light (Cohen, 1982).

In chapter 3, we show that sediment loading dominates the state of stress at passive margins. Taking into account only the age-dependence of the gravitational instability of the lithosphere, it was reasonable to expect that the chances for initiation of subduction of oceanic lithosphere increase with the age of the margin (Vlaar and Wortel, 1976). The present study demonstrates that owing to the continuing accumulation of sediments at passive margins, the stress level induced increases with the age of the margin. However, an important feature following from the rheological considerations given in chapter 2 and implemented in the models, is that the strength of the oceanic lithosphere increases with age as well. We found that the aging of passive margins alone does not make them more susceptible to initiation of subduction. In general, the stresses generated at passive margins are not sufficient to induce lithospheric failure. Extensive sediment loading on a young margin (age below 20 m.y.) might, however, be an effective mechanism for closing of small ocean basins.

Closure of small oceanic basins plays an important role in the process of mountain building. Orogenic belts ranging in age from Precambrian to Alpine (Kröner, 1981; Winterer and Bosellini, 1981; Frisch, 1979) show evidence for extensive deformation of passive margins bordering small oceanic basins.

In the appendix, a summary is given of aspects of the finite element analysis employed in the present work, which are potentially useful in other fields of geodynamics.

The supplement contains reprints of publications by the author on the topic considered in this thesis.

CHAPTER 2

DEFORMATION OF OCEANIC LITHOSPHERE

A thorough understanding of the deformation characteristics of oceanic lithosphere is essential to a quantitative analysis of mechanisms underlying lithospheric processes. This applies in particular to initiation of subduction. It is, therefore, appropriate to begin here with a survey of lithospheric properties pertinent to its deformation. This chapter is divided into three sections dealing respectively with gravitational stability, the system of forces acting on the lithosphere, and the flexural characteristics of oceanic lithosphere for various rheologies.

2.1 GRAVITATIONAL STABILITY OF OCEANIC LITHOSPHERE

Gravitational stability is a key factor determining the possibility of subduction of oceanic lithosphere. Vlaar (1975) and Vlaar and Wortel (1976) pointed out that, whereas near the oceanic ridge crest the lithosphere is stably stratified with respect to the underlying upper mantle, the lithosphere-asthenosphere system away from the ridge may become increasingly unstable as a result of cooling and associated thermal contraction of the lithosphere.

Oxburgh and Parmentier (1977) presented a petrological model for the lithosphere in which the total stability of the oceanic lithosphere is the sum of the positive buoyancy of its stable petrological stratification and the negative buoyancy resulting from thermal contraction upon cooling.

An important parameter in the analysis of lithospheric stability is the density defect thickness δ defined as $\delta = \int \frac{\rho_m - \rho}{\rho_m} dz$, where the integration is over the thickness of the lithosphere. ρ and ρ_m are the densities of the lithosphere and the underlying asthenosphere respectively. Oxburgh and Parmentier (1977) found for the compositional component $\delta_c = 1.3 \times 10^3$ meter. This compositional component does not depend on lithospheric age; the thermal component $\delta_{th} = \beta \int (T(z,t) - T_m) dz$ does. β, $T(z,t)$ and T_m are the thermal expansion coefficient, the temperature profile within the lithosphere, and the temperature at the base of the lithosphere respectively. Wortel (1980) has calculated the stability for a model of oceanic lithosphere consistent with observations of heat flow and topography. The result, expressed by the density defect thickness, is given in Fig.2.1.

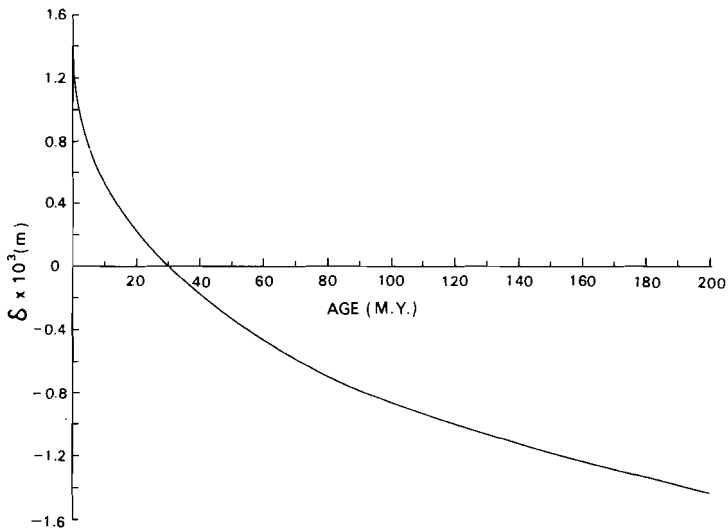

Fig.2.1 - The density defect thickness plotted as a function of age. This curve illustrates the increase of the gravitational instability of oceanic lithosphere with age, induced by cooling and associated thermal contraction. The figure is taken from Wortel (1980).

At an age of 30 m.y. the positive buoyancy of the chemical layering is compensated by the negative buoyancy resulting from cooling. Sediment accumulation at the margin has a stabilizing thermal effect on the underlying lithosphere. Fig.2.1 shows that for lithospheric ages below 200 m.y. the relation $|\delta_{th}|<2|\delta_c|$ applies. A reduction of 15% in the thermal component implies a reduction of approximately 30% in the total instability for the case of a 200 m.y. old lithosphere. The compositional component δ_c is independent of the age of the lithosphere and, therefore, the latter reduction increases with decreasing age. For the reference model of sediment loading (see section 2.2) adopted in our analysis, it is assumed that sedimentation is keeping up with the thermal subsidence of the underlying lithosphere (Turcotte and Ahern, 1977). It can then be shown (Wortel, 1980) that the maximum age at which oceanic lithosphere is still gravitationally stable is extended from 30 m.y. to 45 m.y.; the new ocean basin would nowhere be gravitationally unstable during the first 45 m.y. after opening.

In dealing with initiation of subduction, attention must be given to the role that is played by the forces acting on the lithosphere. The magnitude of the external forces exerted on the lithosphere, for instance, might be sufficiently large to overcome the buoyancy effect. Another important point to be considered is the considerable strength of the lithosphere. Before oceanic lithosphere can be subducted, external forces acting on it must induce stresses sufficiently large to induce lithospheric failure. After plate rupture has taken place, gravitationally *unstable* lithosphere can be subducted. Subduction of gravitationally *stable* lithosphere is hampered by resistive forces active in the process of trench formation. In this case, continuous action of external forces is needed to sustain subduction. These considerations make it necessary to study in detail the forces acting on the lithosphere and to quantify the levels of the stresses that are induced.

2.2 FORCES ACTING ON THE LITHOSPHERE WITH IMPLICATIONS FOR THE STRESS DISTRIBUTION

Lithospheric plates are in motion under the influence of plate tectonic forces. These driving forces are schematically indicated in a

cross section through the lithosphere (Fig.2.2). They are: 1. the ridge push (F_{RP}) resulting from the elevation of the spreading ridge to the adjacent ocean floor and the thickening of the lithosphere with cooling (Hales, 1969), 2. the forces associated with the buoyancy of the cooling lithosphere (F_B) (Vlaar and Wortel, 1976), 3. the drag exerted at the base of the lithosphere (F_D) (Richter, 1973) due to the action of viscous shear forces associated with the relative motion with respect to the underlying asthenosphere, and 4. the forces acting on the downgoing slab in a subduction zone (F_{SP}) (McKenzie, 1969).

The forces, associated with an already existing subduction zone are irrelevant to a study of the processes underlying the creation of a *new* subduction zone in a passive margin setting. They are mentioned here for completeness only (see England and Wortel (1980) for further details on this topic).

Apart from the "driving" forces of plate tectonics, other forces are acting on the lithosphere, which might locally even dominate the stress field. Examples are stresses (σ_{TO}) associated with topographic anomalies (Artyushkov, 1973) and crustal thickness inhomogeneities (σ_{CT}) at passive margins (Bott and Dean, 1972). Further, temperature variations may induce thermal stresses (σ_{TH}) in the cooling lithosphere (Turcotte, 1974), while membrane stresses (σ_{ME}) (Oxburgh and Turcotte, 1974) are

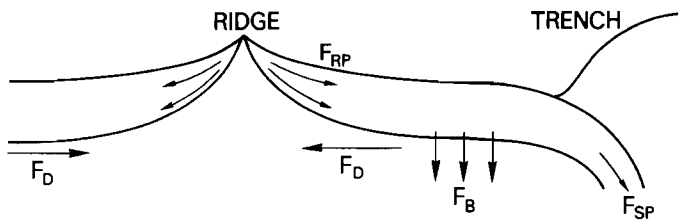

Fig.2.2 - The forces associated with plate tectonics: The ridge push (F_{RP}), the negative buoyancy associated with cooling (F_B), the resistive drag exerted at the base of the lithosphere (F_D), and the slab pull (F_{SP}).

possibly induced by plate motion on a non-sperical Earth. A number of these stress mechanisms have been reviewed earlier by Turcotte and Oxburgh (1976).

Finally, flexural stresses (σ_{FL}) are generated due to vertical loads on the lithosphere, in particular by seamount loading (Heiskanen and Vening Meinesz, 1958) and sedimentary sequences at passive margins (Walcott, 1972). Sediment loading may also generate overburden stresses (σ_{OV}) (Haxby and Turcotte, 1976) and stresses induced by a hypothetical phase change (σ_{PC}) in the underlying lithosphere (Neugebauer and Spohn, 1978).

A systematic analysis is necessary to determine the relevance of these forces for the problem under consideration. This applies in particular to the order of magnitude of the stresses induced by the various mechanisms. Unless otherwise stated, order of magnitude calculations of stresses are made for a uniform elastic plate with a thickness of 100 km. As the seismologically defined Young's modulus E is not applicable to analysis of stresses associated with processes on geological timescales, the relaxed E modulus (Anderson and Minster, 1980) is used. Values of $E = 700$ kbar and $\nu = 0.25$ for Young's modulus and Poisson's ratio respectively are taken throughout the analysis. The results of this survey are summarized in table 2.1. Below, an explanatory treatment of the separate mechanisms is given. This section is concluded with a discussion of table 2.1.

TABLE 2.1. STRESS MECHANISMS OPERATING ON THE LITHOSPHERE

Mechanism	*Stress*	*(order of magnitude)*	*Incorporated*
Ridge push	σ_{RP}	(100 bar)	yes
Buoyancy	σ_{B}	(100 bar)	yes
Drag	σ_{D}	(10 bar)	no
Slab pull	σ_{SP}	(kbar)	no
Topography	σ_{TO}	(100 bar)	no
Crustal thickness contrast	σ_{CT}	(10-100 bar)	no
Thermal	σ_{TH}	(kbar)	no
Membrane	σ_{ME}	(100 bar)	no
Flexure	σ_{FL}	(kbar)	yes
Phase change	σ_{PC}	(10 bar)	no
Overburden	σ_{OB}	(100 bar)	yes
Isostasy	σ_{IS}	(100 bar)	yes

1. *The ridge push*

Richter and McKenzie (1978) have derived the following expression for this driving force: $F_{RP} = gh\ (\rho_m - \rho_w)\ (S_L/3 + h/2)$, where h is the difference in elevation between the ridge crest and the depth the ocean basin at the adjacent continental margin would have in the absence of sediment loading. ρ_m and ρ_w are the densities of mantle and seawater, respectively and S_L is the lithospheric thickness. The ridge push results from the thickening of the oceanic lithosphere with age. For ages below 65 m.y., both h and S_L are linearly dependent on the square root of age function, which gives a linear relation between ridge push and age (England and Wortel, 1980). The ridge push is to be considered as an integrated horizontal pressure gradient distributed over the adjacent oceanic lithosphere (Lister, 1975), rather than as a line force, as usually is done. The integrated pressure gradient per unit width along the ridge for oceanic lithosphere with an age of 100 m.y. is 2.3×10^{12} N/m, inducing stresses with O(100 bar) in a 100 km thick elastic plate.

2. *The forces associated with buoyancy of the cooling lithosphere (F_B)*

As argued in section 2.1, the oceanic lithosphere becomes gravitationally unstable for ages in excess of 30 m.y. For that reason, the lithosphere will experience the action of a body force resulting from density differences with the underlying asthenosphere. From Fig.2.1 we can estimate the magnitude of F_B. For 100 m.y. old lithosphere the density defect thickness δ equals 1 km. This is equivalent to a load of 1 km of mantle material (density $\rho_m = 3.3$ g/cm^3) on the lithosphere. This results in stresses of O(100 bar) in a uniform elastic lithosphere.

3. *Drag at the base of the lithosphere (F_D)*

Viscous shear forces are exerted on a lithosphere in motion with respect to the underlying asthenosphere. For a proper assessment of the shear, the rheology and the plate velocities must be quantified. Another fundamental question to be answered is, whether the mantle passively resists the plate motions, or on the contrary moves the plates on top of the convection cells. The latter mechanism involves large shear stresses

necessary to maintain a firm coupling between lithosphere and asthenosphere (Hanks, 1977). On rheological grounds, large shear stresses are improbable in this depth range of the mantle (see further section 2.3). This reasoning is further supported by inversion studies of global plate velocities (Forsyth and Uyeda, 1975), which point to small shear forces acting at the base of the plate. These results are confirmed by more recent work by Wortel and Cloetingh (1982). Their detailed modelling of the forces acting on the Nazca plate shows that only force models characterized by the presence of a small resistive drag fulfil the condition of mechanical equilibrium of the Nazca plate. Thus, drag forces are difficult to specify in the absence of a good understanding of the basic physical properties, and are probably very small. Drag forces will, therefore, be neglected.

4. *The effect of topographic anomalies*

Assuming isostatic compensation for a linear topographic anomaly, the compressive force F per unit length, induced by this feature on the adjacent plate, can be inferred from $F = \int (\sigma_x - \sigma_z) dz$. σ_x and σ_z are horizontal and vertical normal stress components. The integration is over the thickness z (see for a derivation Artyushkov, 1973). Using this equation, it is easily demonstrated that linear topographic elevations of a few km height generate compressive forces of the order of 10^{12} N/m. This is equivalent to stresses of a few hundred bars in a 100 km thick elastic plate. Linear topographic anomalies in the oceanic realm are, apart from the spreading centres, the "aseismic" ridges, of which the Ninety-east ridge in the Indian Ocean is perhaps the most prominent example. For continents, the equation can be used to quantify the effect of elongated mountain chains such as the Appalachians.

5. *Crustal thickness inhomogeneities at passive margins*

Passive margins furnish a special case of the previous category. Here, lateral variations in crustal thickness occur, which result in an unequal loading of the lithosphere across the margin. A fairly accurate knowledge of the crustal structure is required for a proper evaluation of the resulting stress distribution at the margin. At passive margins,

however, the penetration depth of high resolution seismic methods is very often limited due to the presence of very thick sedimentary deposits. On account of this, knowledge of the crustal structure is often incomplete (Curray, 1980; Bally, 1982). In particular, the position of the Moho is frequently unknown or inferred from non-unique gravity modelling. Rayleigh wave group velocity investigations of passive margins (Cloetingh et al., 1979; 1980a, b) may prove a more useful tool for this purpose. Bott and Dean (1972) have calculated the stress distribution for a simplified model of passive margins, with a column of seawater on the oceanic side of the margin adjacent to a rock column on the continental side. This is accompanied by the presence of a root under the continent, which is absent under the ocean. Bott and Dean showed that the unequal density distribution across the margin can result in shear stresses of the order of a few hundred bars in the continental crust. However, the stresses generated by this mechanism in the oceanic crust were found to be negligible (O(10 bar)).

6. *Thermal stresses*

Temperature variations inside an elastic medium induce thermal stresses. Simple expressions for the thermal stresses can be derived for the case of plane strain. It is assumed that the medium cools from an initial temperature T_i to a temperature T_e. T_y is the yield temperature. The following equations hold for the thermal stresses σ_{TH} (Nadai, 1963):
$\sigma_{TH} = \beta E(T_i - T_e)$ when T_i and T_e are both below T_y and
$\sigma_{TH} = \beta E(T_i - T_y)$ when the yield temperature lies between T_i and T_e.
β is the thermal expansion coefficient. Thermal stresses are zero for temperatures T_e in excess of the yield temperature. Substitution of values from the temperature profiles for the cooling lithosphere (Crough, 1975) in these equations, shows that large thermal stresses (order of magnitude tens of kilobars) can be generated by lithospheric cooling following creation at spreading centres. It is to be expected that such high stresses are relieved very early in the evolution of the lithosphere by the formation of transform faults (Turcotte, 1974; Collette, 1974). Other authors argue for a stress relaxation by deformation on a grain size level as a result of anisotropic thermal expansion of mineral grains (Solomon et al., 1975), the ultimate result on the stresses being the same.

7. *Membrane stresses*

A lithospheric plate moving in a north-south direction experiences a change in the radius of curvature owing to the Earth's ellipticity. This results in the generation of so-called membrane stresses.

An early treatment of membrane stresses in geophysics has been given by Heiskanen and Vening Meinesz (1958). Various authors following them have proposed membrane stresses as a mechanism for plate rupture, in particular in the context of the slow northward movement of the African plate in the last hundred m.y. (Oxburgh and Turcotte, 1974; Freeth, 1979).

However, most of the Earth's plates have velocities with large east-west components, which reduces the potential effect of ellipticity considerably. The effect is further reduced by incorporating rheological constraints, as has been shown by Dickman and Williams (1981), to a level of only a few hundred bars under the most favourable conditions.

8. *Vertical loads*

Examples of vertical loading on oceanic lithosphere are provided by individual seamounts, seamount chains (of which the Hawaii-Emperor chain is the best known) and the presence of sediment loads on passive margins. These loads result in flexural stresses in the underlying oceanic lithosphere. The case of an individual seamount is irrelevant to our analysis. The magnitude of the stresses induced by a seamount chain can be easily estimated by using the analogy of a line load on an elastic plate (see section 2.3). Although capable of generating stresses on a kilobar level locally, seamount chains are on the average much shorter in length and have a much lower height, than sediment loads along passive margins. An elaborate discussion of seamount loading can, therefore, be omitted. The remainder of this section concentrates on the effect of sediment loading on oceanic lithosphere.

Sediment loading

Passive margins are usually characterized by the presence of extensive sedimentary deposits (e.g. Burk and Drake, 1974). Recent estimates (Southam and Hay, 1981) are that approximately one-third of all

Phanerozoic sediments are located in passive continental margins formed by the break-up of Pangea (180-200 m.y. ago). Since that event, the total length of segments of passive continental margins on Earth has been increasing with time to the present length of approximately 70.000 km (Southam and Hay, 1981). These observations make passive continental margins a prominent subject for both academic and industrial research, the latter in particular as a result of their potential as source beds for hydrocarbons (e.g. Emery, 1980; Dow, 1978; Royden et al., 1980).

The sediment loading capacity of the oceanic lithosphere increases with age through continued cooling and densification of the lithosphere (which controls the subsidence of the ocean floor (Parsons and Sclater, 1977)). One might, therefore, expect a coupling of the height of the sedimentary column deposited at the passive margin with the age-dependent subsidence of the underlying oceanic lithosphere (Sleep, 1971; Kinsman, 1975; Turcotte and Ahern, 1977). Two adjacent major depocentres are found at the margin: under the shelf and under the continental rise. The sediment deposits are often in the form of two wedges of more or less triangular form. The wedges join at the continental slope, where the maximum sedimentary thicknesses are found. Assume that the height of the wedges corresponds with the thickness that can be expected if the sedimentation has been keeping up with the subsidence of a boundary layer model of the cooling oceanic lithosphere (Turcotte and Ahern, 1977; Wortel, 1980). This implies that the maximum height of the sedimentary wedge will gradually increase and reach a maximum of 9.4 km at 200 m.y. (see Fig.2.3), following roughly a square root of age relation. In Fig.2.3, observational data are plotted on post-rift sedimentary thicknesses, inferred from many geophysical surveys carried out at passive margins during the last few years. Inspection of Fig.2.3 shows that the reference model of sediment loading constitutes a fair average of the sediment loading histories and resulting thicknesses observed at passive margins.

Other authors (Southam and Hay, 1981) have reached similar conclusions, stating that "the general principle of sediment accumulation rates decreasing with time after the breaking apart of a passive margin is confirmed by a large number of geophysical sections".

The huge sediment accumulations found at deltas, however, exceed clearly the thicknesses depicted by the reference model. Therefore,

a second model of sedimentation, the full load model, is adopted, in which the entire full loading capacity of oceanic lithosphere is taken up by sediments. In this model, the maximum height of the sedimentary wedges reaches 16 km at 200 m.y. (see Fig.2.3). The sedimentary thicknesses of

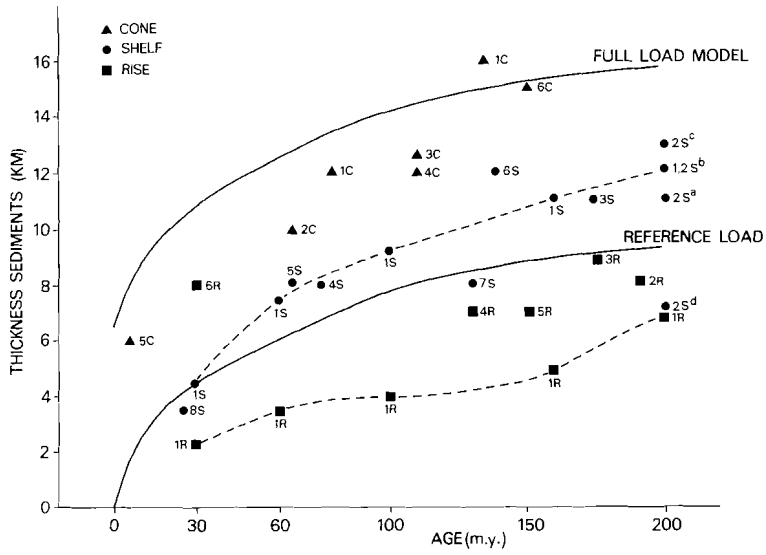

Fig.2.3 - The increase of sediment thickness versus age adopted for the reference load and full load models (solid curves), compared with data on post-rift sedimentary thicknesses at passive continental margins.
Symbols ● , ■ , ▲ denote maximum thicknesses of post-rift shelf, rise and fan deposits respectively.

Data are taken from the following sources:

- ● 1S, Eastern U.S. shelf off New Jersey based on the Cost-B2 well. Dashed (- - -) curve gives the sediment loading history (Grow et al., 1979); 2S, Carolina through (2a), Blake plateau (2b), Baltimore Canyon (2c) and Georges Bank (2d) (Grow and Sheridan, 1981); 3S, Nova Scotia shelf (Keen, 1979); 4S, Labrador shelf (Hinz et al., 1979); 5S, Western Indian shelf (Closs et al., 1974); 6S, Shelf off Kenya (Kent, 1974); 7S, South Argentina shelf (Urien et al., 1976); 8S, Gulf of Lyon (Watts and Ryan, 1976)
- ■ 1R, Eastern U.S. continental rise off New Jersey based on the Cost-B2 well. Dashed (- - -) curve gives the sediment loading history (Grow et al., 1979); 2R, Morocco rise (Goldflam et al., 1980); 3R, Nova Scotia rise (Watts and Steckler, 1979); 4R, South Argentina rise (Urien et al., 1976); 5R, Gulf of Mexico rise (Buffler et al., 1981); 6R, Baffin Bay (Keen and Keen, 1974)
- ▲ 1C, Bengal fan (Curray and Moore, 1974); 2C, Indus cone (Naini, 1980); 3C, Niger cone (Lehner and De Ruiter, 1977); 4C, Amazon cone (Houtz et al., 1977; Cloetingh et al., 1979, 1980b); 5C, Colorado fan (Crowell, 1974); 6C, Mississippi fan (Buffler et al., 1981)

the full load model are representative for deltas. It should be noted that only deltas which at least partly overlie oceanic lithosphere are plotted. Therefore, thicknesses of sedimentary deposits of the Nile Cone (thickness at least 8 km, Malovitskyi et al., 1975) and the Po fan (thickness of the order of 7 km, Finetti and Morelli, 1973), which are deposited on (thinned) continental crust of the eastern Mediterranean (Cloetingh et al., 1980a) and the Adriatic Sea (Nolet et al., 1978) respectively, are excluded from Fig.2.3.

The average shelf width of passive margins formed during the last 180-200 m.y. is 108 km, while the average slope width is only 11 km (Southam and Hay, 1981). The total width of the sedimentary wedges is on the average 250 km, although, for young margins, widths as small as 150 km are found, e.g. some western Mediterranean basins (see also Burk and Drake, 1974; Watkins and Drake, 1982). On the margin, sediments replace water. A reasonable value for the density difference of water and sediments is $\Delta\rho = \rho_{sediments} - \rho_{water} = 1.4\ g/cm^3$ (e.g. Kinsman, 1975).

In section 2.3., it is shown that thick sedimentary sequences at passive margins are capable of inducing flexural stresses up to several kilobars, assuming a simple uniform elastic plate analogy for the lithosphere. In comparison with the flexural stresses, the effect of a hypothetical phase change in the lithosphere under the influence of sedimentary loading, is very small: a few tens of bars (Neugebauer and Spohn, 1978).

For gravitational stresses in the Earth, hydrostatic conditions prevail (Jaeger and Cook, 1976). When sediments are deposited on the lithosphere, however, deviatoric stresses are generated. Sediment loading induces a tensional deviatoric overburden stress with a magnitude a fraction of the overburden load. Depending on lateral confinement, deviatoric stresses up to several hundreds of bars can be generated (Haxby and Turcotte, 1976).

9. *Isostasy*

The forces associated with downward displacements of the lithosphere are counteracted by isostasy. Isostasy can be expressed as a hydrostatic restoring force $(\rho_m - \rho_w)gw$, which is proportional to the displacement w ,

and the density difference between the asthenosphere (density ρ_m) and the medium overlying the lithosphere (usually water with density ρ_w). g is the acceleration due to gravity. For displacements of the lithosphere of a few kilometers, differential stresses σ_{IS} of 0(100 bar) are induced by the isostatic forces.

Discussion

The stress level associated with the mechanisms summarized in table 2.1 varies between 0(10 bar) and 0(kbars). Note that only *differential* stresses are considered here.

The effect of drag at the base of the lithosphere can be ignored, as the effect is small 0(10 bar). Moreover, essential points as whether drag is resistive, or not, and whether drag under continents is larger than under oceanic plates are not resolved.

Membrane stresses are of a low order of magnitude 0(100 bar) and irrelevant to the present study. The same applies to the effect of a hypothetical phase change induced by sedimentary loading of 0(10 bar). The contribution of the stresses due to changes in crustal thickness at the ocean-continent boundary is of minor importance. This mechanism induces shear stresses of 0(100 bar) in the continental crust, while the contribution to the stresses in the oceanic lithosphere is very small: 0(10 bar).

Thermo-elastic stresses due to cooling of the lithosphere (0(kbars)) are probably relieved to a large extent in the early stages of lithospheric evolution. The exact mechanism of relaxation of thermo-elastic stresses is uncertain. Formation of fracture zones may be one of the mechanisms involved here. The topographic load of a mountain belt can locally induce stresses of 0(100 bar) in continental lithosphere. An aseismic ridge could generate stresses of this order of magnitude in the adjacent oceanic lithosphere. The presence of topographic anomalies of these types, is not standard in a passive margin setting, and the effect will be ignored here.

The ridge push and the forces associated with the buoyancy of the cooling lithosphere generate stresses of 0(100 bar) throughout the lithospheric plate. These mechanisms can be quantified easily and are taken into account in the present analysis, as are the overburden stresses of 0(100 bar) generated by sedimentation.

Flexure induced by sediment loading at passive margins forms the most important stress mechanism. Flexural stresses are strongly influenced by the rheological constitution of the lithosphere. Therefore, the following section focuses on the subject of plate bending and rheological structure of oceanic lithosphere.

2.3 LITHOSPHERIC BENDING AND RHEOLOGY

In this section, the classical bending theory of an elastic plate on an inviscid substratum for linear and triangular loads, is reviewed. This is followed by an analysis of the flexural behaviour of a more realistic rheological model of the lithosphere. This model consists of an upper elastic part and a lower elastic-plastic part. Finally, a rheological model of the oceanic lithosphere, based on recent experimental studies, and characterized by a depth-dependent strength, is presented. This model provides the framework for considering the differential stresses generated by flexure in relation to the differential strength of the lithosphere.

2.3.1 *Bending of a uniform elastic plate with a hydrostatic restoring force*

The classical theory of bending of thin plates on an inviscid substratum as developed in engineering literature, is the first step in the analysis of lithospheric flexure. Assuming an entirely elastic lithosphere with uniform properties, floating on an inviscid fluid, the following equation for flexure under a load is easily derived (Hetényi, 1946; Nadai, 1963; Heiskanen and Vening Meinesz, 1958):

$$D\frac{d^4w}{dx^4} + \Delta\rho_1 gw + N\frac{d^2w}{dx^2} = P \qquad (2.3.1)$$

where $\Delta\rho_1$ is the density difference between the asthenosphere and any medium overlying the plate (usually water or sediments). w is the deflection resulting from a horizontal load N and a vertical load P. x is the horizontal coordinate. D is the flexural rigidity ($D = ES_e^3/12(1-\nu^2)$, where E is Young's modulus, S_e the plate thickness and ν the Poisson's ratio).

There are two special cases:

1. In the first case, *only horizontal forces* such as ridge push and slab pull act upon the plate (e.g. Wortel and Cloetingh, 1981). These forces induce a state of plane stress in the horizontal plane. The lithosphere cannot undergo longitudinal buckling under a horizontal load without failing. This can be illustrated simply by using eq.(2.3.1), with P=o:

$$D\frac{d^4w}{dx^4} + \Delta\rho_1 gw + N\frac{d^2w}{dx^2} = 0 \qquad (2.3.2)$$

Jeffreys (1976) has derived the eigenvalue for horizontal buckling (see also Turcotte et al., 1977b):

$$N = (4D\Delta\rho_1 g)^{\frac{1}{2}}$$

Assuming a thickness S_e for the elastic plate, yields:

$$N = \left(\frac{ES_e^3 \Delta\rho_1 g}{3(1-\nu^2)}\right)^{\frac{1}{2}} = \sigma_b S_e$$

A plate thickness of 100 km then gives for the buckling stress σ_b:

$$\sigma_b = \left(\frac{ES_e \Delta\rho_1 g}{3(1-\nu^2)}\right)^{\frac{1}{2}} = 75.6 \text{ kbar}$$

Recall that 700 kbar is taken for the value of Young's modulus E and 0.25 for Poisson's ratio ν. The density difference $\Delta\rho_1$ is 2.3 g/cm^3. A reduction of the plate thickness to the very small value of 5 km, yields a buckling stress of 16.9 kbar. These values for σ_b are far above estimates for lithospheric strength (see section 2.3.3) and, therefore, lithospheric failure will take place before the buckling stage is reached.

2. In the second case *only vertical loading* is taken into account. Vertical loading is important at passive margins, owing to the presence of thick sedimentary sequences.

Equation 2.3.1 then reduces to

$$D\frac{d^4w}{dx^4} + \Delta\rho_1 gw = P \qquad (2.3.3)$$

Two special cases are of particular interest for the present study: the case of a line load on the lithosphere and the case of flexure under the

influence of a load with the shape of a triangular wedge.

Line load

For a line load P on an infinite uniform elastic plate, the solution for the plate deflection is given by Hetényi (1946) (see also Walcott, 1976; McNutt, 1980) :

$$w = \exp(-\lambda x)\, A[\cos\lambda x + \sin\lambda x]$$

where $\lambda = \left(\frac{\Delta\rho_1 g}{4D}\right)^{\frac{1}{2}} = \frac{1}{\alpha}$. α is the flexural parameter (see Fig.2.4). x is taken to be the positive horizontal distance from the point where the line load is applied.

The value of A follows from the isostatic condition:

$$P = 2 \int_0^\infty \Delta\rho_1\, gw(x)\, dx$$

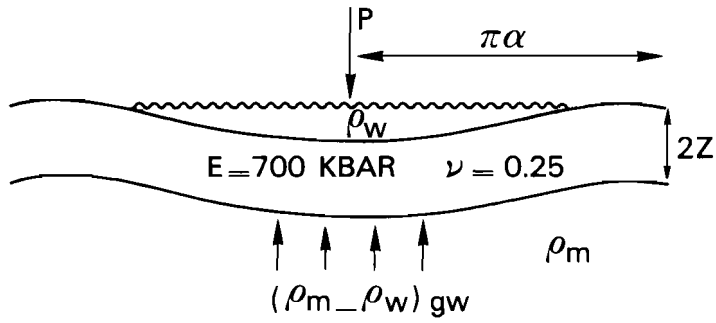

Fig.2.4 - Specific features associated with the flexure of an infinite elastic plate under the influence of a line load P, with a hydrostatic restoring force $(\rho_m - \rho_w)gw$. ρ_m and ρ_w are densities of the underlying mantle and the overlying medium (usually water) respectively. w and 2z are the displacements and the thickness of the plate. α is the flexural parameter. Values taken for Young's modulus E and Poisson's ratio ν are given in the figure.

and hence

$$A = P\lambda/2\Delta\rho_1 g$$

resulting in the following equation for the displacements:

$$w = \frac{P\lambda}{2\Delta\rho_1 g} \exp(-\lambda x)\ (\cos\lambda x + \sin\lambda x) \qquad (2.3.5)$$

For the bending stresses, which are proportional to $\frac{d^2w}{dx^2}$,

follows

$$\sigma = Ez \frac{d^2w}{dx^2} \qquad (2.3.6)$$

where z is the distance from the neutral surface. Combining eq.(2.3.5) and eq.(2.3.6) gives, in a straightforward manner

$$\sigma = \frac{EzP\lambda^3}{\Delta\rho_1 g} \exp(-\lambda x)\ (\cos\lambda x - \sin\lambda x) \qquad (2.3.7)$$

The maximum stress is at the point of loading (x = 0) where

$$\sigma_{max} = \frac{ES_eP\lambda^3}{2\Delta\rho_1 g}$$

Fig.2.5 shows the deflection and bending stress as a function of the distance from the point where the load is applied. Adopting a plate thickness of 100 km and a density difference $\Delta\rho_1 = \rho_{mantle} - \rho_{water}$ = 2.3 g/cm^3, the following values for the flexural rigidity and the flexural parameter α are obtained:
D = 6.222 x 10^{24}Nm., α = 181.4 km and $\lambda = 1/\alpha$ = 0.005 km^{-1}

The analysis given above is for an infinite plate. This is a simplification as plates are obviously finite. Consequently, the effect of finiteness of the plate should be taken into account theoretically (Hetényi, 1946).

The assumption of the load being concentrated into a line load is a more serious limitation of the model. A distributed load is a far better model for loading at passive margins. In particular, the triangular wedge is an appropriate representation of sedimentary loads.

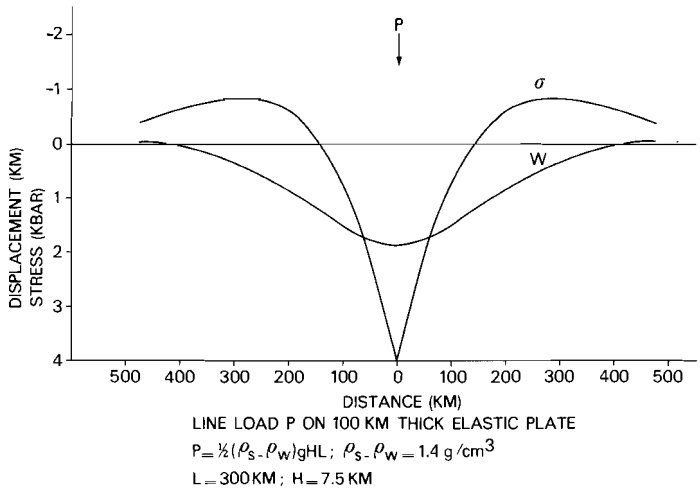

Fig. 2.5 - Vertical displacements w(km) and bending stresses σ(kbar) due to a concentrated line load, equivalent with the mass of a sedimentary triangular wedge on a 100 km thick uniform elastic plate. The vertical displacements are for the upper surface of the plate. The bending stresses are given for the lower surface of the plate. Sign convention: downward displacements and tensional stresses positive, upward displacements and compressional stresses negative. Loading specifications are given in the figure.

Triangular wedge

Consider the case of one dimensional bending of a thin plate due to a triangular wedge, with a density difference of water and sediments $\Delta\rho_2$, height H and width L. Other variables receive the same names as before. The top of the wedge is located directly above x = 0. The toe of the wedge is at x = L. Note that left is taken here as the positive direction.

The displacements under the load (L > x > 0) are (Hetényi, 1946) given by

$$w = \frac{\Delta\rho_2 gH}{4\lambda k L} \{\exp(-\lambda L)\ \exp(\lambda x)[\ (\cos\lambda x)(\cos\lambda L - \sin\lambda L)$$

$$+ (\sin\lambda x)(\sin\lambda L + \cos\lambda L)] + \exp(-\lambda x)[\sin\lambda x - \cos\lambda x\ (1+2\lambda L)]$$

$$+ 4\lambda(L-x)\} \qquad (2.3.8)$$

where $k = (\rho_m - \rho_w)g$.

For the bending stress follows

$$\sigma = \frac{\Delta\rho_2 gHEz}{8\lambda^3 LD} \{\exp(-\lambda L)\ \exp(\lambda x)\,[(\cos\lambda x)(\cos\lambda L+\sin\lambda L)$$

$$+ (\sin\lambda x)(\sin\lambda L-\cos\lambda L)] - \exp(-\lambda x)\,[(1+2\lambda L)\sin\lambda x + \cos\lambda x]\} \quad (2.3.9)$$

which simplifies for x = 0 to

$$\sigma = \frac{\Delta\rho_2 gHEz}{8\lambda^3 LD} [\exp(-\lambda L)(\cos\lambda L+\sin\lambda L)-1] \quad (2.3.9a)$$

Similar expressions apply for the displacements and stresses to the left of the load ($x \geqslant L$), where

$$w = \frac{\Delta\rho_2 gH}{4\lambda kL} \{\exp(-\lambda x)\ \exp(\lambda L)\ [(\cos\lambda L+\sin\lambda L)\cos\lambda x$$

$$-(\sin\lambda x)(\cos\lambda L-\sin\lambda L)] - \exp(-\lambda x)\ [(1+2\lambda L)\cos\lambda x-\sin\lambda x]\} \quad (2.3.10)$$

and

$$\sigma = \frac{\Delta\rho_2 gHEz}{8\lambda^3 LD} \{\exp(\lambda L)\ \exp(-\lambda x)\ [(\cos\lambda x)(\cos\lambda L-\sin\lambda L)$$

$$+(\sin\lambda x)(\cos\lambda L+\sin\lambda L)] - \exp(-\lambda x)\ [(1+2\lambda L)\sin\lambda x+\cos\lambda x]\} \quad (2.3.11)$$

and to the right of the load ($x \leqslant 0$), where

$$w = \frac{\Delta\rho_2 gH}{4\lambda kL} \{\exp(-\lambda L)\ \exp(\lambda x)\ [(\cos\lambda x)(\cos\lambda L-\sin\lambda L)$$

$$+(\sin\lambda x)(\cos\lambda L+\sin\lambda L)] - \exp(\lambda x)\ [(1-2\lambda L)\cos\lambda x+\sin\lambda x]\} \quad (2.3.12)$$

and

$$\sigma = \frac{\Delta\rho_2 gHEz}{8\lambda^3 LD} \{\exp(-\lambda L)\ \exp(\lambda x)\ [(\cos\lambda x)(\cos\lambda L$$

$$+ \sin\lambda L) + \sin\lambda x(\sin\lambda L-\cos\lambda L)] - \exp(\lambda x)$$

$$[(-1+2\lambda L)\sin\lambda x+\cos\lambda x]\} \quad (2.3.13)$$

Using these expressions for w and σ, the deflections and bending stresses are calculated for a load distributed over a triangle with a length of 300 km and with a mass equal to the line load applied in the previous section. It should be noted that the solutions obtained by Hetényi (1946) are not subject to the restrictions imposed on more recent formulas by Menke (1981). The equations given by Menke are of limited use since they

apply only for distances greater than those of the distributed load. However, the primary concern of the present work is with stress maxima located *under* the load.

The deflections and bending stresses calculated with the equations 2.3.8 - 2.3.13 are plotted in Fig.2.6, adopting the flexural characteristics given in the previous section. A comparison of Figs.2.5 and 2.6 demonstrates the inadequacy of the line load analogy, which grossly overestimates stresses, to provide a reliable picture of stresses resulting from distributed loads encountered in the real world. A second important point, illustrated by Fig.2.6, is that, assuming a simple elastic plate analogy for the lithosphere, a sediment load of a height typical for passive margins is capable of inducing flexural stresses of several kilobars. This is a conservative estimate, as a plate thickness of 100 km is a considerable overestimate of the actual elastic plate thickness. More realistic values for the thicknesses of the plate will yield still higher stresses (see chapter 3).

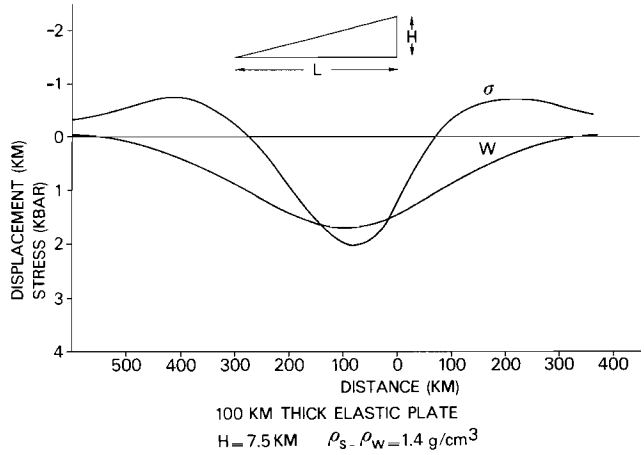

Fig. 2.6 - Displacements and stresses induced by the distributed triangular load. Other properties and conventions as in the previous figure.

2.3.2 *Bending of an elastic-perfectly plastic plate*

The elastic formulation given in the previous section provides a first order description of the mechanical behaviour of the oceanic lithosphere. The concept of the elastic plate is an important one, as is known from studies of seamount loading (Watts et al., 1980) and of lithospheric bending at trenches (McAdoo et al., 1978) that the lithospheric deformation has an important elastic component. From this work, it also becomes clear that the lithosphere is capable of supporting stresses on the kilobar level for long periods on a geological timescale. However, the lithosphere also has a non-elastic rheological component on a geological timescale.

At temperatures in excess of approximately half the melting point, rocks under deformation will relax their stresses by creep (Ashby and Verrall, 1978; Weertman and Weertman, 1975). The thickness of the part of the lithosphere which responds elastically to bending,is controlled by the depth at which the first thermally activated deformation mechanism becomes effective. The thermally defined lithosphere has its lower boundary at a depth corresponding approximately with the 1200^{o}C isotherm. For this reason it is expected that only the upper part of the lithosphere will respond in an elastic mode. The material at temperatures above 600^{o}-700^{o}C will experience ductile flow. Thus, as a reasonable first order approximation, the transition between the upper elastic part of the lithosphere and the lower plastic part, can be placed in the middle of the lithosphere. A second argument follows from studies on the seismicity at subduction zones (Chapple and Forsyth, 1979): the maximum focal depths at which earthquakes occur are reported to be 40-50 km below the upper surface of the lithosphere. A simple elastic-plastic model of the lithosphere is consistent with these observations (Forsyth, 1980).

Another line of evidence follows from detailed analysis of the bending of lithosphere at trenches. Although modelling the bending of the lithosphere at oceanic trenches with a uniform elastic plate generally yields results that are in good agreement with observations (Caldwell et al., 1976), discrepancies arise with respect to the large curvatures and widths of the forebulges observed at some trenches. This applies in particular to the Tonga- and Kuril Trenches, where an elastic-plastic model for the rheology of the lithosphere is required to fit the data. (McAdoo et al., 1978). The most satisfactory results have been obtained by these workers for yield

strengths of the lithosphere between 2.5 and 9.8 kbar.

The thickness of the lithosphere (defined by the 1200°C isotherm) is a function of its age. The thickness of the elastic part of the lithosphere (defined by the isotherms of 600°-700°C) must therefore exhibit the same age-dependence (see Fig.2.7). The isotherms are calculated from Crough's (1975) model, which model combines the merits of the boundary layer model (Turcotte and Oxburgh, 1967) and the plate model (McKenzie, 1967; Parsons and Sclater, 1977) (see Wortel (1980) for a review). This is corroborated by the results of more recent studies of seamount loading and bending of lithosphere at trenches, using a simple elastic-perfectly plastic model (Caldwell and Turcotte, 1979).

Caldwell and Turcotte (1979) found (see Fig.2.8) an increase in the thickness of the elastic part of the lithosphere, from a few kilometers near the spreading centre to about 40 km for 100-200 m.y. old lithosphere.

Once a lithospheric plate with an elastic-plastic rheology is loaded, rapid stress relaxation takes place in its lower part (Minster and Anderson, 1980) and stresses are concentrated in its upper elastic part.

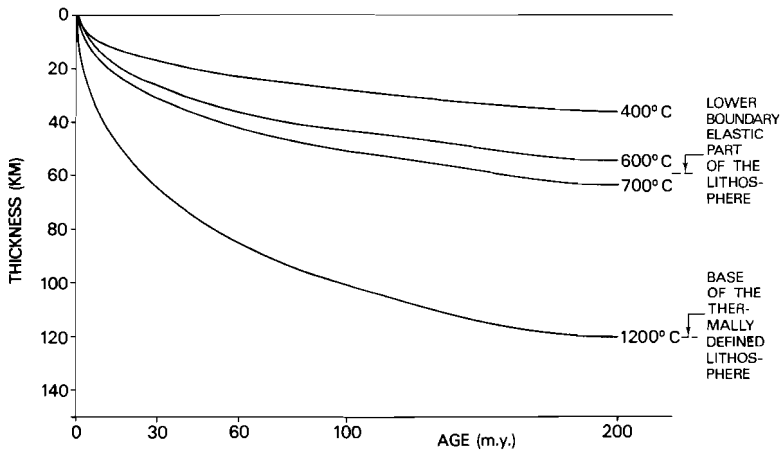

Fig.2.7 - Lithospheric growth as a function of age. The isotherms of the cooling oceanic lithosphere are calculated from Crough's (1975) model. The lower boundary of the thermal lithosphere is defined by an isotherm of 1200°C. The elastic upper part of the oceanic lithosphere has its lower boundary at approximately 600°-700°C.

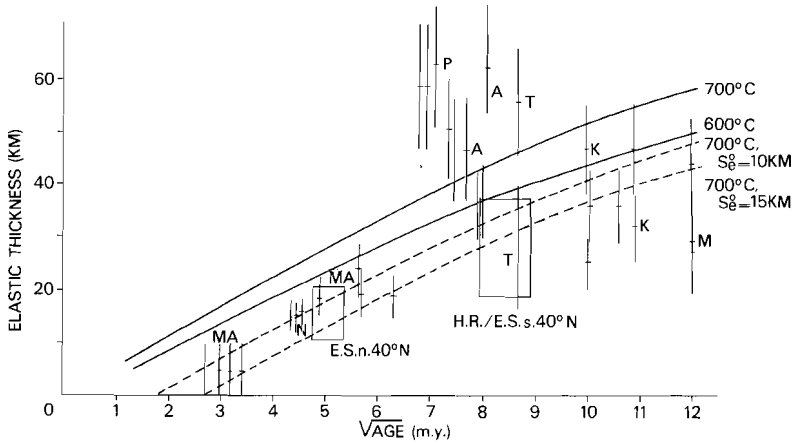

Fig.2.8 - Comparison of estimates of the elastic thickness of oceanic lithosphere based on data from Caldwell and Turcotte (1979), with elastic thicknesses inferred from the 600°C and 700°C isotherms given in Fig.2.7 (solid lines). Dashed (- - -) lines show the reduction in the elastic thickness when a top layer with thickness S_e^o and a zero strength is included in the upper part of the lithosphere. Data points are labelled by the following abbreviations: Trenches: MA, Middle America; M, Mariana; N, Nankai; P, Philippines; T, Tonga; K, Kuril. Seamounts: E.S.n.40°N: Emperor seamounts north of 40°N, H.R./E.S.s.40°N: Hawaiian ridge and Emperor seamounts south of 40°N. Figure modified from Caldwell and Turcotte (1979).

The concentration factor is approximately the ratio of the total lithospheric thickness and the thickness of the elastic upper part (e.g. Kusznir and Bott, 1977). When the upper part is assumed to have a certain strength in bending, flexural stresses can be generated at its top and bottom which may exceed the yield strength. Although, the stress analysis of elementary elastic-plastic structures under simple loading conditions can be made by analytical methods, the complicated geometry and loading conditions encountered in the real world usually require a numerical approach. An example of a numerical stress analysis for an elastic-perfectly plastic rheology of the lithosphere is given in Cloetingh et al. (1982a) (supplement).

2.3.3 *The depth-dependent rheology*

The simple elastic-perfectly plastic model of the lithosphere has two obvious shortcomings:

1. The abruptness of the transition from the strong elastic upper to the weak plastic lower part.
2. The uniformity of the rheological properties within the elastic upper plate.

In the following, implications of these assumptions are discussed and, subsequently, the modification of the simple elastic-plastic model is treated in detail. The outcome of this latter is a depth-dependent rheology.

The transition of the elastic part to the plastic part

From the previous section, it follows that the yield strength of the lower part of the lithosphere is small (O(100 bar)). This holds for the average strength. However, for a more detailed analysis of the transition of the elastic part to the plastic part, a closer inspection of the rheology of the plastic part is necessary.

Recent experimental and theoretical work on the deformation of olivine, which mineral is the dominant constituant of oceanic lithosphere, has provided a framework for understanding the creep properties of the lower lithosphere (Goetze, 1978). In particular, the important role that temperature plays in creep processes has been demonstrated. A very important creep process takes place by thermally activated climb of dislocations, obeying a non-linear relation between stress and strain-rate (Goetze, 1978):

$$\dot{e} = \dot{e}_o \sigma^3 \exp[-\frac{Q}{RT}] \qquad (2.3.14)$$

with Q the activation energy, R the universal gas constant, σ the differential stress, $\dot{e}$ the strain-rate, T the temperature. Q = 122 kcal/mole. For σ measured in bars, the value of the pre-exponential constant $\dot{e}_o$ is 70 $bar^{-3}s^{-1}$. Power-law creep holds for conditions of high temperatures and relatively low deviatoric stresses (Ashby and Verrall, 1978).

Consider the transition of the uniform elastic upper part to the lower plastic part, where the rheology is described by power-law creep.

For a given strain-rate, the eq.(2.3.14) can be used to calculate the transition stress between both parts as a function of temperature. The result is given in Fig.2.9, adopting a strain-rate of $\dot{e} = 10^{-18} s^{-1}$ (representative for sediment loading on oceanic lithosphere).

Using the equation for power-law creep and deriving temperature profiles (given in Fig.2.10) from Crough's (1975) model, strength profiles can be calculated for a simplified rheological model of the oceanic lithosphere.

This model is characterized by uniform rheological properties for the elastic upper part of the lithosphere, while the strength of the lower part of the lithosphere is limited by power-law creep. Strength profiles for lithospheric ages between 10 and 200 m.y., are given in Fig.2.11. From this figure, it appears that the transition between the uniform elastic part and the plastic (power-law) part is quite narrow.

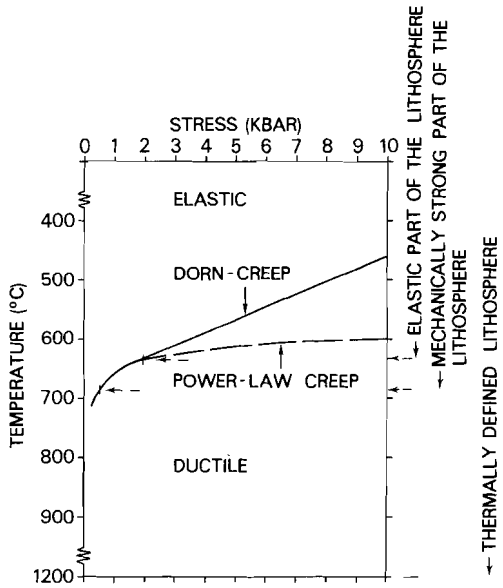

Fig.2.9 - The transition stress between the elastic upper part of the lithosphere and the ductile lower part of the lithosphere as a function of temperature based on two different flow laws for olivine, given by Goetze (1978). A strain-rate of $10^{-18} s^{-1}$ is adopted. The lower boundary of the thermally defined lithosphere is at 1200°C. The lower boundaries of the mechanically strong part of the lithosphere and the elastic lithosphere, defined by stress levels of 0.5 kbar and 2 kbar, are indicated in the figure.

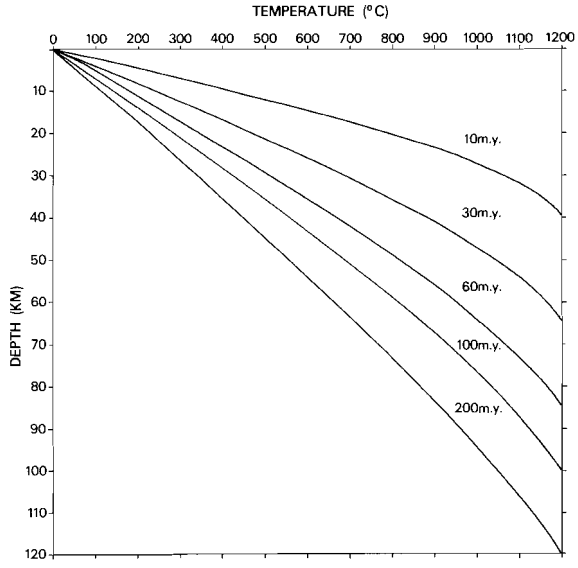

Fig.2.10 - Temperature profiles for oceanic lithosphere with ages varying between 10 and 200 m.y., derived from Crough's (1975) model.

This figure also shows that the transition is at temperatures between 600 and 700°C. The lower boundary of the *elastic part of the lithosphere* is defined as the point where the yield strength falls below 2 kbar. The flexural parameters for various lithospheric ages can be calculated, using Fig.2.11, and are plotted in Fig.2.12. The flexural rigidity D shows a linear relation with age, since the thickness of the elastic part of the lithosphere has a dependence on age that follows more closely an $age^{1/3}$ instead of an $age^{1/2}$ function. The flexural parameter α increases according to an $age^{1/4}$ function to values of about 120 km at 200 m.y.

From Fig.2.11 follows that the assumption made of an abrupt transition between the uniform elastic upper part and the plastic lower part would be valid under the assumption of deformation of the lower lithosphere by power-law creep. However, as mentioned earlier, power-law creep only applies under conditions of high temperatures and low deviatoric stresses (below 2 kbar).

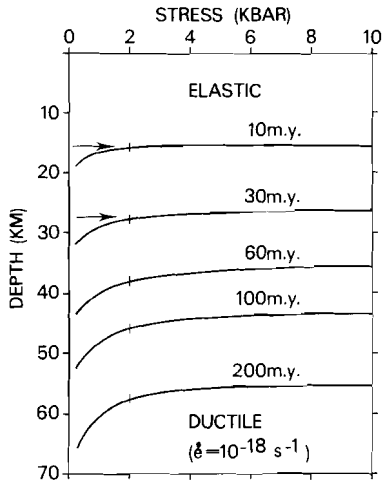

Fig.2.11 - Transition stress between the elastic upper part of the lithosphere and the ductile lower part with deformation described by power-law creep (Goetze, 1978) plotted as a function of depth. Transition stresses are given for a set of lithospheric ages, using the temperature profiles given in Fig.2.10, and a strain-rate of $10^{-18}s^{-1}$. Elastic thicknesses are indicated by arrows.

The constitutive equation (2.3.14) certainly does not hold for the transition between the elastic and ductile regimes in the lithosphere, where stresses are high and temperatures relatively low.

Under these stress and temperature comditions, dislocation glide is the dominating creep process. For dislocation glide, the velocity of the dislocations (or the strain-rate) is limited by obstacles in the gliding plane. These obstacles can be dislocation interactions or the Peierls resistance coupled with the position in the lattice (see for further details: Weertman and Weertman, 1965; Nicolas and Poirier, 1976). A much better description of the deformation in this region is provided by the Dorn-type creep formulation developed by Goetze and his co-workers (Goetze, 1978; Goetze and Evans, 1979). The constitutive equation for Dorn-creep, which holds for stresses in excess of 2 kbar, is

$$\dot{e} = \dot{e}_o \exp[-Q/RT(1-\sigma/\sigma_p)^2] \qquad (2.3.15)$$

where σ_p = 85 kbar and Q = 128 kcal/mole.

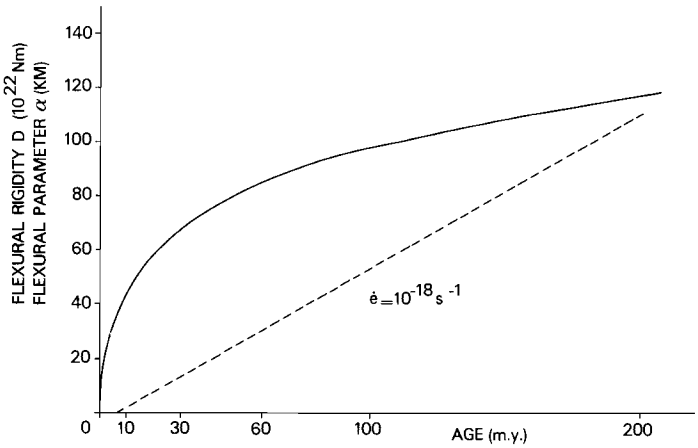

Fig.2.12 - Flexural rigidity D (dashed line) and flexural parameter α (solid line), which are based on Fig.2.11, plotted as a function of lithospheric age.

The value of the pre-exponential constant $\dot{e}_o$ is $5.7 \times 10^{11} s^{-1}$. The occurrence of deformation by creep in a high stress regime, implies a much wider transition zone than indicated in Fig.2.11. This feature is demonstrated in Fig.2.9.

Another point to be reconsidered is, the assumption of uniform rheological properties in the elastic upper part of the lithosphere. In the following section, the evidence for non-uniform rheological properties is discussed.

The elastic upper part of the lithosphere

The rheology of the upper part of the lithosphere is different from the material properties in the lower part in several aspects. Whereas, in the plastic regime, the effect of temperature plays a dominant role, pressure effects on brittle strength dominate at shallow depths. The deformation is in the brittle regime and the Coulomb strength strongly increases with depth. Goetze and Evans (1979) pointed out that the deformation in this region is essentially insensitive to temperature and strain-rate variations. At the same time, the strength is expected to be insensi-

tive to rock type. An important point is the linear increase of the brittle strength with depth. For tension, the fracture strength σ_f at a depth z equals $(2/3)\rho gz$, where ρ is the density of the lithosphere (Goetze and Evans, 1979). The strength in compression fulfils the equation $\sigma_f = 2\rho gz$. Right at the surface of the lithosphere, the strength is close to zero (Brace and Kohlstedt, 1980). The above equation gives rise to compressional strengths increasing rapidly with depth to unrealistically high levels (Fig.2.14). These are in excess of 10 kbar, which exceeds by far estimates obtained from flexural studies. Moreover, ductile faulting (Post, 1977; Ashby and Verrall, 1978) is expected to occur at these high stress levels. Therefore, unless otherwise stated, equality of compressional and tensional strengths is assumed, i.e. $\sigma_f = (2/3)\rho gz$.

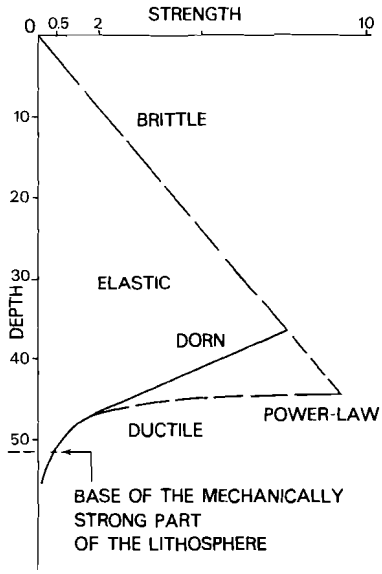

Fig.2.13 - Rheological model for the upper part of the lithosphere, characterized by a depth-dependent brittle strength. The model is derived from Fig.2.9 by specifying the temperature function inside the lithosphere according to Crough's (1975) thermal model. Three zones are present in the mechanically strong part of the lithosphere: The top is characterized by brittle fracture, the central core is in the elastic regime, and the lower part is deforming according to ductile flow with power-law creep and Dorn-creep dominating at stresses respectively below and above 2 kbar. Depths are given in km, stresses in kbar.

A depth-dependent rheological model of the oceanic lithosphere, with non-uniform brittle properties and Dorn-creep and power-law creep

A detailed rheological model of the oceanic lithosphere can be constructed by superposing the brittle/elastic part, upon its ductile part. In Fig.2.13, the various zones of a rheological profile through the lithosphere are indicated. It is important to realize that, although the brittle strength is not dependent on temperature and strain-rate, the intersection of the brittle and ductile parts of the strength envelope is.

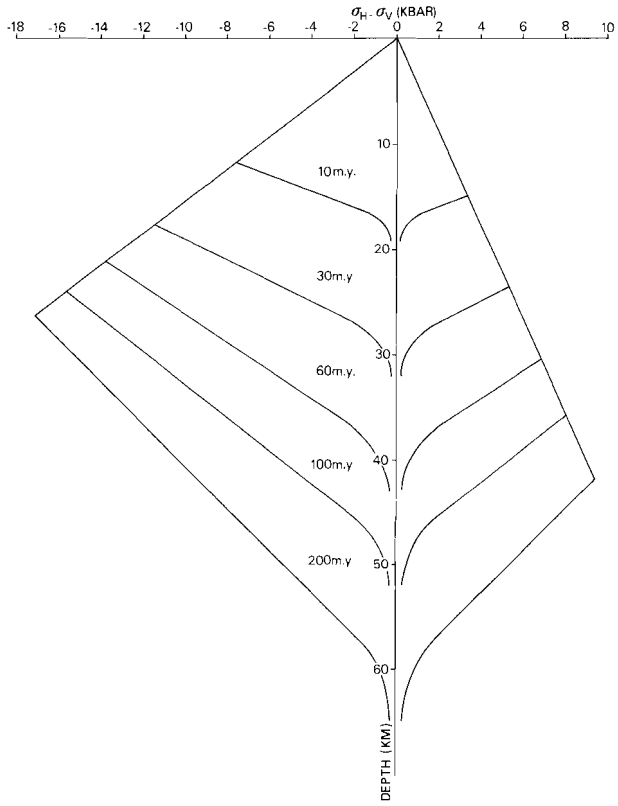

Fig. 2.14 - Strength envelopes for the rheology given in Fig. 2.13, for oceanic lithosphere with ages varying between 10 and 200 m.y., adopting a strain-rate of $10^{-18}s^{-1}$. Differential stresses ($\sigma_H - \sigma_V$) are plotted versus depth. σ_H and σ_V are horizontal and vertical principal stresses, respectively. Sign convention for the stresses: tension positive, compression negative. In the figure different values for brittle strengths in tension ($\sigma_f = (2/3)\rho gz$), and compression ($\sigma_f = 2\rho gz$) are adopted. Note that we attribute significance only to the tensional part of the envelope.

Since the temperature profile is prescribed by lithospheric age, the age of the lithosphere directly controls its rheological structure. The depth at which the strength is 500 bar is defined here to be the lower boundary of the *mechanically strong upper part of the lithosphere*. The thickness of the mechanically strong upper part of the lithosphere S_{me} and the maximum strength in tension σ_{YT} are two quantities of particular interest for the characterization of the mechanical structure of the lithosphere. In Fig.2.14, strength envelopes are plotted for lithospheric ages between 10 and 200 m.y. A transition stress between power-law creep and Dorn-creep of 2 kbar is adopted. A similar approach was followed by Bodine et al. (1981). From an inspection of this figure, it follows immediately that not only the thickness S_{me} (c.f. the elastic thickness S_e in the elastic-plastic model presented in section 2.2), but also the strength of the lithosphere is strongly age-dependent. Note that we attribute significance only to the tensional part of the strength envelope.

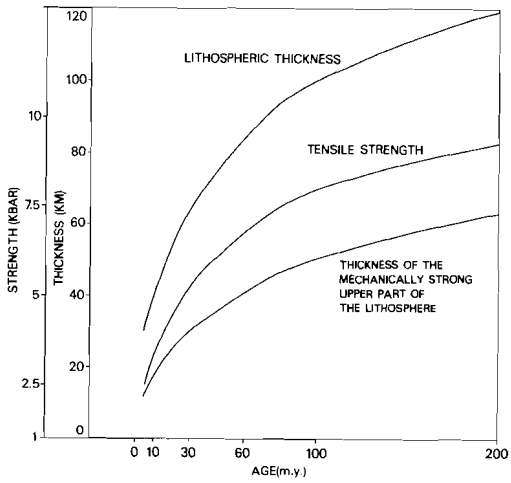

Fig.2.15 - Lithospheric thickness and mechanical properties of the lithosphere inferred from Fig.2.14 plotted as a function of lithospheric age.

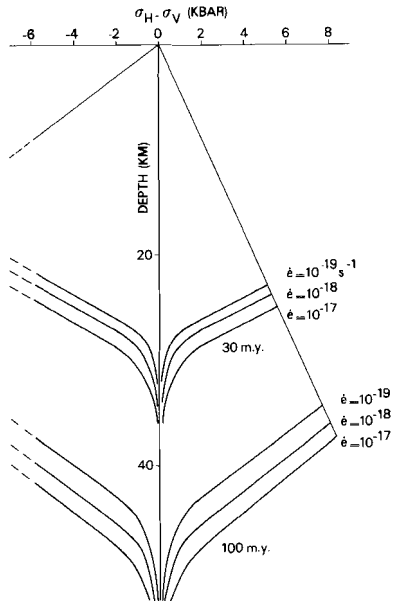

Fig. 2.16 - The effect of variations in strain-rate on the strength and the thickness of the mechanically strong upper part of the lithosphere. Figure conventions as in Fig. 2.14.

Both S_{me} and σ_{YT} increase according to a square root of age function from a few kilometers, respectively a few kilobars, for young lithosphere to values of approximately 50 km and 10 kbar for old oceanic lithosphere (see Fig.2.15). The effect of variations in strain-rate is much less pronounced, as demonstrated in Fig.2.16; an order of magnitude variation in strain-rate corresponds to only a 1-2 km change in the thickness of the mechanically strong upper part of the lithosphere.

An important implication of this rheological model is that the maximum stresses generated inside the strong upper part of the lithosphere are no longer to be found at its base, but are relaxed upwardly into the elastic "core" of the upper part of the lithosphere. This was realized by Lago and Cazenave (1980). However, by confining themselves to an analytical treatment, these authors could not explore the effects of a rheology which

combines power-law creep and Dorn-creep.

The depth-dependent rheology, even for configurations with a very elementary geometry and a simple system of forces, is practically intractable for analytical methods. Therefore, following a short intermezzo dealing with the analytical treatment with simplified rheological models, the following chapter concentrates on a numerical analysis of the state of stress at passive margins with a depth-dependent rheology, using the finite element technique for the stress calculations.

CHAPTER 3

ANALYSIS OF THE STATE OF STRESS AT PASSIVE MARGINS

The preceding review of the rheology of the lithosphere and the forces acting on the lithosphere, shows that lithospheric flexure dominates the state of stress at passive margins. This mechanism generates differential stresses of the order of several kilobars, in an elastic lithosphere. We, therefore, first concentrate our attention on flexure induced by sediment loading at passive margins.

To this end, we follow in section 3.1, a simple analytical approach, using the model of a triangular load on an infinite elastic plate. The results are subsequently used in section 3.2 as a guideline for the complete numerical treatment of the state of stress at passive margins, in which we incorporate the set of forces and the depth-dependent rheology treated in section 2.3.3.; see also Cloetingh et al. (1982b)(supplement).

To assess the potential of a passive margin for initiation of subduction, its evolution from youth to maturity must be considered. In the previous chapter, we have demonstrated that changes in lithospheric age imply changes in the parameters which control the state of stress. We, there-

fore, calculate the state of stress at *different* stages of the evolution of passive margins. For computational reasons, the emphasis of section 3.2 will be on a set of model calculations, in which the loads are applied instantaneously. The effect of the assumption of instantaneously applied loads is investigated numerically. For this purpose, we have constructed an additional set of models for a limited number of lithospheric ages, in which time-varying loads on passive margins are applied in small steps.

In section 3.3, we evaluate the results of the model calculations in the light of pertinent geological evidence.

3.1 ONE DIMENSIONAL BENDING OF AN INFINITE UNIFORM ELASTIC THIN PLATE DUE TO AN INSTANTANEOUSLY APPLIED TRIANGULAR SEDIMENT WEDGE: ANALYTICAL SOLUTIONS

The analytical solution for one dimensional bending of an infinite uniform elastic thin plate due to an instantaneously applied triangular sediment load, presented in section 2.3, can be used to illustrate some critical features of flexural stresses induced at passive margins. To this end, we adopt the reference model of sediment loading (section 2.2.2), which specifies the height H of the triangular load. The elastic thickness of the plate is inferred from the simple rheology of a uniform elastic-plastic plate, with the rheology of the ductile part described by power-law creep (section 2.3.2, Fig. 2.11). We take a width L = 300 km for the triangle. We have calculated displacements for plates with variable age-dependent elastic thicknesses loaded by sedimentary triangles with age-dependent heights H, prescribed by the reference model. Ages up to 200 m.y. were considered. Fig.3.1a shows that the wavelength and amplitude of the flexure increase with age. Fig.3.1b demonstrates a similar behaviour for the bending stresses. Tensional stresses up to 3.5 kbar are generated under the load. The age-dependent behaviour of the flexural stresses results from two opposing effects. These are the thickening and stiffening of the lithosphere with age, which result in lower values of the stress level, and the growth of the load with age, which gives an increase in stresses with age. The net result is an increase in the stress maximum with age, with a flattening in the increase

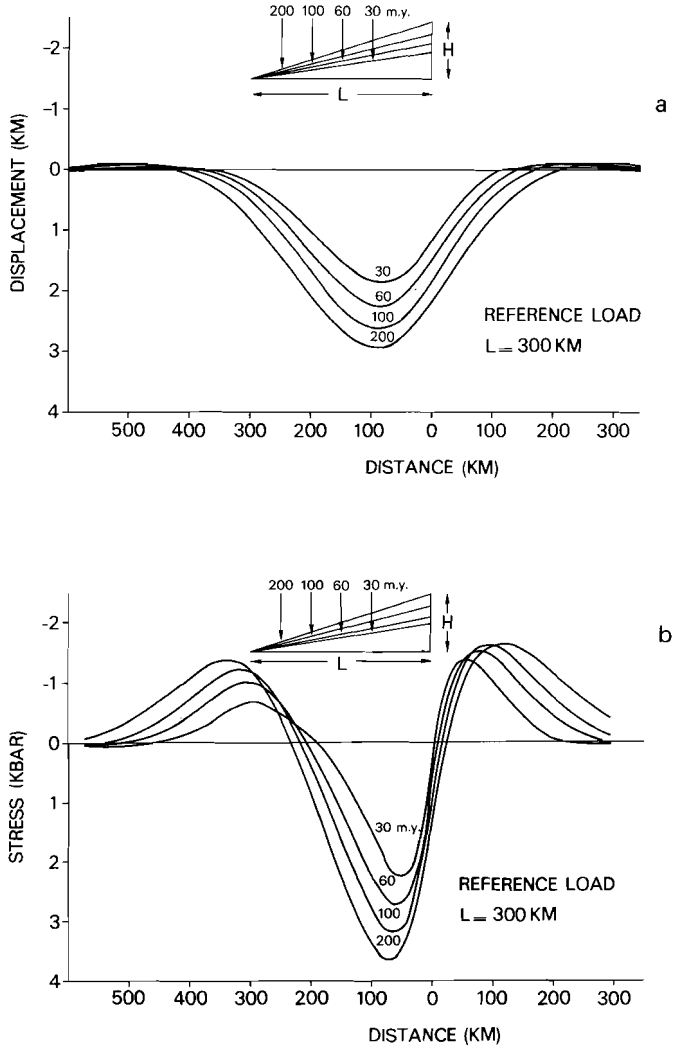

Fig.3.1 – Deflections and bending stresses of uniform elastic plates with age-dependent flexural rigidities (inferred from Fig.2.12) loaded by sedimentary triangles with a height H defined by the reference model of sediment loading. Distance (km) is taken from the point directly under the vertical side of the triangle. The width L of the load is 300 km. a (upper), The vertical displacements (km) of the upper surface of the plate. b (below), The bending stresses (kbar) at the lower surface of the plate. Sign convention: tension positive, compression negative.

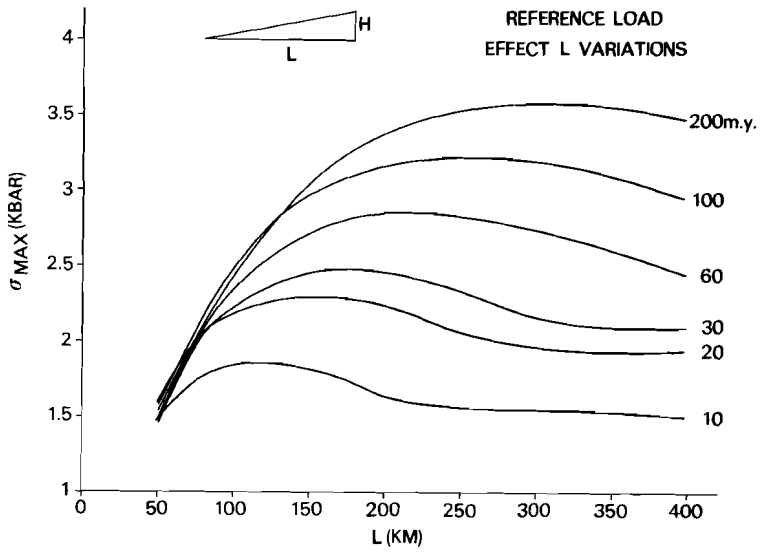

Fig.3.2 - The stress maximum as a function of the width L of the load for various ages of the lithosphere.

for ages beyond 100 m.y. This behaviour does not depend on the width and the exact form of the load, as shown in Figs. 3.2 and 3.3 respectively. In the first figure, we have plotted the maximum stress as a function of the width of the load for various ages. This figure shows that the conclusions made on the basis of models with a load width L of 300 km, hold for values of L above 75 km. Widths of sedimentary prisms encountered at passive margins, are usually much greater than 75 km. The stresses increase with L to a maximum value and then decrease. For large values of L ($L >> 4\alpha$) the isostatic limit for the stresses $\sigma = (\rho_s - \rho_w)gH$ is ultimately reached. Recall that α is the flexural parameter. The most "effective" width L varies from L = 125 km, for 10 m.y. old lithosphere, to L = 325 km, at 200 m.y. A reshaping of the triangular form of the load into a set of two adjacent triangles results in a shift with some 50 km of the position of the stress maximum, and does not influence the essence

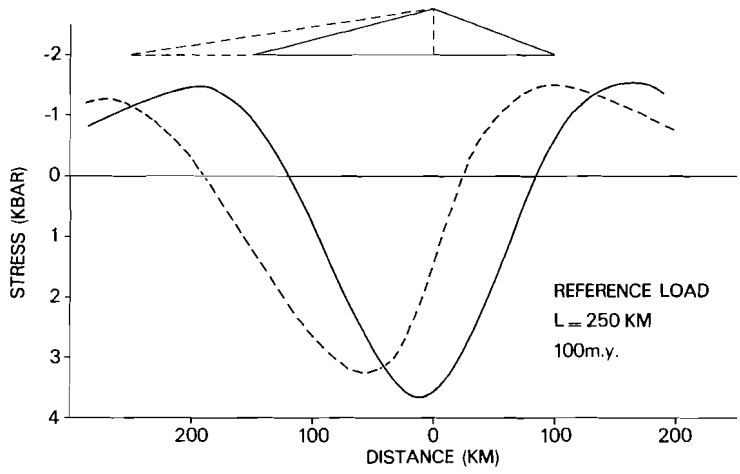

Fig.3.3 - The effect of variations in load shape. The width L of the load is taken to be a constant value of 250 km. Solid line: stresses due to a set of two adjacent triangular loads. Dashed line: stresses induced by an isolated triangular wedge.

of the results obtained for a simple triangular load.

Although instructive, these simple analytical models suffer from serious shortcomings, which restrict their value for detailed flexural analysis at passive margins. An important point is that the lithosphere at passive margins is characterized by lateral variations in thickness and rheology. Further, the uniform elastic model is an oversimplification of the depth-dependent rheology of the lithosphere. Finally, the analytical solution is based on thin plate theory which overestimates flexural stresses (Timoshenko and Woinowsky-Krieger, 1959). A numerical approach is, therefore, warranted to explore more fully the state of stress at passive margins. This allows the incorporation of the sediment loading and other forces, with more realistic boundary conditions and rheology in the models.

3.2 NUMERICAL MODELS

For our numerical analysis of the state of stress at passive margins, we have selected the finite element technique. This method (see Zienkiewicz, 1977) allows the accurate calculation of stresses in an irregular, inhomogeneous structure deformed by a system of distributed loads. In finite element analysis, the structure is divided into a number of so-called finite elements connected at nodal points. The displacements of the nodal points become the basic unknown quantities of the problem. The state of displacement within each element is chosen as a function of the nodal displacements. These functions also define the state of strain in the elements in terms of the nodal displacements. The strains, in turn, lead to the stresses within the element by way of a constitutive law. Finally, a system of forces consistent with the nodal displacements is found. These forces must be in equilibrium with the loads. A short description of the finite element method is given in the appendix.

In the present section, a description of the general features of the numerical models is given. This is followed by a presentation of the results of the model calculations.

3.2.1 *Description of the models*

We have constructed finite element models for passive margins with ages between 5 and 200 m.y.

The model features are illustrated in Fig. 3.4. For all models, we take a half-spreading rate of 1 cm/yr, characteristic for oceanic lithosphere without attached downgoing slabs (Forsyth and Uyeda, 1975). Age-dependent lithospheric thicknesses are based on Crough's (1975) model for the oceanic lithosphere and are taken from Wortel (1980). A thickness of 150 km, inferred from a number of independent geophysical approaches (e.g. Pollack and Chapman, 1977) is assigned to the continental lithosphere.

Eventual weakness zones associated with the initial break-up phase of passive margin evolution, possibly influence the stress pattern, in particular in the early post-rift phase. Both the extent in depth of such

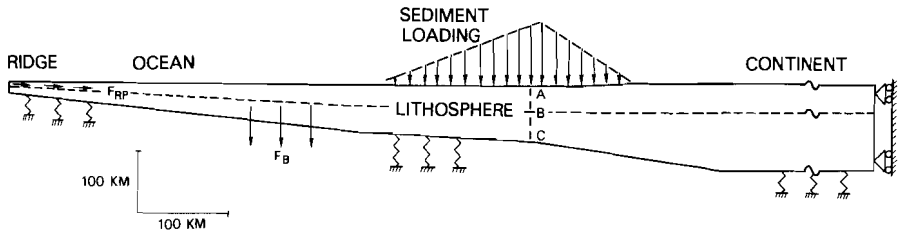

Fig.3.4 - Features of the numerical model: geometry, rheology, system of forces and boundary conditions. The bottom of the mechanically strong part of the lithosphere is indicated by a broken horizontal line. Young's modulus E = 700 kbar and Poisson's ratio ν = 0.25. F_{RP} is the push exerted by the oceanic ridge, F_B is the negative buoyancy associated with the cooling of the oceanic lithosphere when it moves away from the spreading centre. Isostatic forces counteracting the deflection are indicated by springs.

fault zones and the degree of decoupling are unclear. It has been argued (Turcotte et al., 1977a) that, due to the existence of a break-up fault system at passive margins, oceanic and continental lithosphere are effectively decoupled. Observations of more or less simultaneous subsidence of wells located on oceanic, transitional and continental crust off the eastern U.S. margin, however, imply that there has been little, if any differential motion between the oceanic and continental lithosphere across the United States Atlantic margin, at least from the early Cretaceous through Paleogene time (Heller et al., 1982). Modelling of subsidence at passive margins (Steckler and Watts, 1981) provides strong evidence that faults associated with the break-up phase are locked very early in the post-rift evolution, and are no longer active. Therefore, we refrain from incorporating mechanical weakness zones and discontinuities (fossil fault zones), and model the transition between oceanic and continental lithosphere as continuous. We adopt a width of 200 km for the transition, taking into account the evidence for the presence of rift-stage crust at the margin (Hutchinson et al., 1982).

The rheology of the oceanic lithosphere is based on Fig. 2.14 (section 2.3). A recent investigation of the gravity anomalies at passive margins (Karner and Watts, 1982) confirms the validity of our assump-

tion that the mechanical properties of oceanic lithosphere at passive margins are not essentially different from the rheological properties of standard oceanic lithosphere (as inferred from studies of seamount loading). This applies in particular to the increase of the thickness of the mechanically strong upper part of the lithosphere, with the age of the passive margin (Karner and Watts, 1982). We take brittle strengths in compression equal to the tensile strengths $\sigma_f = (2/3)\rho gz$, for reasons given in the previous chapter. In section 3.2.2, we demonstrate by a comparison of model calculations with equal and different brittle strengths in tension and compression, that the assumption made here does not influence the major conclusions of the present study. The depth-dependent rheology has been incorporated in the finite element models. Essentially, we implement the strength envelope via the integration points of the elements. This approach allows an accurate strength representation, without strength discontinuities between adjacent elements.

A thickness of 60 km for the mechanically strong upper part of the adjacent continental lithosphere is inferred from studies of the loading of continental lithosphere (Haxby et al., 1976; Molnar et al., 1980; Cochran, 1980). Rheological profiles under the shelf and in the rift-stage crust have been constructed by linear interpolation between the rheologies of the adjacent oceanic and continental lithosphere. This approach is supported by the results of temperature calculations by Zielinski (1979), which show a gradual linear transition of 100-300 km from the ocean, towards the continent, across the margin. This applies in particular to the isotherms below 600°-700°C, which are most pertinent to the mechanical properties at the margin.

Two models for sediment loading are considered in the analysis: the reference model, which implies sediment loading keeping up with the thermal subsidence of the underlying lithosphere, and the full load model, where the full loading capacity of the oceanic lithosphere is taken up by sediment loading at the ocean-continent boundary (see section 2.2). Note that in both sediment loading models the height of the sedimentary wedge is derived from a model where the sedimentation is related to the thermal subsidence of the underlying lithosphere. Sedimentary wedges at the continental shelf and the continental rise (with widths of respectively 100 and 50-150 km) are incorporated in the models.

Sediment loading also has implications for the rheological stratification at passive margins. The increase with depth of the shear strength *inside* the sedimentary section is usually linear, as pointed out by Bryant et al. (1981). These authors observe that, presumably due to porosity contrasts, the shear strength-depth profile is a function of sediment type and age. They demonstrate also that, even amongst seemingly similar sediment types, a considerable range of shear strengths versus depth has been measured at shallow levels. Further downward, large uncertainties in strength arise. Therefore, instead of making an uncertain estimate, we attribute a zero strength to the sediments deposited on the margin. Numerical calculations have shown us that strength variations in the top ten km of the plate have a very small effect on the stress distribution within the plate as a whole. This applies in particular to the stresses generated at the base of the mechanically strong part of the lithosphere. The hydrostatic pressure exerted by the sedimentary load increases the differential strength of the underlying lithosphere. This effect has been incorporated in our rheological models. If we assume a state of thermal equilibrium, the presence of sediments with zero-strength results in a reduction of the thickness of the mechanically strong part of the lithosphere (see Fig. 3.6). This is the case when continuous sedimentation occurs according to the reference model of sediment loading. Wortel (1980) has demonstrated that for reference loading the effect on the temperature distribution is very small at depths corresponding with the transition of the elastic to the ductile regime. For deltas, where rapid sedimentation often takes up the full loading capacity of the underlying lithosphere, the situation is different. Initially, sudden deposition of a sedimentary sequence results in a zero temperature and a non-zero pressure perturbation. With time, thermal equilibrium is restored. We have performed simple thermal calculations, using a finite difference scheme, to estimate this effect. The results indicate that within 10 m.y. thermal equilibrium is restored. Deviations from thermal equilibrium result in an underestimate by only a few km of the elastic thickness. We neglect this effect and assume thermal equilibrium throughout our analysis.

The flexure of the lithosphere under the influence of loading is counteracted by isostasy. Isostatic forces, proportional to the deflec-

tion due to loading, are included by modifying the stiffness matrix at the basal nodes of the model (e.g. Cloetingh and Wisse, 1981).

The magnitudes of the forces associated with the ridge push, and the negative buoyancy of the oceanic lithosphere are calculated on the basis of Oxburgh and Parmentier's (1977) model for the formation of oceanic crust, and Crough's (1975) model for the thermal evolution of oceanic lithosphere. Following Lister (1975), we model the ridge push not as a line force, but as a pressure gradient, excluding in this way artificial stress concentrations at the ridge. The integrated pressure gradient per unit width along the ridge for oceanic lithosphere with an age of 100 m.y. is 2.3×10^{12} N/m. We ignore drag at the base of the lithosphere. Zero horizontal displacements are prescribed for the right hand boundary of the model to simulate a ridge push transmitted through the continent from an adjacent oceanic plate.

Our finite element model is made up of plane strain elements. For flexural analysis, constant strain elements are inadequate and an element is required with linearly varying strain over its surface. For this reason, the displacement field has to be at least quadratic and, hence, an eight-node quadrilateral element was chosen.

Since we investigate for the most part pure in-plane bending, only a few elements are needed in areas where strains and stresses are anticipated to vary linearly with position. This is the case in the vertical direction. In the horizontal direction, the stress distribution is more complex, so that up to 50 elements were necessary here. This conclusion is based partly on tests that were made for the case of bending of a uniform elastic plate under a triangular load with a hydrostatic restoring force. The results of the finite element solution were tested and confirmed by the analytical solution. The finite element calculations were carried out with MARC (Marc, 1980). An initial stress procedure was used to solve the plane strain equations for plasticity.

The largest model (the 200 m.y. model) has about 2000 degrees of freedom, and 20 (plastic) load increments were necessary to reach the final state of loading. The results of the elastic-plastic analysis (presented in section 3.2.2.) were checked and confirmed by convergence tests and an analysis of the internal reaction forces of the model. It should be noted that the finite element approach followed here is not

hampered by the limitations and the assumptions of the classical thin plate theory, encountered in other methods of flexural analysis (Lambeck and Nakiboglu, 1980; Bodine et al., 1981). In particular, the assumptions of a zero shear stress neutral surface and of zero shear forces in the vertical plane are avoided.

As mentioned before, the emphasis of our analysis is on a set of model calculations, in which the loads are applied instantaneously on the lithosphere. However, simultaneous with the growth of the load, the elastic core of the lithosphere thickens with age by a continuous transition of cooling lithospheric material from a ductile state to an elastic state. Significant stresses can only be accomodated once the material has become part of the mechanically strong upper part of the lithosphere. This implies that the part of the sedimentary wedge, deposited in an interval between ages t_1 and t_2, effectively determines the state of stress at t_2 at the bottom of the mechanically strong part of the lithosphere (itself created between t_1 and t_2). This follows from the fact that loading prior to t_1 can only induce low stresses in the then weak part of the lithosphere.

In the following section, we present the results of numerical models, which are characterized by an instantaneously applied sedimentary load. From the arguments given above, we infer that the stress maxima calculated at the bottom of the mechanically strong part of the lithosphere tend to be overestimated. This might be important for the reference model of sediment loading. Most of the Earth's deltas have, measured on geological timescales, been deposited instantaneously (within a few hundred thousand years) in particular, during Pleistocene times (Nelson et al., 1970). For deltas, the approximation of an instantaneously applied load is anticipated to be a very good one. To evaluate the effect of this assumption more quantitatively, we have developed in section 3.2.3, an additional class of models for a limited set of lithospheric ages, in which incremental loads are placed on the lithosphere.

3.2.2 *Results*

The stress calculations are made for a passive margin in different stages of evolution in which the two sediment loading models and the depth-dependent rheologies are incorporated.

Reference load model

Fig. 3.5 shows the results for the case of a reference load on a 100 m.y. old passive margin. This figure strengthens and extends some conclusions reached earlier on the basis of our simple analytical models. The deformation of the lithosphere and the resulting stress field, with an order of magnitude of some kilobars, is dominated by the sediment loading: the contribution of the plate tectonic forces to the stress field is an order of magnitude smaller. Differential stresses are largest at the points of maximum flexure. The largest stress maximum is located under the rise in the oceanic lithosphere close to the transition of oceanic and rift-stage lithosphere. The extreme lowermost and uppermost regions of the mechanically strong upper part of the lithosphere fail. This is due to the high stresses developed at the top and at the base. The main part of the mechanically strong part of the lithosphere remains in the elastic state. In Figs. 3.6a and 3.6b, the stress maxima for 100 m.y. and 30 m.y. are displayed for the reference load, as a function of depth, down to the base of the mechanically strong upper part of the lithosphere. Hatched areas indicate failure by brittle fracture in the uppermost part and by ductile flow in the lowermost region of the mechanically strong part of the lithosphere; the main part is in the elastic state. These figures illustrate some of the points made before. From a comparison of these figures, the dependence on age of the state of stress at passive margins is evident.

In order to summarize this dependence, we have plotted in Fig. 3.7 the maximum differential (tensional) stresses as a function of age for the four cases (30, 60, 100 and 200 m.y.) considered in the reference load models. The age-dependence is strongest for ages below 100 m.y. From 30 to 100 m.y., an interval in which the sedimentary loading and the thickness of the mechanically strong part of the lithosphere and its strength increase, the differential stress maxima are also seen to

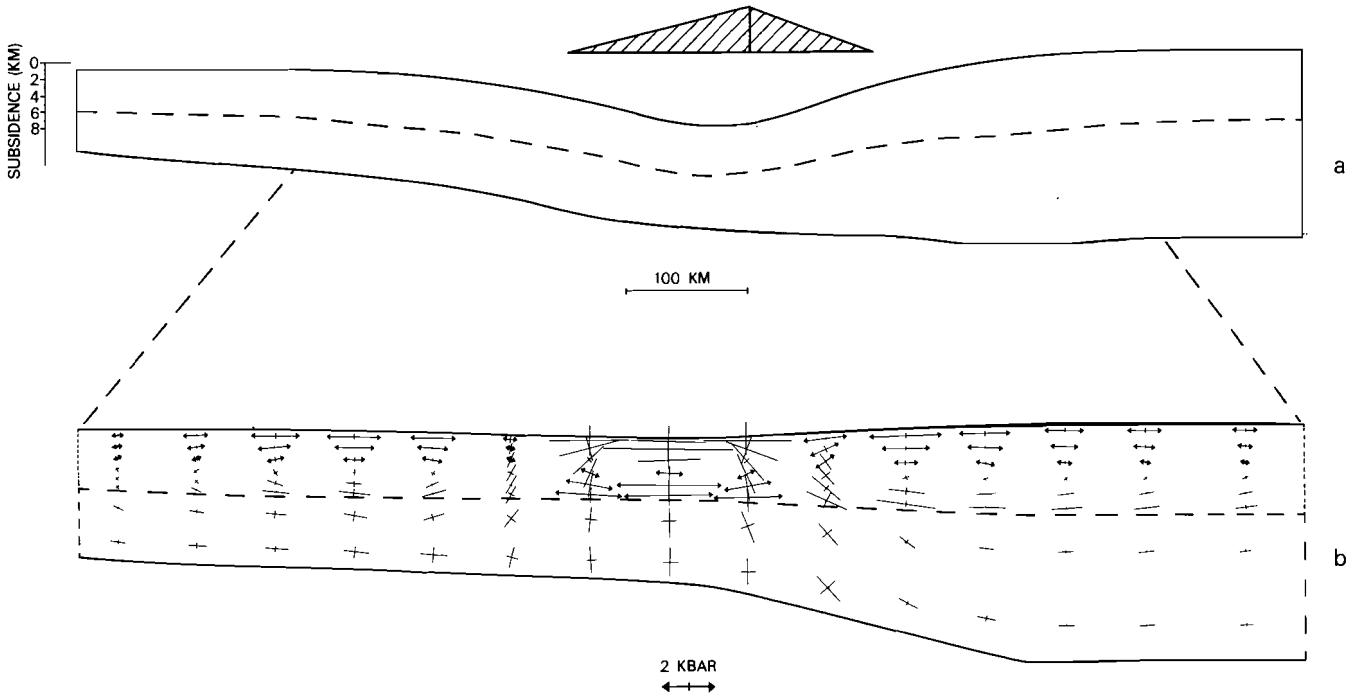

Fig.3.5 - Deflections and stresses calculated for a passive margin with an age of 100 m.y., based on the reference model of sediment loading, given in Fig.2.3. Flexure caused by sediment loading forms the dominant deformation mode at the margin. Principal stresses, denoted by arrows, are plotted in the undeformed configuration. Stresses and displacements are plotted only for the parts of the lithosphere where the deformation is significant. a (above), displacements of the lithosphere (km). Note that the scale of the displacements (vertical axis) and geometry (indicated by a horizontal bar at the bottom of the figure) are not the same. b (below), Principal stresses (kbar) at the margin. Symbols (⟵⟶) and (⟶⟵) denote tension and compression respectively. The scale is indicated at the lower part of the figure.

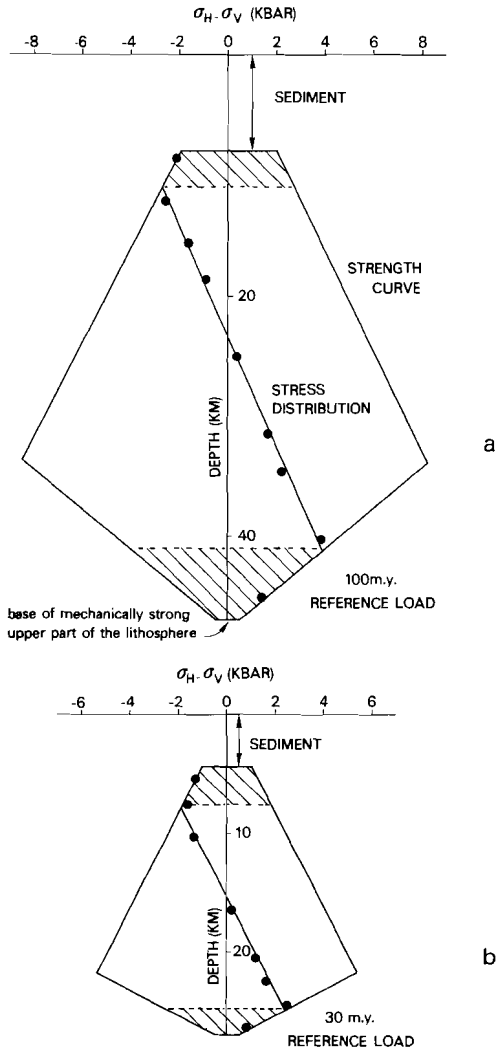

Fig.3.6 – Comparison of stresses generated at the margin with lithospheric strength. Strength envelope and results of stress calculations (solid dots) are given as a function of depth, down to the base of mechanically strong upper part of the lithosphere at the point of maximum flexure (AB of cross section ABC in Fig.3.4; see also Fig.3.5). The line inside the strength envelope connecting the solid dots is the stress distribution. Differential stresses (σ_H-σ_V) are plotted versus depth. Sign convention for the stresses: tension positive, compression negative. Zero-strength has been assumed for the sediments. Hatched areas in the upper and lower part of the mechanically strong upper part of the lithosphere denote failure by brittle fracture and ductile flow respectively. a (upper), b (lower), The results for the reference model of sediment loading for ages of 100 m.y. and 30 m.y. respectively.

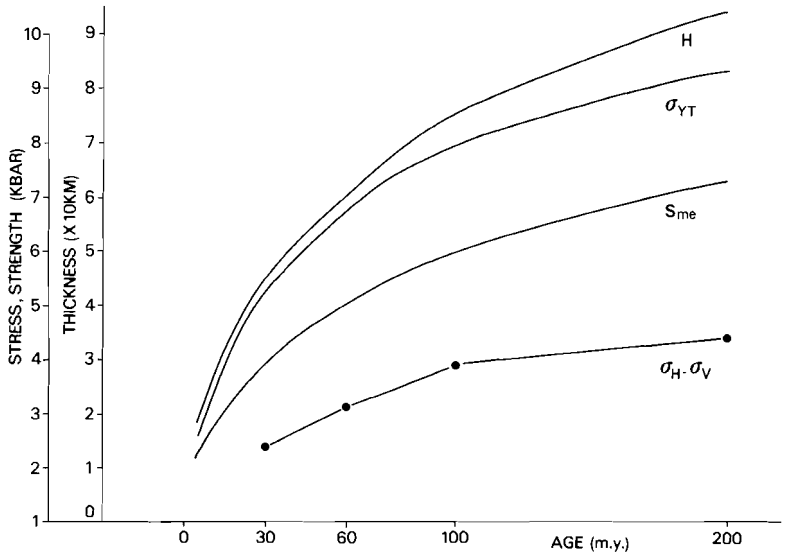

Fig.3.7 - Maximum differential stresses (σ_H-σ_V), load height H, tensional strength σ_{YT} and thickness of the mechanically strong upper part of the lithosphere plotted as a function of lithospheric age. The figure demonstrates the similarity in the age-dependence of these quantities.

increase with age. From 100 to 200 m.y., the strength and thickness of the mechanically strong part of the lithosphere show only a gradual increase. The increase in sediment load, according to our reference model, results only in a minor increase of the stresses. Interesting quantities are: the ratio of the maximum stress generated and the maximum strength in tension; the relative thickness of the mechanically strong upper part in failure S_Y/S_{me}; and the ratio of A_Y, corresponding with the hatched area (inside the strength envelope (Fig.3.6)), and the total area A of the envelope. For the reference model of sediment loading, these quantities prove to be essentially independent of age (Figure 3.8).

Stresses are on a level too low to result in rupture of the lithosphere, no matter whether the margin is in a youthful or mature stage.

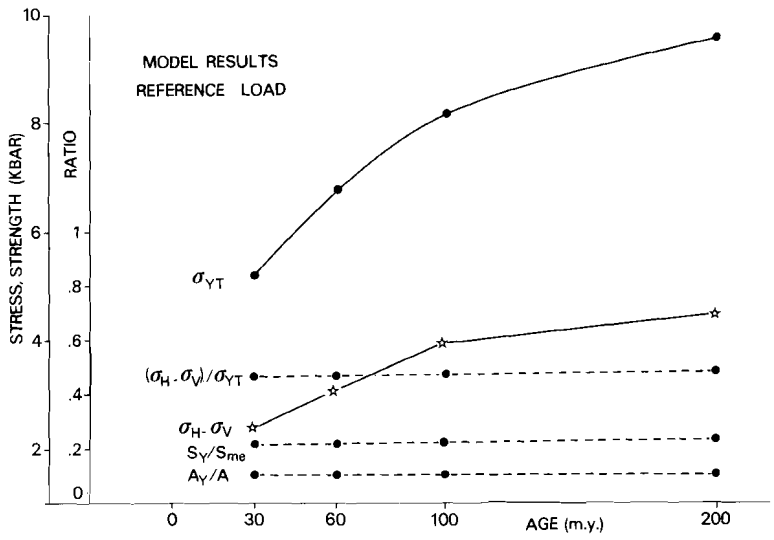

Fig.3.8 - Model results for the analysis with the reference load: maximum differential stresses ($\sigma_H - \sigma_V$), tensile strength σ_{YT}, their ratio, the relative thickness of the mechanically strong part of the lithosphere in failure (S_Y/S_{me}) and the ratio of A_Y (the hatched area inside the strength envelope, see Fig.3.6) and A (total area of the envelope) plotted as a function of lithospheric age. Stresses are on a level too low to result in rupture of the lithosphere, no matter whether the margin is in a youthful or mature stage.

Full load model

The situation is drastically different when the full loading capacity is taken up by the sediments. For the full load analysis, we constructed seven models for ages varying between 15 and 200 m.y. The surplus load of sediments added to the reference load will be most effective in creating high stresses when deposited on a young (weak) margin.

This is demonstrated in Figure 3.9, which shows the stresses at the point of maximum flexure generated by full loading on a 20 m.y. old passive margin. Complete failure of the lithosphere is induced. Of the three ratios $(\sigma_H - \sigma_V)/\sigma_{YT}$, S_Y/S_{me} and A_Y/A, we select the latter as the most meaningful quantity to illustrate the evolution of the stress pattern under full loading conditions. Quantity A (or A_Y) is a

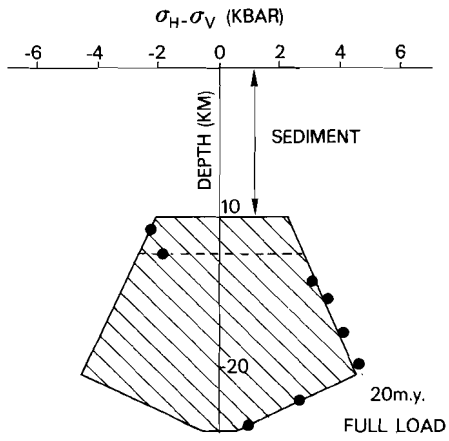

Fig.3.9 - The results for the full load model for 20 m.y. The horizontal dashed line indicates the neutral surface just before complete failure of 20 m.y. old lithosphere takes place. Figure conventions as in Fig.3.6.

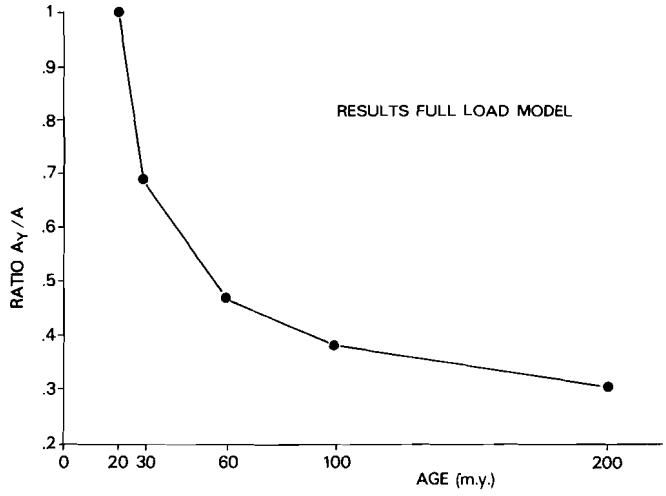

Fig.3.10 - The results of the full load model: ratio of A_Y (the hatched area inside the strength envelope, see Fig.3.9) and A (total area of the envelope) as a function of lithospheric age. For ages below 20 m.y., lithospheric failure and consequently initiation of subduction is induced.

combined measure of the thickness and the strength of the mechanically strong part of the lithosphere. The ratio A_Y/A is plotted in Figure 3.10 as a function of the age of the margin.

Figure 3.10 and results of numerical calculations made for ages below 20 m.y. (not shown here), shows that full loading on passive margins with ages *below* 20 m.y. leads to complete failure of the lithosphere. For ages in excess of 20 m.y., the relative amount of failure strongly decreases with age.

The implementation of a strength envelope with different brittle strengths in compression and tension, shifts the maximum age, at which complete failure is induced, from 20 m.y. to 15 m.y. (see Figure 3.11). Such modifications of the model do not alter the essence of our conclusions.

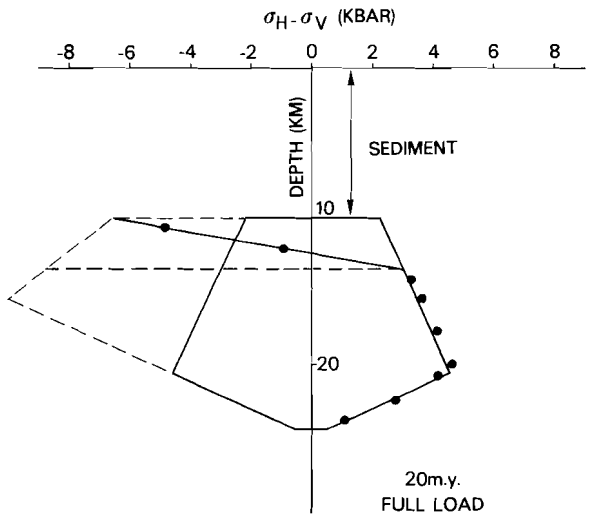

Fig.3.11 - The result for the full load model for 20 m.y. when different values for strengths in compression and tension are incorporated into the models. Figure conventions as in Fig.3.6.

3.2.3 *Investigation of the assumption of instantaneously applied loads*

In the present section, we investigate the influence on the results presented in section 3.2.2. of the assumption of instantaneously applied loads. To this end, we have constructed models for a limited set of lithospheric ages, in which incremental loads are placed on the lithosphere. Here, we confine ourselves to a short description of the results of the model calculations. An elaborate account of the numerical features of this particular set of calculations will appear elsewhere (Cloetingh and Wisse, in prep.). Small quantities of sediment are stepwise added, as a function of time, to the previously deposited sediments. Considering the results of section 3.2.2, we restrict ourselves to the youthful stages of margin evolution (ages up to 20 m.y.). For this range of litho-

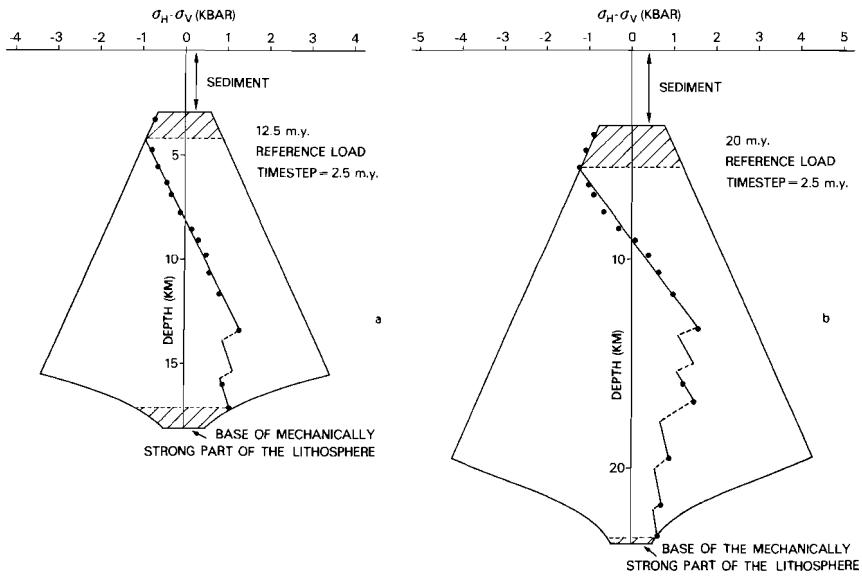

Fig.3.12 - Comparison of the results, obtained with incremental loads, with lithospheric strength for the case of reference loading on passive margins of 12.5 m.y.(a) and 20 m.y.(b). Figure conventions as in Fig.3.6.

spheric ages, the selected timestep of 2.5 m.y. is equivalent to increments in the thickness of the lithosphere of the order of 5 km.
In Fig. 3.12, we present the results of these calculations for the case of *reference loading* on passive margins of 12.5 and 20 m.y. Compared with the results of the calculations in which we applied an instaneous load, a relatively small part of the lithosphere is in failure. The stress maxima are no longer found near the lower boundary of the mechanically strong part of the lithosphere.

Flexural stresses are more evenly distributed over the thickness of the mechanically strong part of the lithosphere, since the position of the neutral plane moves downward with each new loading step. A comparison of Figs 3.12a and 3.12b shows that, with time, several stress maxima are developing at different levels within the mechanically strong part of the lithosphere. In Figure 3.13, we have summarized the results for the reference load in the form of a plot of the maximum differential stresses, and the quantities $(\sigma_H - \sigma_V)/\sigma_{YT}$ for ages up to 20 m.y. The differential

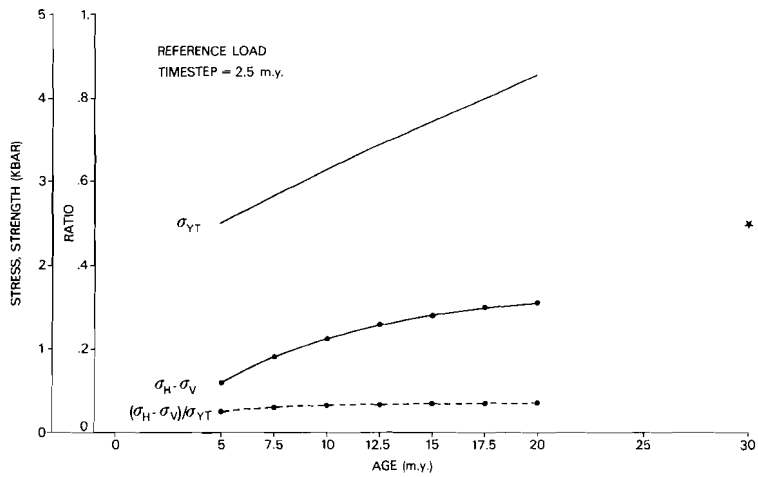

Fig.3.13 - Model results, calculated with incremental loads for reference loading, summarized for a limited range of lithospheric ages. The stress maximum (*) found with an instantaneously applied load on 30 m.y. old lithosphere (see Fig.3.8) is given for comparison. Figure conventions as in Fig.3.8.

stress maxima are far too low to result in failure of the lithosphere. Compared with the case of instantaneously applied loads (Fig. 3.8), the differential stress maxima are lower. The differential stress maxima show a relatively small increase with age, which results for ages in excess of 5 m.y. in values for the ratio $(\sigma_H-\sigma_V)/\sigma_{YT}$ of approximately 0.35. Although the value of 0.35 for $(\sigma_H-\sigma_V)/\sigma_{YT}$ is slightly lower than the value of 0.45 found with the models described in section 3.2.2, the essence of the conclusions reached with models assuming instantaneously applied loads is not altered. For the *full load* model, the deviations from the results obtained with loading in small steps from the results given in section 3.2.2 are even smaller. Loading with small timesteps does not change the age (20 m.y.), at which complete lithospheric failure is induced.

Implications

The calculations for instantaneously applied loads, reported in section 3.2.2,have demonstrated that stresses induced by reference loading on passive margins are too low to result in lithospheric failure. These calculations showed that continuous aging of the passive margin alone, does not result in conditions more favourable for initiation of subduction. The investigation of the assumption of the instantaneously applied load, confirms these conclusions by giving constant, although lower, values for the quantities $(\sigma_H-\sigma_V)/\sigma_{YT}$. More importantly, the results of the calculations with small incremental loads presented in this section, confirm the major conclusion reached with the calculations presented in section 3.2.2: full loading on a young passive margin provides a mechanism for lithospheric failure and initiation of subduction.

3.3 EVALUATION AND DISCUSSION

The results of our calculations show that sediment loading can induce stresses of many kilobars at a passive margin. For the reference model of sediment loading, the increase of the stresses, generated as loading proceeds, is compensated by the stiffening of the aging lithosphere. Therefore, under these loading conditions, stresses at the margin will remain on a level, which is not sufficiently high to rupture the lithosphere; whether the margin is in a youthful or mature stage is immaterial. The situation is drastically different when supplementary sedimentary loads (the full load model) are deposited on young lithosphere. In this case, stresses are generated, that can induce lithospheric failure and initiation of subduction.

3.3.1 *Geological inferences*

From our results, we conclude that extensive sediment loading (following the full load model) might have been an effective mechanism for closure of young, and presumably small, ocean basins in geologic history. Closing of small oceanic basins plays an important role in the process of mountain building. Precise data on the timing of the closing events are lacking, which inhibits a quantitative comparison with our model results. However, much of the available geological evidence is clearly contradictory to activation of passive margins in a late stage of their evolution. In particular, studies of Alpine orogeny show evidence for closing of small oceanic basins in an early stage after opening (Trümpy, 1981). For the central Alps, closure of oceanic basins *within* the first 100 m.y. after their opening, has been demonstrated by Frisch (1979). Winterer and Bosellini (1981) have documented the evolution of a thickly sedimented Jurassic passive margin in the southern Alps. These authors argue for closing of the oceanic basin *within* 50 m.y. after spreading started. Kröner (1981) has presented evidence for the important role small basins have played further back in geological time during the Pan-African orogeny (500-1100 m.y. b.p.). These small basins were closed soon after opening, and were characterized by the presence of extensive sediment loads of up to 8 km thickness. Lithospheric failure associated with downflexing of the lithosphere by the sediments,

might provide a simple explanation for these observations.

The maximum reconstructed sedimentary thicknesses in orogenic belts (Stoneley, 1969) are of the same order of magnitude as the maximum sedimentary thicknesses observed at passive margins.

The classical eugeosynclinal cycle is generally interpreted as the result of the Wilson (1966) cycle of oceanic opening by seafloor spreading and oceanic closure by subduction (Mitchell and Reading, 1978). It seems, however, that in general, the stresses generated by sediment loading at passive margins are insufficient to induce lithospheric failure and initiation of subduction. Only in the very beginning of its evolution, the combination of a very weak lithosphere with a thick sediment load may provide a mechanism for the activation of passive margins. McKenzie (1977) demonstrated that a large slab pull is required to overcome the resistive forces active in the process of trench formation. Such a large slab pull is lacking for young lithosphere (England and Wortel, 1980). However, the compressive stresses needed to sustain the further development of subduction zones involving young stable lithosphere (McKenzie, 1977; England and Wortel, 1980), may be provided by stress concentration of plate tectonic forces during plate reorganizations, and are an order of magnitude smaller than the stresses required to *rupture* the lithosphere. Therefore, plate rupture forms the most essential part of the initiation process.

In our analysis, we ignored the effect of fossil fault systems. Wells drilled off the eastern U.S. margin show simultaneous subsidence across the margin (Heller et al., 1982). Marginal faults are probably locked early in the post break-up stage (Steckler and Watts, 1981). Their presence may be of additional help to decouple oceanic and continental lithosphere at young margins. In conclusion, it has been shown here that if subduction has not been initiated at the margin in a youthful stage, continued aging of the passive margin alone does not result in conditions more favourable for beginning the subduction process.

3.3.2 *Alternative scenarios*

Therefore, in general, existing weakness zones located entirely within oceanic lithosphere, might be more suitable sites for initiation of subduction than passive margins. As such, spreading centres (Turcotte

et al., 1977b) and, in particular, transform faults (Uyeda and Ben Avraham, 1972; Dewey, 1975) have been advocated. Spreading ridges can be considered as the lower bound (0 m.y.) of the young passive margins studied in the present work, the spreading ridge forming an inherently present rupture zone in the lithosphere.

This view is coherent with the results of a survey of recently initiated subduction zones in the Pacific (Karig, 1982) showing that zones initiated in the Neogene either are at the sites of transform faults or are rejuvenated pre-existing subduction zones.

Many of the present circum-Pacific zones are in fact the successors of subduction zones already present in the configuration prior to the break-up of Gondwanaland (Cox, 1978; Burchfiel, 1980). Further back in geological time, different plate configurations and a different thermal regime might have provided conditions more suitable for initiation of subduction. As an extreme example, one might consider the Archaean, where, due to much steeper temperature gradients in the lithosphere (Sharpe and Peltier, 1979), the oceanic plates must have been considerably weaker and thinner (McKenzie and Weiss, 1975) than nowadays. In such a situation, plate rupture requires a considerably lower stress level.

Thus, in general, we do not expect initiation of subduction of oceanic lithosphere at passive margins to play a primary role in plate reorganizations such as documented by Rona and Richardson (1978). However, in an oceanic plate attached to a subduction zone, the pull acting on the subducting slab can be concentrated to a high stress level (order of magnitude many kilobars) (Wortel and Cloetingh, 1981). In particular, Wortel and Cloetingh (1981) have shown that lateral variations in the age of the slab descending in a subduction zone might provide a mechanism for fragmentation of oceanic plates and for the formation of spreading centres. Therefore, plate reorganization may take place predominantly by the formation of new spreading ridges, because stress relaxation in the lithosphere takes place much more easily through this process than through the formation of new subduction zones.

REFERENCES

Anderson, D.L., and Minster, J.B., 1980. Seismic velocity, attenuation and rheology of the upper mantle, Prof. J. Coulomb Symp. on Source mechanisms and Earthquake prediction.

Ashby, M.F., and Verrall, R.A., 1978. Micromechanisms of flow and fracture, and their relevance to the rheology of the upper mantle, Phil. Trans. R. Soc. Lond. A., v. 288, p. 59-95.

Artyushkov, E.V., 1973. Stresses in the lithosphere caused by crustal thickness inhomogeneities, J. Geophys. Res., v. 78, p. 7675-7708.

Bally, A.W., 1982. Keynote to the conference on Continental margin Processes, Galveston, Texas january 12-16, 1981, Am. Assoc. Petrol. Geol. Memoir, in press.

Bodine, J.H., Steckler, M.S., and Watts, A.B., 1981. Observations of flexure and the rheology of oceanic lithosphere, J. Geophys. Res., v. 86, p. 3695-3707.

Bott, M.H.P., and Dean, D.S., 1972. Stress systems at young continental margins, Nature Phys. Sciences, v. 235, p. 23-25.

Brace, W.F., and Kohlstedt, D.L., 1980. Limits on lithospheric stress imposed by laboratory experiments, J. Geophys. Res., v. 85, p. 6248-6252.

Bryant, W.R., Bennett, R.H., and Katherman, C.E., 1981. Shear strength, consolidation, porosity and permeability of oceanic sediments, in: Emiliani, C., (ed.), The Oceanic Lithosphere, The Sea vol. 7, Wiley, New York, p. 1555-1616.

Buffler, R.T., Shaub, F.J., Huerta., R., Ibrahim, A.B., and Watkins., J.S., 1981. A model for the early evolution of the Gulf of Mexico basin, Oceanologica Acta, Colloque C3, Geology of continental margins, 26th Int. Geol. Congr. Paris, 1980, p. 129-136.

Burchfiel, B.C., 1980. Tectonics of noncollisional regimes, The modern Andes and the Mesozoic Cordilleran orogen of the western United States, in: Continental Tectonics, Natl. Acad. of Sci., Studies in Geophysics, Washington, p. 65-72.

Burk, C.A., and Drake, C.L., (eds.), 1974. The Geology of Continental margins, Springer, New York, pp. 1009.

Caldwell, J.G., Haxby, W.F., Karig, D.E., and Turcotte, D.L., 1976. On the applicability of a universal elastic trench profile, Earth Planet. Sci. Lett., v. 31, p. 239-246.

Caldwell, J.G., and Turcotte, D.L., 1979. Dependence of the thickness of the elastic oceanic lithosphere on age, J. Geophys. Res., v. 84, p. 7472-7576.

Chapple, W.M., and Forsyth, D.W., 1979. Earthquakes and bending of plates at trenches, J. Geophys. Res., v. 84, p. 6729-6749.

Cloetingh, S., Nolet, G., and Wortel, R., 1979. On the use of Rayleigh wave group velocities for the analysis of continental margins, Tectonophysics, v. 59, p. 335-346.

Cloetingh, S., Nolet, G., and Wortel, R., 1980a. Crustal structure of the eastern Mediterranean inferred from Rayleigh wave dispersion, Earth Planet. Sci. Lett., v. 51, p. 336-342.

Cloetingh, S., Nolet, G., and Wortel, R., 1980b. Standard graphs and tables for the interpretation of Rayleigh wave group velocities in crustal studies, Proc. Kon. Ned. Akad. Wetensch. B.,v. 83, p. 101-118.

Cloetingh, S., and Wisse, G., 1981. Finite element modelling in Geodynamics: the state of stress at passive continental margins, Finite Element News, no. 3, p. 37-40.
Cloetingh, S.A.P.L., Wortel, M.J.R., and Vlaar, N.J., 1981. On the state of stress at passive continental margins and the problem of initiation of subduction zones, Paper presented at the 1980 EGS-ESC Meeting Budapest, Trans. Am. Geophys. Un. EOS, v. 62, p. 222.
Cloetingh, S.A.P.L., Wortel, M.J.R., and Vlaar, N.J., 1982a. State of stress at passive margins and initiation of subduction zones, Am. Assoc. Petrol. Geol. Memoir, in press.
Cloetingh, S.A.P.L., Wortel, M.J.R., and Vlaar, N.J., 1982b. Evolution of passive continental margins and initiation of subduction zones, Nature, v. 297, p. 139-142.
Closs, H., Narain, H., and Garde, S.C., 1974. Continental margins of India, in: Burk, C.A., and Drake, C.L., (eds.), The Geology of Continental margins, Springer Verlag, New York, p. 629-639.
Cochran, J.R., 1980. Some remarks on isostasy and the longterm behaviour of the continental lithosphere, Earth Planet. Sci. Lett., v. 46, p. 266-274.
Cohen, C.R., 1982. Model for a passive to active continental margin transition: implicationsfor hydrocarbon exploration, Am. Assoc. Petrol. Geol. Bull., v. 66, p. 708-718.
Collette, B.J., 1974. Thermal contraction joints in a spreading seafloor as origin of fracture zones, Nature, v. 251, p. 299-300.
Cox, K.G., 1978. Flood basalts,subduction and the break-up of Gondwanaland, Nature, v. 274, p. 47-49.
Crough, S.T., 1975. Thermal model of oceanic lithosphere, Nature, v. 256, p. 388-390.
Crowell, J.C., 1974. Origin of late Cenozoic basins in southern California, in: Dickinson, W.R., (ed.), Tectonics and sedimentation, Soc. Econ. Paleontol. Mineral. Spec. Publ., v. 22, p. 190-204.
Curray, J.R., 1980. The Ipod programme on passive continental margins, Phil. Trans. R. Soc. Lond. A., v. 294, p. 17-33.
Curray, J.R., and Moore, D.G., 1974. Sedimentary and tectonic processes in the Bengal deep-sea fan and geosyncline, in: Burk, C.A., and Drake, C.L., (eds.), The Geology of Continental margins, Springer Verlag, New York, p. 617-627.
Desai, C.S., and Abel, J.F., 1972. Introduction to the Finite Element Method, van Nostrand Reinhold, New York, pp. 477.
Dewey, J.F., 1969. Continental margins: a model for conversion of Atlantic type to Andean type, Earth. Planet. Sci. Lett., v. 6, p. 189-197.
Dewey, J.F., 1975. Finite plate evolution, some implications for the evolution of rock masses at plate margins, Am. J. Sci., v. 275 A., p. 260-284.
Dickinson, W.R., and Seely, D.R., 1979. Structure and stratigraphy of fore arc regions, Am. Assoc. Petrol. Geol. Bull., v. 63, p. 2-31.
Dickman, S.R., and Williams, D.R., 1981. Viscoelastic membrane tectonics, Geophys. Res. Lett., v. 8, p. 199-202.
Dietz, R.S., 1963. Collapsing continental rises: an actualistic concept of geosynclines and mountain building, J. Geol., v. 71, p. 314-333.
Dow, W.G., 1978. Petroleum source beds on continental slopes and rises, Am. Assoc. Petrol. Geol. Bull., v. 62, p. 1584-1606.
Dziewonski, A.M., and Boschi, E., (eds.), 1980. Physics of the Earth's Interior, North Holland, Amsterdam, pp. 716.

Emery, K.O., 1980. Continental margins - classification and petroleum prospects, Am. Assoc. Petrol. Geol. Bull., v. 64, p. 297-315.
England, P., and Wortel, R., 1980. Some consequences of the subduction of young slabs, Earth Planet. Sci. Lett., v. 47, p. 403-415.
Finetti, I., and Morelli, C., 1973. Geophysical exploration of the Mediterranean Sea, Boll. Geof. Teor. Appl., v. 15, p. 263-340.
Flinn, E.A., 1982. The International lithosphere program, Trans. Am. Geophys. Un. EOS., v. 63, p. 209-210.
Forsyth, D.W., 1980. Comparison of mechanical models of the oceanic lithosphere, J. Geophys. Res., v. 85, p. 6364-6368.
Forsyth, D.W., and Uyeda, S., 1975. On the relative importance of driving forces of plate motion, Geophys. J.R. astr. Soc., v. 43, p. 163-200.
Freeth, S.J., 1979. Deformation of the African Plate as a consequence of membrane stress domains generated by post-Jurassic drift, Earth Planet. Sci. Lett., v. 45, p. 93-104.
Frisch, W., 1979. Tectonic progradation and plate tectonic evolution of the Alps, Tectonophysics, v. 60, p. 121-139.
Goetze, C., 1978. The mechanisms of creep in olivine, Phil. Trans. R. Soc. Lond. A, v. 288, p. 99-119.
Goetze, C., and Evans, B., 1979. Stress and temperature in the bending lithosphere as constrained by experimental rock mechanics, Geophys. J.R. astr. Soc., v. 59, p. 463-478.
Goldflam, P., Hinz, K., Weigel, W., and Wissmann, G., 1980. Some features of the northwest African margin and magnetic quiet zone, Phil. Trans. R. Soc. Lond. A., v. 294, p. 87-96.
Grow, J.A., Mattick, R.E., and Schlee, J.S., 1979. Multi channel seismic depth sections and interval velocities over outer continental shelf and upper continental slope between Cape Hatteras and Cape Cod, in: Watkins, J.S., Montadert, L., and Dickerson, P.W., (eds.), Geological and Geophysical investigations of continental margins, Am. Assoc. Petrol. Geol. Memoir., v. 29, p. 65-83.
Grow, J.A., and Sheridan, R.E., 1981. Deep structure and evolution of the continental margin of the eastern United States, Oceanologica Acta, Colloque C3, Geology of continental margins, 26th Int. Geol. Congr. Paris, 1980, p. 11-19.
Hager, B.H., 1980. Problems in geodynamics, in: Dziewonski, A.M., and Boschi, E., (eds.), Physics of the Earth's Interior, North Holland, Amsterdam p. 707-709.
Hales, A.L., 1969. Gravitational sliding and continental drift, Earth Planet. Sci. Lett., v. 6, p. 31-34.
Hanks, T.C., 1977. Earthquake stress drops, ambient tectonic stresses and stresses that drive plate motions, Pure Appl. Geophys., v. 115, p. 441-458.
Haxby, W.F., and Turcotte, D.L., 1976. Stresses induced by the addition or removal of overburden and associated thermal effects, Geology, v. 44, p. 181-184.
Haxby, W.F., Turcotte, D.L., and Bird, J.M., 1976. Thermal and mechanical evolution of the Michigan Basin, Tectonophysics, v. 36, p. 57-75.
Heiskanen, W.A., and Vening Meinesz, F.A., 1958. The Earth and its gravity field, McGraw Hill, New York, pp. 470.
Heller, P.L., Wenworth, C.M., and Poag, C.W., 1982. Episodic post-rift subsidence of the United States Atlantic continental margin, Geol. Soc. Am. Bull., v. 93, p. 379-390.

Hetényi, M., 1946. Beams on elastic foundation, Theory with applications in the fields of civil and mechanical engineering, University of Michigan Press, Ann Arbor Michigan, pp. 255.
Hinz, K., Schlüter, H-U., Grant, A.C., Srivastava, S.P., Umpleby, D., and Woodside, J., 1979. Geophysical transects of the Labrador Sea: Labrador to Southwest Greenland, Tectonophysics, v. 59, p. 151-183.
Houtz, R.E., Ludwig, W.J., Milliman, J.D., and Grow, J.A., 1977. Structure of the northern Brazilian continental margin, Geol. Soc. Am. Bull., v. 88, p. 711-719.
Hutchinson, D.R., Grow, J.A., and Klitgord, K.D, 1982. Deep structure and evolution of the Carolina Trough, in Watkins, J.S., and Drake, C.L., (eds.), Continental margin Processes, Am. Assoc. Petrol. Geol. Memoir, in press.
Jaeger, J.C., and Cook, N.G.W., 1976. Fundamentals of rock mechanics, second edition, Chapman and Hall, London, pp. 585.
Jeffreys, H., 1976. The Earth, sixth edition, Cambridge University Press, Cambridge, pp. 574.
Kanamori, H., 1980. Stress in the lithosphere, in: Dziewonski, A.M., and Boschi, E., (eds.), Physics of the Earth's Interior, North Holland, Amsterdam, p. 712-713.
Karig, D.E., 1982. Initiation of subduction zones: implications for arc evolution and ophiolite development, preprint Cornell Univ.
Karner, G.D., and Watts, A.B., 1982. On isostasy at Atlantic-type continental margins, J. Geophys. Res., v. 87, p. 2923-2948.
Keen, C.E., 1979. Thermal history and subsidence of rifted continental margins: Evidence from wells on the Nova Scotia and Labrador shelves, Can. J. Earth Sci., v. 16, p. 505-522.
Keen, C.E., and Keen, M.J., 1974. Continental margins of eastern Canada and Baffin Bay, in: Burk, C.A., and Drake, C.L., (eds.), The Geology of Continental margins, Springer Verlag, New York, p. 381-389.
Kent, P.E., 1974. Continental margin of east Africa - a region of vertical movement, in: Burk, C.A., and Drake, C.L., (eds.), The Geology of Continental margins, Springer Verlag, New York, p. 313-320.
Kinsman, D.J.J., 1975. Rift valley basins and sedimentary history of trailing continental margins, in: Fischer, A.G., and Judson, S., (eds.), Petroleum and global tectonics, Princeton Univ. Press, Princeton, N.J., p. 83-126.
Kirby, S.H., 1980. Tectonic stresses in the lithosphere: constraints provided by the experimental deformation of rocks, J. Geophys. Res., v. 85, p. 6353-6368.
Kraus, H., 1980. Creep analysis, Wiley, New York, pp. 250.
Kröner, A., 1980. Precambrian plate tectonics, in: Kröner, A., (ed.), Precambrian Plate Tectonics, Elsevier, Amsterdam, p. 57-90.
Kusznir, N.J., and Bott, M.H.P., 1977. Stress concentration in the upper lithosphere caused by underlying visco-elastic creep, Tectonophysics, v. 43, p. 247-256.
Lago, B., and Cazenave, A., 1981. State of stress in the oceanic lithosphere in response to loading, Geophys. J. R. astr. Soc., v. 64, p. 785-799.
Lambeck, K., and Nakiboglu, S.M., 1980. Seamount loading and stress in the ocean lithosphere, J. Geophys. Res., v. 85, p. 6403-6418.
Lehner, P., and de Ruiter, P.A.C., 1977. Structural history of Atlantic margin of Africa, Am. Assoc. Petrol. Geol. Bull., v. 61, p. 961-981.

Lister, C.R.B., 1975. Gravitational drive on oceanic plates caused by thermal contraction, Nature, v. 257, p. 663-665.
Malovitskiy, J.P., Emelyanov, E.M., Karakov, O.V., Moskalenko, V.N., Osipov, G.V., Shimkus, K.M., and Chumakov, I.S., 1975. Geological structure of the Mediterranean sea floor (based on geological-geophysical data), Mar. Geol., v. 18, p. 231-261.
Marc Analysis Research Corporation, 1980. Marc general purpose finite element program, User manual, v. A-E., Palo Alto.
McAdoo, D.C., Caldwell, J.G., and Turcotte, D.L., 1978. On the elastic-perfectly plastic bending of the lithosphere under generalized loading with application to the Kuril Trench, Geophys.J.R.astr. Soc., v. 54, p. 11-26.
McKenzie, D.P., 1967. Some remarks on heat-flow and gravity anomalies, J. Geophys. Res., v. 72, p. 6261-6273.
McKenzie, D.P., 1969. Speculations on the consequences and causes of plate motions, Geophys. J.R. astr. Soc., v. 18, p. 1-32.
McKenzie, D.P., 1977. The initiation of trenches: a finite amplitude instability, in: Talwani, M., and Pitman III, W., (eds.), Island arcs, deep sea trenches and back-arc basins, Am. Geophys. Un., Maurice Ewing Series, v. 1, p. 57-62.
McKenzie, D.P., and Weiss, N.O., 1975. Speculations on thermal and tectonic history of the earth, Geophys. J.R. astr. Soc., v. 42, p. 131-174.
McNutt, M., 1980. Implications of regional gravity for state of stress in the Earth's crust and upper mantle, J. Geophys. Res., v. 85, p. 6377-6396.
Menke, W., 1981. The effect of load shape on the deflection of thin elastic plates, Geophys. J.R. astr. Soc., v. 65, p. 571-577.
Minster, J.B., and Anderson, D.L., 1980. Dislocations and non-elastic processes in the mantle, J. Geophys. Res., v. 85, p. 6347-6352.
Mitchell, A.H.G., and Reading, H.G., 1978. Sedimentation and tectonics, in: Reading, H.G., (ed.), Sedimentary environments and facies, Blackwell, Oxford, p. 439-476.
Molnar, P., Chen, W.P., Fitch, T.J., Tapponier, P., Warsi, W.E.K., and Wu, F.T., 1980. Structure and tectonics of the Himalaya: a brief summary of relevant geophysical observations, in: Ecologie et Geologie de l'Himalaya, C.N.R.S. Colloq., v. 268, p. 269-294.
Nadai, A., 1963. Theory of flow and fracture of solids, volume 2, McGraw Hill, New York, p. 250-348.
Naini, B.R., 1980. A geological and geophysical study of the continental margin of western India, and the adjoining Arabian Sea including the Indus Cone, Ph.D. Thesis Columbia University, New York, pp. 172.
Nelson, C.H., Carlson, P.R., Byrne, J.V., and Alpha, T.R., 1970. Development of the Astoria canyon-fan physiography and comparison with similar systems, Mar. Geol. v. 8, p. 259-291.
Neugebauer, H.J., and Spohn, T., 1978. Late stage development of mature Atlantic-type continental margins, Tectonophysics, v. 50, p. 275-305.
Nicolas, A., and Poirier, J.P., 1976. Crystalline plasticity and solid state flow in metamorphic rocks, Wiley, New York, pp. 444.
Nolet, G., Panza, F., and Wortel, R., 1978. An averaged model for the Adriatic subplate, Pure Appl. Geophys., v. 116, p. 1284-1298.
Owen, D.R.J., and Hinton, E., 1980. Finite elements in plasticity: theory and practice, Pineridge press, Swansea, pp. 594.

Oxburgh, E.R., and Parmentier, E.M., 1977. Compositional and density stratification in oceanic lithosphere-causes and consequences, J. Geol. Soc. London, v. 133, p. 343-355.
Oxburgh, E.R., and Turcotte, D.L., 1974. Membrane tectonics and the East African rift, Earth Planet. Sci. Lett., v. 22, p. 133-140.
Parsons, B., and Sclater, J.G., 1977. An analysis of the variation of ocean floor heat flow and bathymetry with age, J.Geophys.Res., v. 82, p. 803-827.
Pollack, H.N., and Chapman, D.S., 1977. On the regional variation of heat flow, geotherms and lithospheric thickness, Tectonophysics, v. 38, p. 279-296.
Post, R.L., 1977. High-temperature creep of Mt. Burnet dunite, Tectonophysics, v. 42, p. 75-110.
Richter, F., 1973. Dynamical models for sea floor spreading, Rev. Geophys. Space Phys., v. 11, p. 223-287.
Richter, F., and McKenzie, D., 1978. Simple plate models of mantle convection, J. Geophys., v. 44, p. 441-471.
Rona, P.A., and Richardson, E.S., 1978. Early Cenozoic global plate reorganization, Earth Planet. Sci. Lett., v. 40, p. 1-11.
Royden, L., Sclater, J.G., and von Herzen, R.P., 1980. Continental margin subsidence and heat flow: important parameters in formation of petroleum hydrocarbons, Am. Assoc. Petrol. Geol. Bull., v. 64, p. 173-187.
Sharpe, H.N., and Peltier, W.R., 1979. A thermal history model for the Earth with parameterized convection, Geophys. J.R. astr. Soc., v. 59, p. 171-203.
Sleep, N.H., 1971. Thermal effects on the formation of Atlantic continental margins by continental break up, Geophys. J.R. astr. Soc., v. 24, p. 325-350.
Solomon, S.C., Sleep, N.H., and Richardson, R.M., 1975. On the forces driving plate tectonics: inferences from absolute plate velocities and intra-plate stress, Geophys. J.R. astr. Soc., v. 47, p. 769-801.
Southam, J.R., and Hay, W.W., 1981. Global sedimentary mass balance and sea level changes, in: Emiliani, C., (ed.), The Oceanic Lithosphere, The Sea vol. 7, Wiley, New York, p. 1617-1684.
Speed, R.C., and Sleep, N.H., 1982. Antler orogeny: a model, submitted to Geol. Soc. Am. Bull.
Steckler, M.S., and Watts, A.B., 1981. Subsidence history and tectonic evolution of Atlantic-type Continental margins, Geodynamics Series, v. 6, Am. Geophys. Un., p. 184-196.
Stoneley, R., 1969. Sedimentary thicknesses in orogenic belts, in: Kent, P.E., et al., (eds.), Time and Place in orogeny, Geol. Soc. London, p. 215-238.
Timoshenko, S.P., and Woinowsky-Krieger, S., 1959. Theory of plates and shells, McGraw Hill, New York, pp. 580.
Trümpy, R., 1981. Alpine paleography - a reappraisal, paper presented at the Mountain building symposium, Zürich, July 14-18, 1981.
Turcotte, D.L., 1974. Are transform faults thermal contraction cracks, J. Geophys. Res., v. 79, p. 2573-2577.
Turcotte, D.L., and Ahern, J.L., 1977. On the thermal and subsidence history of sedimentary basins, J. Geophys. Res., v. 82, p. 3762-3766.
Turcotte, D.L., Ahern, J.L., and Bird, J.M., 1977a. The state of stress at continental margins, Tectonophysics, v. 42, p. 1-28.

Turcotte, D.L., Haxby, W.F., and Ockendon, J.R., 1977b. Lithospheric instabilities, in: Talwani, M., and Pitman III, W., (eds.), Island arcs, deep sea trenches and back-arc basins, Washington D.C., Am. Geophys. Un., Maurice Ewing Series, v. 1, p. 63-69.
Turcotte, D.L., and Oxburgh, E.R., 1967. Finite amplitude convective cells and continental drift, J. Fluid Mech., v. 28, p. 29-42.
Turcotte, D.L., and Oxburgh, E.R., 1976. Stress accumulation in the lithosphere, Tectonophysics, v. 35, p. 183-199.
Urien, C.M., Martins, L.R., and Zambrano, J.J., 1976. The geology and tectonic framework of southern Brazil, Uruguay and northern Argentina continental margin: their behaviour during the southern Atlantic opening, in: De Almeida, F.F.M., (ed.), Continental margins of Atlantic type, An. Acad. Bras. Cienc., v. 48 (suppl.),p. 365-376.
Uyeda, S., and Ben-Avraham, Z., 1972. Origin and development of the Philippine sea, Nature, v. 240, p. 176-178.
Vlaar, N.J., 1975. The driving mechanism of plate tectonics: a qualitative approach, in: Borradaile, G.J., Ritsema, A.R., Rondeel, H.E., and Simon, O.J., (eds.), Progress in Geodynamics, North-Holland, Amsterdam, p. 234-245.
Vlaar, N.J., and Wortel, M.J.R., 1976. Lithospheric aging, instability and subduction, Tectonophysics, v. 32, p. 331-351.
Walcott, R.I., 1972. Gravity, flexure and the growth of sedimentary basins at a continental edge, Geol. Soc. Am. Bull., v. 83, p. 1845-1848.
Walcott, R.I., 1976. Lithospheric flexure, analysis of gravity anomalies and the propagation of seamount chains, in: Sutton, G.H., et al., (eds.), The geophysics of the Pacific Ocean Basin and its margin, Am. Geophys. Un., Geophys. Monograph, v. 19, p. 431-438
Watkins, J.S., and Drake, C.L., 1982. Continental margin Processes, Am. Assoc. Petrol. Geol. Memoir, in press.
Watts, A.B., Bodine, J.H., and Steckler, M.S., 1980. Observations of flexure and the state of stress in the oceanic lithosphere, J. Geophys. Res., v. 85, p. 6369-6376.
Watts, A.B., and Ryan, W.B.F., 1976. Flexure of the lithosphere and continental margin basins, Tectonophysics, v. 36, p. 25-44.
Watts, A.B., and Steckler, M.S., 1979. Subsidence and eustasy at the continental margin of eastern North America, in: Talwani, M. et al., (eds.), Deep drilling results in the Atlantic Ocean: continental margins and paleo-environment Washington D.C., Am. Geophys. Un., Maurice Ewing Series, v. 3, p. 218-234.
Weertman, J., and Weertman, J.R., 1965. Mechanical properties, strongly temperature dependent, in: Cahn, R.W., (ed.), Physical Metallurgy, North Holland, Amsterdam, p. 793-819.
Weertman, J., and Weertman, J.R., 1975. High temperature creep of rock and mantle viscosity, Ann. Rev. Earth Planet. Sci., v. 3, p. 293-315.
Wilson, J.T., 1966. Did the Atlantic close and then re-open?, Nature, v. 211, p. 676-681.
Winterer, E.L., and Bosellini, A., 1981. Subsidence and sedimentation on Jurassic passive continental margin, Southern Alps, Italy, Am. Assoc. Petrol. Geol. Bull., v. 65, p. 394-421.
Wortel, R., 1980. Age-dependent subduction of oceanic lithosphere, Ph.D. Thesis Utrecht University, Utrecht, pp.147.

Wortel, R., and Cloetingh, S., 1981. On the origin of the Cocos-Nazca spreading center, Geology, v. 9., p. 425-430.
Wortel, R., and Cloetingh, S., 1982. A mechanism for fragmentation of oceanic plates, Am. Assoc. Petrol. Geol. Memoir, in press.
Zielinski, G.W., 1979. On the thermal evolution of passive continental margins, thermal depth anomalies and the Norwegian-Greenland Sea, J. Geophys. Res., v. 84, p. 7577-7588.
Zienkiewicz, O.C., 1977. The finite element method, McGraw Hill, Maidenhead, pp. 787.

APPENDIX

THE FINITE ELEMENT ANALYSIS

In the finite element method (F.E.M.), the structure under consideration is divided into a number of *finite* elements. The elements are connected at nodal points, whose displacements become the basic unknown quantities of the problem. This is the so-called displacement formulation. The state of displacement within each element is chosen as a function of the nodal displacements. Such a function also defines the state of strain in the elements in terms of the nodal displacements. The strains, in turn, lead to the stresses within the element through a constitutive law. Finally, a system of forces consistent with the nodal displacements is found. The forces must be in equilibrium with the loads. Excellent descriptions and derivations of the method have been given by Desai and Abel (1972) and Zienkiewicz (1977). Here, we limit ourselves to a short summary of the essential features of the method. Subsequently, we concentrate on aspects of the finite element technique that are of particular relevance for stress analysis in geodynamics.

A1. BASIC FEATURES OF THE FINITE ELEMENT METHOD

For an outline of the basic features we follow Kraus (1980) and Zienkiewicz (1977). We consider the case of plane strain and use the simple triangle shown in Fig. A1 as the basic element of the F.E. mesh. The triangle has nodal points i, j and k. At each of these nodal points are two displacement components r and s.

For convenience, we assume the following simple linear displacement distribution in the element:

$$\begin{aligned} r &= \alpha_1 + \alpha_2 x + \alpha_3 y \\ s &= \alpha_4 + \alpha_5 x + \alpha_6 y \end{aligned} \qquad \text{(A1)}$$

These relations imply a strain constant over the element. The α_j in the above equations are found easily by applying them to the nodes and substituting the result back into the equations. Subsequently, we can describe the displacements ϕ (inside the element) as a function of the displacements $w^e = \{\begin{matrix} r_i \\ s_i \end{matrix}\}$ of the nodal points, as the linear relation

$$\phi = N w^e \qquad \text{(A2)}$$

where N is the so-called *displacement matrix*. We can derive the strains ε from

$$\varepsilon = B w^e \qquad \text{(A3)}$$

For a constant strain triangle, the *strain displacement matrix* B is independent of position. Assuming linear isotropic elasticity, stresses can be calculated from the strains by means of

$$\sigma = D\varepsilon \qquad \text{(A4)}$$

where D is the *elasticity matrix*.

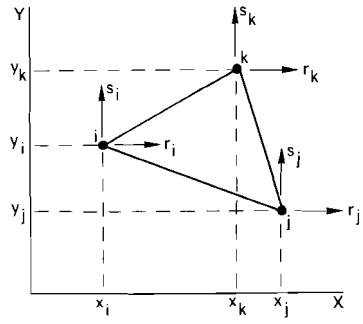

Fig.A1 - A constant strain triangle, with nodal points i, j and k. At each node of the triangle two displacement components r and s are present.

Suppose that forces F^e are acting at each node to equilibrate the boundary loads and external loads. (Another class of loads is given by the body loads P). We impose a virtual displacement on the element and equate the internal and external virtual work. This ensures static equivalence between nodal forces and boundary and external loads.

The virtual displacements $d\phi$ and strains $d\varepsilon$ in the element are expressed in terms of the virtual displacements dw^e with the relations

$$d\phi = N dw^e \tag{A5a}$$

$$d\varepsilon = B dw^e \tag{A5b}$$

The virtual work done by the nodal forces then becomes

$$dW_F = (dw^e)^T F^e \tag{A6}$$

where T denotes the transpose. Similarly, the internal virtual work is

$$dW_I = d\varepsilon^T \sigma - d\phi^T P \tag{A7}$$

where the first term is the strain energy and the second term is the virtual work of the body forces.

This relation is equivalent with

$$dW_I = (dw^e)^T (B^T \sigma - N^T P) \tag{A8}$$

Equating internal and external work yields

$$(dw^e)^T F^e = (dw^e)^T \int_V B^T \sigma - N^T P dV \tag{A9}$$

The volume integral represents the total internal work in the element.

For an arbitrary virtual displacement, the two sides of the equation (A9) must be equal. Substituting eq. (A4) in this equality gives

$$F^e = \int_V B^T DBw^e dV - \int_V N^T P dV \qquad (A10)$$

Define $$K^e = \int_V B^T DB dV \qquad (A11)$$

where K is the *stiffness matrix*, in which the geometrical and rheological properties of the element are condensed.

We now can write

$$F^e = K^e w^e - F_P^e \qquad (A12)$$

where $$F_P^e = \int_V N^T P dV \qquad (A13)$$

is the matrix of the nodal forces due to distributed body loads.

Concentrated forces may be applied at the nodal points together with distributed loads G (per unit area) at the boundaries of the structure. In this case an additional term

$$F_b^e = \int_A N^T G dA \qquad (A14)$$

(integration over the boundary area of the element) is introduced in eq. A12 yielding

$$F^e = K^e w^e - F_P^e - F_b^e \qquad (A15)$$

The next step is the *assembly of the elements* to represent the total structure. We can write

$$\phi = Nw \qquad (A16)$$

where w refers to the displacements at all nodal points. Similarly, we write

$$\varepsilon = Bw \qquad (A17)$$

The principle of virtual work gives

$$dw^T R + \int_V d\phi^T P dV + \int_A d\phi^T G dA = \int_V d\varepsilon^T \sigma dV \qquad (A18)$$

with R the vector of the force components at all nodes. The eqs.A11 and A18 yield

$$R = Kw - F_P - F_b \qquad (A19)$$

where all quantities are obtained from the element quantities by summation, for example

$$K = \Sigma K^e \qquad (A20)$$

The unknown displacements w are simply obtained by solving the linear system (A19). Finally, the stresses in the assembly are found from

$$\sigma = DBw = Sw \qquad \text{(A21)}$$

with S the *stress matrix* of the structure.

The derivation given above is restricted to the case of linear elasticity, using constant strain triangles. In the following sections, we focus on extensions and modifications of this simple scheme, that are of special concern for our analysis.

A2. FINITE ELEMENT ANALYSIS OF PLATE BENDING WITH A HYDROSTATIC RESTORING FORCE

The implementation of isostasy in F.E.M. analysis

The classical one dimensional equation describing the flexure of a uniform elastic plate under the influence of a load F, with a hydrostatic restoring force, is

$$D \frac{d^4 w}{dx^4} + (\rho_m - \rho_w) g w = F \qquad \text{(A22)}$$

where the hydrostatic restoring force $(\rho_m - \rho_w)gw$ is proportional to the deflection w and the density difference between the mantle (density ρ_m) and the medium overlying the plate (usually water with density ρ_w). D is the flexural rigidity of the plate and g is the acceleration due to gravity. Eq. A22 is equivalent to the linear system

$$Kw + K^1 w = F \qquad \text{(A23)}$$

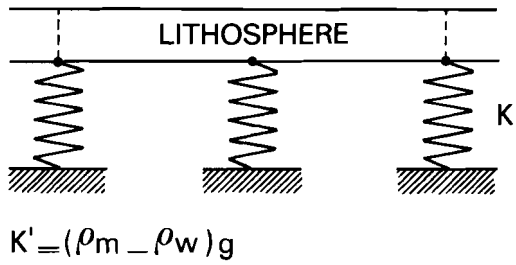

Fig.A2 - The finite element representation of the hydrostatic restoring force $(\rho_m - \rho_w)gw$ by a spring with a stiffness $K^1 = (\rho_m - \rho_w)g$, applied at the basal nodes of the lithosphere.

where K is the operator $\frac{Dd^4}{dx^4}$, and K^1 is $(\rho_m - \rho_w)g$ at the lower boundary of the plate and zero elsewhere. Translated into finite element language, the operator $(K+K^1)$ is the stiffness matrix K_i. The system (A23) can now be written in the familiar form

$$K_i w = F$$

where $K_i = K+K^1$ at the basal nodes of the plate, and $K_i = K$ elsewhere. Thus, isostasy can be incorporated into the analysis by modifying the stiffness matrix at the basal nodes of the model. This is accomplished by the implementation of springs or an elastic foundation with a stiffness $(\rho_m - \rho_w)g$ in the model (Fig. A2).

Selection of element displacement function order

Simple plate theory provides an obvious instrument for the selection of the appropriate order of the element displacement function required for accurate flexural analysis.

A simple linear displacement function

$$w_1 = a + bx + cy$$

yields as its second derivative

$$\frac{\delta^2 w_1}{\delta x^2} = 0$$

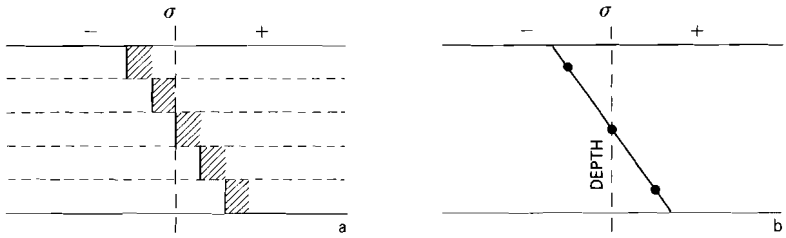

Fig.A3 - F.E.M. analysis of flexure with constant strain elements and linear strain elements. Bending stresses (solid lines) are plotted versus depth for a uniform elastic plate, with a thickness 2Z.
a, Bending stresses calculated with an F.E.M. mesh of five layers of constant strain elements. Boundaries between the layers are indicated by dashed lines. A large number of elements is required for a reasonable approximation of the (linear) variation of bending stresses with depth.
b, The linear variation of bending stress with depth, calculated with a single layer of linear strain elements, provides an excellent representation of stresses caused by flexure.

which implies for the bending stress σ:

$$\sigma = EZ \frac{\delta^2 w_1}{\delta x^2} = 0$$

where Z is the vertical distance from the neutral plane. A zero bending stress within the element is clearly contrary to the assumptions of plate theory.

A quadratic displacement function

$$w_2 = a + bx^2 + cxy + dx + ey + fy^2$$

gives, after differentiation,

$$\frac{\delta^2 w_2}{\delta x^2} = 2b$$

which implies for the bending stress

$$\sigma = \frac{\delta^2 w_2}{\delta x^2} = 2bEZ$$

or a linear variation within the element, which is consistent with plate theory.

From the above, it follows that flexural analysis *requires* elements with a displacement function order that is at least quadratic. An element with a linear displacement function (constant strain element), which is still the most widely used element type in F.E.M. analysis, obviously is inadequate. Using constant strain elements in flexural analysis results in stress discontinuities between adjacent elements, because stresses are not allowed to vary *within* the separate constant strain elements. Fig. A3 provides an extreme example encountered in the case of pure bending where an F.E.M. approximation using only one layer of elements with a quadratic displacement function (linear strain) is obviously superior to modelling with a much larger number of constant strain triangles. Therefore, we have used elements with a quadratic displacement function throughout the present work. The use of these linear strain elements also allows an accurate representation of variations of material properties with depth in F.E.M. models, since material properties are allowed to vary linearly within a separate element. Therefore, the linear variations of the lithospheric strength with depth encountered in the rheological models discussed in section 2.3 could be incorporated straightforwardly into the models presented in section 3.2.

Accuracy - Comparison with analytical solutions

In general, the accuracy of a finite element calculation is improved by increasing the number of elements in the mesh. The number of elements that is required depends strongly on the element type. The use of linear strain elements permits a considerable reduction of the number of elements that would otherwise be needed for the same calculation using constant strain elements.

We can test the accuracy of the finite element calculations by a comparison with analytical solutions available for some simple cases of flexure. To this end, we have selected the case of a triangular wedge on a thin, infinite plate, presented in section 2.3.

The finite element discretisation was made for a plate sufficiently long to simulate infinity.

The rheological features and loading specifications are taken from the analytical model for 100 m.y. old lithosphere given in section 3.1. (Fig. 3.1). The load is applied at the centre of the plate far from the two ends. The plate is clamped at one end, in order to suppress rigid body modes of translation. The hydrostatic restoring force (isostasy) is incorporated using the technique described earlier. The finite element mesh is made up of 28 elements with variable lengths between 200 km, far from the load, and 50 km, at the points where flexure is most pronounced. The finite element solution is plotted in Fig. A4. Comparison of the resulting stresses and displacements, with the analytical solution based on Hetényi (1946) given in section 3.1 for this case, shows that the finite element mesh is sufficiently fine for accurate analysis.

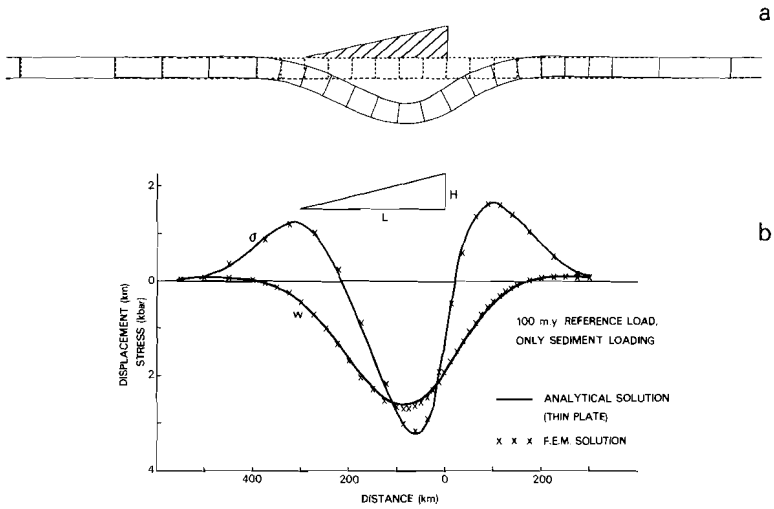

Fig.A4 - The deflection of a uniform elastic infinite plate under the influence of a triangular load, counteracted by isostasy. Load characteristics (density, width L = 300 km, and height H) are for the reference model of sediment loading on 100 m.y. old lithosphere. Flexural properties are for a plate thickness of 44 km.
a (upper), The flexural response (solid line) calculated with the finite element method using the mesh indicated in the figure. Element size varies between 50 km under the load and 200 km outside the bending area. The undeformed configuration is indicated by a dashed (- - -) line.
b (lower), Comparison of numerical and analytical solutions. Solid lines show the displacements (w) and maximum bending stresses (σ) according to the analytical test solution given by Hetényi (1946). Crosses (x) denote the displacements and stresses calculated with the finite element method.

It should be noted that finite element analysis is not hampered by the assumptions and limitations of classical thin plate theory encountered in methods of flexural analysis used by other workers (Lambeck and Nakiboglu, 1980; Bodine et al., 1981).

In particular, the assumption of a zero shear stress neutral surface and zero shear forces in the vertical plane are avoided. Thin plate theory overestimates the stiffness of the plate. Therefore, deflections are underestimated and bending stresses are (to a lesser extent) overestimated. Small deviations of the analytical solution from the finite element solution, as observed in Fig. A4, can be attributed to this effect.

A3. FINITE ELEMENTS AND NON-LINEAR RHEOLOGY

In the above sections of this appendix, we have confined our F.E.M. formulation to the case of linear elasticity. However, as the strain-displacement relationship is non-linear for an elastic-plastic lithosphere, the formulation has to be reorganized.

While for linear elasticity, the solution of the linear system of equations

$$K\mathrm{w} = \mathrm{F}$$

is straightforward, the solution of the non-linear systems associated with elastic-plastic finite element analysis requires small step incremental procedures. The two extreme approaches that can be followed are a large number of small steps, and one large step with many iterative cycles. In practice, a combination is usually employed. In the MARC program, a mid-increment state is found for each point, based on an incremental strain prediction (MARC, 1980). For the first iterative cycle of each step, this prediction is based on the preceding strain increment. The secant stiffness method (Owen and Hinton, 1980) is used to calculate the elastic-plastic response. In the case of a two-dimensional stress state, the secant stiffness method cannot be used and therefore the elastic-plastic response is calculated with the tangent modulus method (Bathe and Wilson, 1976; Owen and Hinton, 1980).

The first step in elastic-plastic analysis is made by assuming a fully elastic response. For a given strain increment, the stress increment is calculated from eq. A4.
The stress is checked with the yield criterion. The increment of the plastic strain and the elastic-plastic constitutive matrix D^{e-p} follows iteratively from the calculation of the normal to the yield surface at the current stress state (Owen and Hinton, 1980).

Finally, during the assembly phase, D^{e-p} is used for the calculation of the stiffness matrix $K = \int_V B^T D^{e-p} B \, dV$.

At the start of each increment during the first stiffness calculation, the element contributions to the residual load vector are found from the element stresses, using

$$\Delta = \int_V B^T \sigma \, dV$$

These element contributions are summed at the nodal points, and the out-of-equilibrium forces or the *residual load vector* Φ is found from

$$\Phi = \Sigma\Delta + P$$

where P represents the total nodal force vector due to concentrated and distributed loads. This residual load vector is added to the existing incremental nodal forces to be distributed over the system during the increment. This method is designed to prevent cumulative equilibrium violation during the course of a non-linear incremental analysis.

A new increment will be calculated when the difference between the calculated and estimated strain energy change is less than a certain tolerance. If this condition is not fulfilled, the increment is recycled.

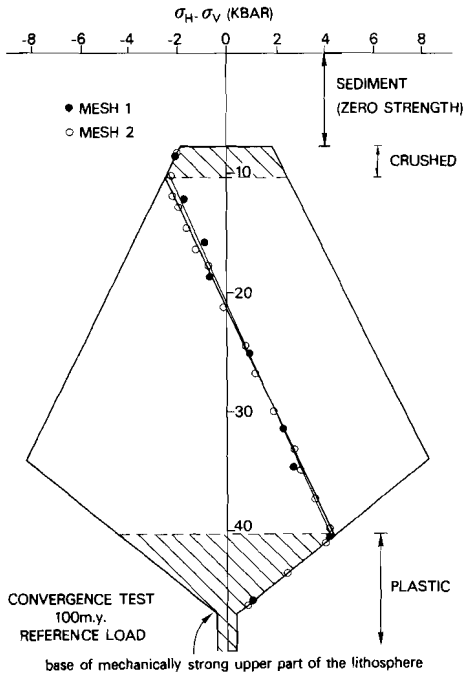

Fig.A5 - Results of a convergence test on the coarsest (100 m.y.) model used in the analysis (mesh 1). Geometrical and depth-dependent rheological properties vary across the margin. Plate tectonic forces and sediment loading following the reference model are assumed. Mesh 2 is the finite element mesh constructed by doubling the number of elements of mesh 1. Solid dots and open circles denote the results of the finite element stress calculations for mesh 1 and mesh 2, respectively. Their close correspondence confirms the accuracy of the model calculations.

In cases where convergence is not achieved within a specified number of recycles, step size reduction should follow. Incipient collapse may also be indicated by near singularity of the stiffness matrix and by a rapid increase of the displacement increments.

For the reasons given above, elastic-plastic finite element analysis requires considerably more computing time than the simple linear elastic calculations. The same applies for the computer memory needed to store the various parameters involved. Careful analysis is required to ensure convergence of the non-linear solution. Therefore, thorough insight in and knowledge of the finite element method, element features, and rheology are required for a successful elastic-plastic analysis.

Accuracy - convergence tests for non-linear rheology

As a matter of fact, analytical test solutions are not available for the deformation of a plate with a depth-dependent non-linear elastic plastic rheology under the influence of sediment loading and plate tectonic forces. Therefore, the accuracy of the model calculations presented in this work was checked by convergence tests made by refining the finite element meshes. An example of such a test is given in Fig. A5. A comparison of the results of two model calculations carried out with meshes differing by a factor two in the number of elements, shows that the coarsest mesh spacing (mesh 1) used in the work guaranteed accurate analysis. Finally, the reaction forces of the model were checked to ensure equilibrium of external and internal forces.

SUPPLEMENT

In Press in: Continental Margin Processes,
American Association of Petroleum Geologists Memoir, v.34,
edited by J.S.Watkins and C.L.Drake.

STATE OF STRESS AT PASSIVE MARGINS AND INITIATION OF SUBDUCTION ZONES ★

S.A.P.L.Cloetingh, M.J.R.Wortel and N.J.Vlaar

Vening Meinesz Laboratory, Instituut voor
Aardwetenschappen, University of Utrecht,
Budapestlaan 4, 3584 CD Utrecht,
The Netherlands.

Abstract

In this paper we present the results of a finite element analysis of the state of stress at passive continental margins, which we performed in order to investigate whether these margins are potential sites for initiation of subduction. The state of stress is determined by the effect of sediment loading at the rise, and to a lesser extent by plate tectonic forces. For a model of sedimentation at the margin, coupled to the subsidence of the cooling oceanic lithosphere, stresses up to 3 kbar can be generated. Stresses of this order may cause failure of the lithosphere and initiation of subduction. In general, however, an additional cause (e.g. plate interaction and geometrical focusing effect) not included in the modelling is required to start the subduction process. If, after 100 m.y. of evolution, subduction has not yet started, continued aging of the passive margin alone, does not result in conditions significantly more favourable for initiation of subduction.

★ *Paper presented at the Hedberg Research Conference on Continental Margin Processes, Galveston, Texas, January 12-16, 1981.*

INTRODUCTION

The problem of initiation of subduction of oceanic lithosphere is one of the major issues in geodynamics. However, as stated by Dickinson and Seely (1979) "the mechanisms that initiate plate consumption at new subduction zones and thus generate arc-trench systems are incompletely known". These authors summarize the possible mechanisms for initiation of subduction of oceanic lithosphere. The following two classes can be distinguished:

1. Plate rupture, either within an oceanic plate, or at a passive margin.
2. Reversal of the polarity of an existing subduction zone, eventually after a collision of an island arc with a passive margin (see also Speed and Sleep, 1982; Speed, this volume).

Another class, although not mentioned by these authors, is initiation of subduction by inversion of transform faults into trenches (see below). We shall concentrate here on the mechanisms for the formation of a *new* plate boundary and, therefore, refrain from dealing with the mechanisms of polarity reversals.

A key factor determining the possibility of subduction of oceanic lithosphere in general is its gravitational stability. The total stability of the oceanic lithosphere is the sum of the positive buoyancy of its stable petrological stratification and the negative buoyancy resulting from thermal contraction upon cooling (Oxburgh and Parmentier, 1977). Wortel (1980) has shown that for a model of oceanic lithosphere consistent with observations of heat flow and topography the system is stable for ages less than 30 m.y., due to the stabilizing effect of the density changes accompanying the formation of oceanic crust (according to Oxburgh and Parmentier's model); as a result of its further cooling and thermal contraction, the lithosphere becomes unstable for ages above 30 m.y. (see also Oxburgh and Parmentier, 1977). Taking into account the age-dependence of the lithospheric instability, it is reasonable to expect that the chances for initiation of subduction of oceanic lithosphere increase with age (Vlaar and Wortel, 1976). However, to allow initiation of subduction of gravitationally unstable lithosphere, stress conditions must be favourable for the creation of a failure zone within the lithosphere. Failure of oceanic lithosphere and initiation of subduction might preferentially take place at existing weakness zones. As such, transform faults have been advocated by several authors (Uyeda and Ben-Avraham, 1972; Uyeda and Miyashiro, 1974; Dewey, 1975). Turcotte et al. (1977a) argue in favour of initiation of subduction by penetration of mantle material through the lithosphere at the location of oceanic spreading centers. Although at ridge-transform intersections high stresses might be generated (Fujita and Sleep, 1978), this young lithosphere is still gravitationally stable. Initiation of subduction of *stable* oceanic lithosphere is hampered by resistive forces active in the process of trench formation (McKenzie, 1977). Thus, apparently spreading centers are not the most appropriate sites for initiation of subduction to occur.

Geological evidence and speculation for margins with widely different ages, ranging from early Proterozoic to recent (Dewey, 1969; Hoffman, 1980; Williams, 1979; Karig et al., 1980), have been put forward to support the thesis that in particular passive margins might be potential

sites for the formation of plate boundaries. There are several reasons why such a process might preferentially take place at a passive margin. Important factors are the contrast in mechanical properties across the margin (in general much greater than the contrast between oceanic lithosphere adjacent to a transform fault) and pre-stressing of the lithosphere by the effect of sediment loading at the margin. The above consideration led us to focus here on the possibilities for initiation of subduction of oceanic lithosphere at a passive margin.

The state of stress at a passive margin is determined by its local geometrical and rheological lithospheric properties, and by the system of forces acting on the lithosphere. Of these features the thickness of the oceanic lithosphere (Parsons and McKenzie, 1978), its rheological stratification (Caldwell and Turcotte, 1979; Bodine et al., 1981), the push exerted by the elevation of the oceanic ridge (Richter and McKenzie, 1978; England and Wortel, 1980), and the forces associated with the (negative) buoyancy of the lithosphere (Vlaar and Wortel, 1976) are a function of the age of the oceanic lithosphere. The sediment loading capacity of oceanic lithosphere increases with age, through continued cooling and densification of the lithosphere. One might, therefore, expect a coupling between the height of the sedimentary column deposited at the passive margin and the age-dependent thermal subsidence of the underlying oceanic lithosphere (Turcotte and Ahern, 1977).

In previous studies of the state of stress at passive margins (Walcott, 1972; Bott and Dean, 1972; Turcotte et al., 1977b; Neugebauer and Spohn, 1978), the possible implications of age-dependent properties of the oceanic lithosphere were not taken into account. In the present work an attempt is made to study the interrelations between age-dependent forces, geometry, and rheology and to decipher their net effect on the state of stress at passive margins, using the finite element technique for the stress calculations. The models presented here deal only with gross features of passive margin evolution and no detailed modelling of a specific margin is intended. As input of (local) detailed stratigraphy is essential before gravity anomalies can be used as a successful constraint for flexural modelling, we refrained from incorporating gravity data as a constraint in the present work. Subsequently we shall discuss the implications for initiation of subduction.

MODELS FOR THE STATE OF STRESS AT A PASSIVE MARGIN

We have constructed finite element models for a passive continental margin in four different stages of evolution, at ages of 30, 60, 100 and 200 m.y. respectively. For all models, a half-spreading rate of 1 cm/yr is taken, characteristic for oceanic lithosphere without downgoing slabs attached to it (Forsyth and Uyeda, 1975). The calculations were carried out with the MARC finite element package (MARC, 1980) using linear strain quadrilateral elements. For more details on the numerical aspects of the work, the reader is referred to Cloetingh and Wisse (1981). The model features are summarized in Fig. 1.

Forces

As a model for sedimentary loading we adopt a triangular sediment wedge at the continental rise. As our reference, we assume that the maximum thickness of the sediments at the continental rise corresponds with the thickness that would result if the sedimentation has been keeping

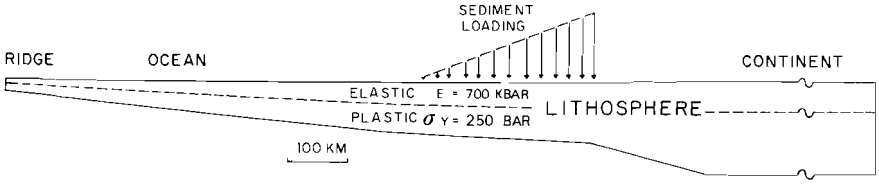

Fig. 1 - Geometry and other features of the models, illustrated for a passive margin with an age of 100 m.y. Vertical scale equals horizontal scale.

up with the subsidence of a boundary layer model of the cooling oceanic lithosphere (Turcotte and Ahern, 1977; Wortel, 1980). This implies for the maximum height of the sedimentary wedge an increase from 4.5 km at 30 m.y. to 9.4 km at 200 m.y., following roughly a square-root of age relation (Fig.2). The width of the sedimentary wedge is taken to be 300 km, a value typical for wedges at continental rises (e.g.Sheridan et al., 1979). Only excess densities are considered. As the sediments on the rise replace water we take a $\Delta\rho = 2.4\text{-}1 = 1.4$ g/cm^3. Although related to age in a somewhat similar way as sediment loading at the rise, sediment loading at the shelf is more difficult to generalize. The position of the shelf edge is not controlled by tectonic subsidence but probably by the local features of sedimentary processes (Watts and Steckler, 1979). On some margins (e.g. off Nova Scotia) the shelf edge has not built out far, it is located landward of the maximum sediment thickness, and maximum sediment loading is at the rise. The amount of lithospheric thinning under the shelf varies strongly (Watts and Steckler report 10 km thinning off Nova Scotia and 20 km thinning off New York) and is therefore hard to be caught in our modelling. Therefore, although in more detailed modelling of specific margins careful attention should be paid to sediment loading at the shelf we refrain from incorporating this feature in our models.

Isostatic forces proportional to the deflection of the lithosphere under the influence of loading are included by modifying the stiffness matrix at the basal nodes of the model. In order to suppress rigid body translation, zero horizontal displacements are prescribed for the right hand boundary of the model. The horizontal extent of the continental lithosphere is sufficient to ignore any artificial effects of this boundary condition in the region of interest.

Of the plate tectonic forces implemented in the models, the magnitudes of the forces associated with the ridge push and the negative buoyancy of the oceanic lithosphere are calculated on the basis of Oxburgh and Parmentier's (1977) model for the formation of oceanic crust, and Crough's (1975) model for the thermal evolution of oceanic lithosphere. Following

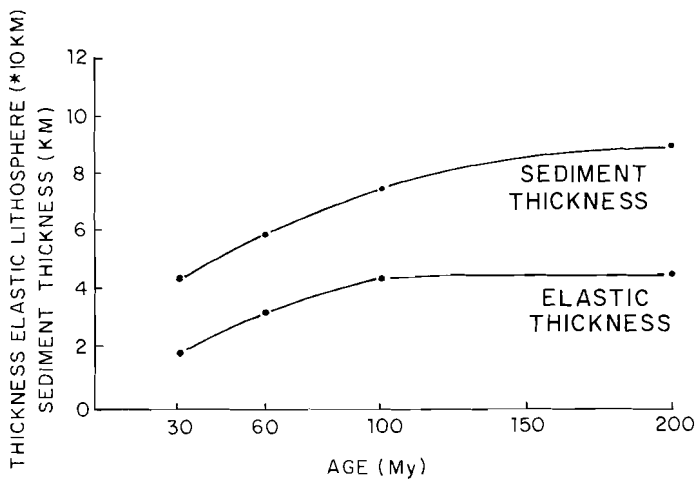

Fig. 2 - Maximum height of the sedimentary prism and the thickness of the elastic part of the lithosphere as functions of age.

Lister (1975) we model the ridge push not as a line force, but as a pressure gradient, excluding in this way artificial stress concentrations at the ridge. The integrated pressure gradient per unit width along the ridge for oceanic lithosphere with an age of 100 m.y. is 2.3 x 10^{12}N/m. For completeness we assume a resistive drag at the base of the lithosphere, acting in a direction opposite the spreading direction with a magnitude per unit area of 1% of the pressure exerted by the elevation of the ridge (Solomon et al., 1977).

Lithospheric thickness and rheology

Age-dependent lithospheric thicknesses are based on Crough's (1975) model for the oceanic lithosphere and are taken from Wortel (1980). A thickness of 150 km, inferred from a number of independent geophysical approaches (e.g. Pollack and Chapman, 1977), is assigned to the continental lithosphere.

It has been argued (Turcotte et al., 1977b) that oceanic and continental lithosphere at a passive margin are effectively decoupled due to the existence of a marginal fault system. As both the extent in depth of such a fault zone and the degree of decoupling are unclear, we model the transition between oceanic and continental lithosphere as continuous. We adopt a width of 200 km for the transition, taking into account the reported evidence for the presence of rift-stage crust at the margin (e.g. Hutchinson et al., 1982). Implications of the presence of fault systems at the margin are briefly discussed further on.

Based on evidence from studies on seismicity (Chapple and Forsyth, 1979) and flexure (McAdoo et al., 1978) of oceanic lithosphere at trenches, we model the oceanic lithosphere as a plate with an elastic upper layer

(Young's modulus E = 7 x 10^{10} N/m^2, Poisson's ratio ν = .25) and a perfectly plastic lower part. From studies on steady-state flow of rocks (Mercier et al., 1977), we adopt a yield stress of 250 bar for the lower part of the oceanic lithosphere. Based on data on the width of the outer rise seaward of oceanic trenches, Caldwell and Turcotte (1979) argue that the thickness of the elastic upper part of the oceanic lithosphere is a strong function of its age. The thickness increases approximately proportional to the square-root of age function from a few km near the ridge to 45 km for ages round 100 m.y., with negligible increase beyond 100 m.y. (see Fig. 2). These values are confirmed by estimates inferred from microrheology of olivine by Beaumont (1979). One might argue, that if the base of the elastic lithosphere coincides with the depth to an isotherm, the thermal effect of sediment loading may reduce the elastic thickness of the lithosphere. However, since the reduction in the elastic thickness is found to be relatively small (at most 15%) we refrain from incorporating this effect in the models. As a result, the stresses inferred from our calculations are somewhat conservative.

Because of cooling, the elastic upper part of the lithosphere thickens with age by a continuous transition of lithospheric material from a plastic to an elastic constitution. Stresses induced by loading, which are higher than the yield strength, can only be accommodated once the material has gone through the plastic-elastic transition. For our reference model of sediment loading, this implies that only that part of the sedimentary wedge deposited in an interval between ages t_1 and t_2 effectively determines the state of stress at t_2 in the bottom part of the elastic part of the lithosphere (that is created between t_1 and t_2). This follows from the fact that loading prior to t_1 can only induce stresses up to the yield strength in the plastic part of the lithosphere. Therefore, the stresses calculated with our "static" models for the bottom of the elastic lithosphere tend to be overestimated. Numerical experiments showed an overestimation in the magnitudes of the stress maxima for the four ages considered in this study, varying between 15 and 22%.

We take a thickness of 50 km for the elastic part of the adjacent continental lithosphere, based on Haxby et al. (1976).

RESULTS

Stress calculations are made for a passive margin in four different stages of evolution, in which the reference model of sediment loading, and the age-dependence of the elastic thickness and other features (as given in Figs. 1 and 2) are incorporated. The results for ages of 30 and 100 m.y. are given in Figs. 3a and 3b respectively. The deformation of the lithosphere and the resulting stress field (order of magnitude a few kbar) is dominated by the sediment loading at the rise; the contribution of the plate tectonic forces to the stress field is an order of magnitude smaller. Differential stresses are largest at the points of maximum flexure. Tensional stresses up to 3 kbar are generated at the base of the elastic lithosphere. Note once again that the magnitudes of the tensional stresses at the bottom of the elastic lithosphere are somewhat overestimated. The concentration of stresses in the elastic part of the lithosphere results from the division of the lithosphere into an elastic and a plastic part (e.g. Kusznir and Bott, 1977). The displacements outside the bending area shown in Fig. 3b are an expression of the equilibrium of the forces associated with the negative buoyancy of the (unstable) oceanic litho-

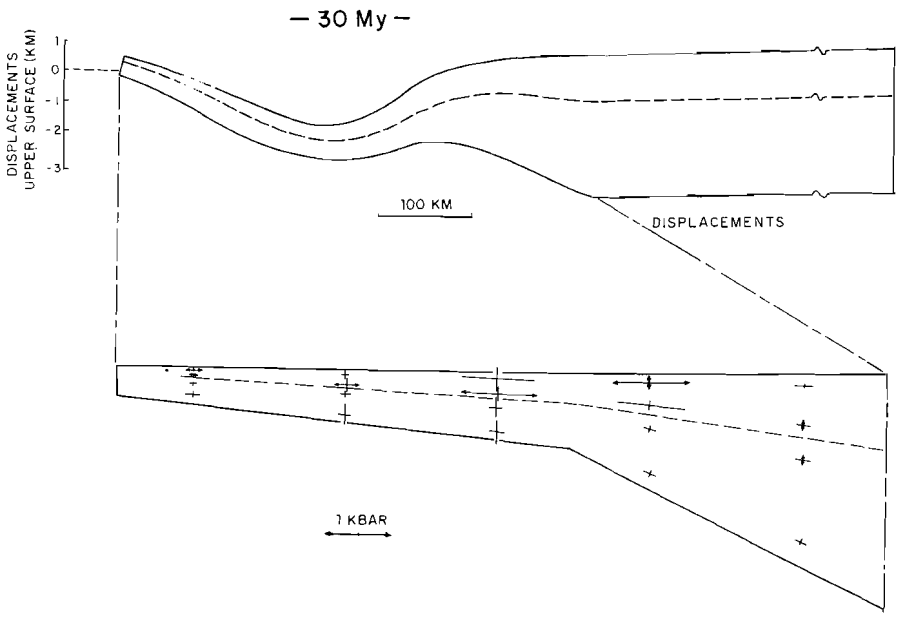

Fig. 3a - *Displacements and stresses calculated for a passive margin with an age of 30 m.y., based on the reference model of sediment loading given in Fig. 2. Stresses are plotted only for the parts of the lithosphere where the displacements are significant. These sections are bounded by the dashed (- . - . -) lines indicated in the figure. The rheological boundary between the elastic upper part and the plastic lower part of the lithosphere is marked by a broken (- - - -) line.*
Above: Displacements of the lithosphere (km) due to the effect of sediment loading. Note that the scale of displacements (vertical axis) and geometry (indicated by a horizontal bar at the bottom of the figure) are not the same.
Below: Principal stresses (kbar) at the margin. Symbols (⟷) and (———) denote tension and compression respectively. Scale indicated at the lower part of the figure.

sphere and the opposing isostatic forces. The resulting depth profile is a well-known feature of oceanic basins (e.g. Parsons and Sclater, 1977) From a comparison of Figs. 3a and 3b it follows that the state of stress at a passive margin depends on the age of the adjacent oceanic lithosphere. It should be noted that as sediment loading on the shelf is related to age in a similar way as sediment loading at the rise, incorporating this feature in the models would not alter this conclusion. In order to summarize this dependence we have plotted (see Fig. 4) the maximum differential (tensional) stresses ($\sigma_1 - \sigma_3$) as a function of age for all our four cases.

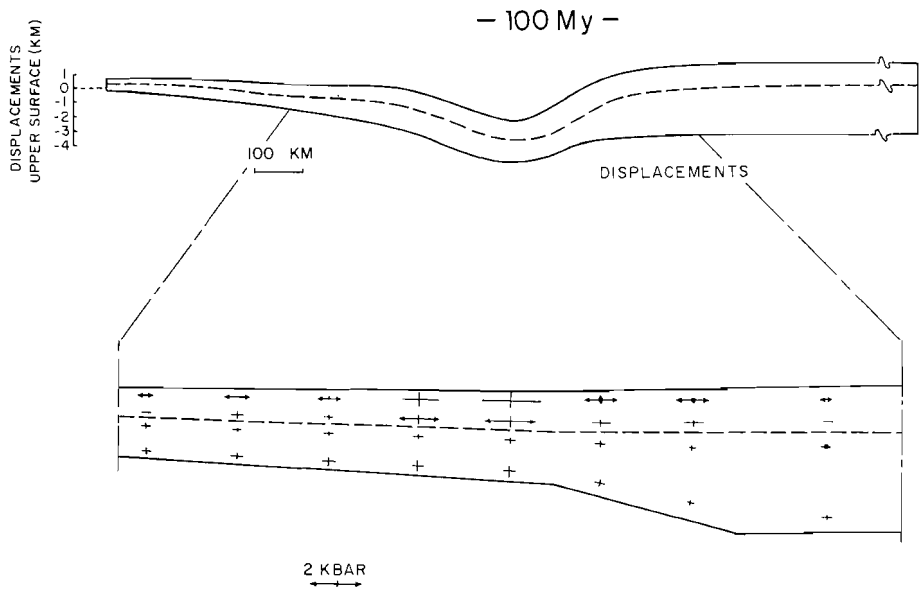

Fig. 3b – Displacements and stresses calculated for a passive margin with an age of 100 m.y. Only the displacements due to sediment loading and the forces associated with the negative buoyancy above 30 m.y. are plotted. Figure conventions as in Fig. 3a.

The age-dependence is strongest for ages below 100 m.y. From 30 to 100 m.y., an interval in which both the sedimentary loading and the elastic thickness increase (see Fig. 2), the differential stress maxima are also seen to increase with age. From 100 to 200 m.y., the thickness of the elastic part of the lithosphere is constant (Fig. 2). The increase in sediment load according to our time-dependent sedimentation model, results only in a minor increase of the stresses.

DISCUSSION

The results of our calculationsfor the reference model of sediment loading show that stresses up to 3 kbar can be generated at a passive margin. However, can stresses of this magnitude create failure zones in the lithosphere? The critical point in answering this question is the strength of the elastic part of the lithosphere. Marine geophysical work on seamount loading and lithospheric bending at trenches (Watts and Cochran, 1974; Caldwell and Turcotte, 1979; Watts et al., 1980) shows that oceanic lithosphere is capable of supporting stresses of several kbars for long periods of geological time (> 50 m.y.). Pertinent laboratory experiments on olivine (e.g. Ashby and Verrall, 1978; Evans and Goetze, 1979; Kirby, 1980) point to yield stresses of the order of 3 - 10 kbar. The laboratory data should be considered to be an upper limit on the strength

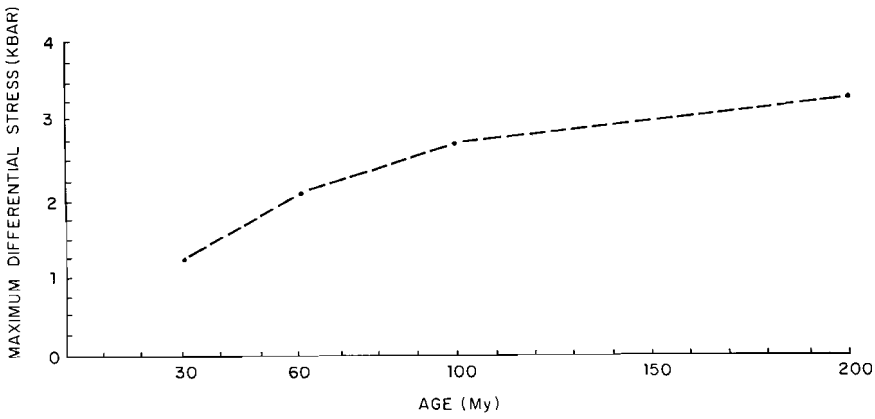

Fig. 4 - Maximum differential stresses as a function of age.

of the lithosphere (Paterson, 1979); nevertheless, a gap remains between the magnitude of the stresses and the strength of the elastic part of the lithosphere. The stresses generated according to our models are for a reference model of sediment loading. Deviations from the reference model occur in the sense of both thicker sediment loads (e.g. the eastern U.S. margin with up to 10 km of sediments at the continental rise) and virtually no sediment loading (e.g. the starved southwest European margin). As a result of the age-dependence of the thickness of the elastic part of the lithosphere, a surplus load of sediments, above the load adopted in the reference model, will be most effective in creating higher stresses, when it is deposited on a young margin.

Several other mechanisms, contributing to the state of stress and not considered here, might be envisaged: thermo-elastic stresses due to cooling of the plate (Turcotte et al., 1977b), stresses due to crustal thickness inhomogeneities (Bott and Dean, 1972), and stresses generated by phase changes in the lithosphere under the influence of sediment loading (Neugebauer and Spohn, 1978). However, thermo-elastic stresses (order of magnitude several kbars) are probably relieved to a large extent in the early stages of lithospheric evolution. The exact mechanism of relaxation of thermo-elastic stresses is uncertain, formation of fracture zones (Turcotte, 1974) being one of the possible mechanisms. The contributions of the stresses due to changes in crustal thickness at the ocean-continent boundary are of relatively minor importance. This mechanism results in shear stresses of the order of a few hundred bars in the continental crust, while the contribution to the stresses in the oceanic lithosphere is negligible (Bott and Dean, 1972). The effect of a hypothetical phase change is even smaller; a few tens of bars (Neugebauer and Spohn, 1978). From the foregoing it might be concluded that the stresses calculated for our models do not provide upper bounds. On the other hand the strength of the lithosphere may be locally reduced by the occurrence of fossil fault systems at passive margins. So in some circumstances, stresses might be generated at passive margins quite close to, or even exceeding, lower bounds of estimates on the lithospheric strength, allowing the creation of failure

zones in the lithosphere and initiating the subduction process.

In general, however, an additional cause is required to trigger the start of the subduction process. Deviations from the two-dimensional situations represented by our models may cause geometrical focusing. At certain stages in the process of global plate reorganization, plate tectonic stresses may be concentrated locally, to a level comparable with the stresses resulting from sediment loading. The short episode (latest Cretaceous-Eocene) of activation of the northern Iberian passive margin inferred by Boillot et al. (1979) might have been caused by this mechanism. The northeastern Indian Ocean might provide a similar example of passive continental margin deformation. Here the onset of the deformation seems to be related to the Himalayan orogenic stage of the collision between India and Asia (Weissel et al., 1980). In this region continental rise sediments up to 12 km thick are present (Curray and Moore, 1974). Apparently this margin combines a number of features that make it an interesting case for further study of the preparatory stages of initiation of subduction.

In summary, our calculations have shown that tensional stresses up to 3 kbar can be generated at passive margins. If subduction has not yet started after 100 m.y. of evolution, continued aging of the passive margin alone does not result in conditions significantly more favourable for initiation of the subduction process.

ACKNOWLEDGEMENTS

Gerald Wisse of the Scientific Applications Group of the Delft University of Technology is gratefully acknowledged for support with the finite element calculations. Discussions held with other participants at the Hollis Hedberg Research Conference, at Carleton University and at L-DGO are highly appreciated.

REFERENCES CITED

Ashby, M.F., and Verrall, R.A., 1978, Micromechanisms of flow and fracture and their relevance to the rheology of the upper mantle: Philos.Trans. Royal Soc.London, v. A288, p.59-95.

Beaumont, C., 1979, On rheological zonation of the lithosphere during flexure: Tectonophysics, v. 59, p.347-365.

Bodine, J.H., Steckler, M.S., and Watts, A.B., 1981, Observations of flexure and the rheology of the oceanic lithosphere: Jour.Geophys. Research, 86, p.3695-3707.

Boillot, G., Auxiètre, J., Dunant, J., Dupeuple, P., and Mauffret, A., 1979, The Northwestern Iberian Margin: A Cretaceous passive margin deformed during Eocene: *in* Talwani, M., and others, eds., Deep drilling results in the Atlantic ocean: Continental margins and paleoenvironment: Am. Geophys. Union, Maurice Ewing Series, v. 3, p.138-153.

Bott, M.H.P., and Dean, D.S., 1972, Stress systems at young continental margins: Nature Phys. Sci., v. 235, p.23-25.

Caldwell, J.G., and Turcotte, D.L., 1979, Dependence of the thickness of the elastic oceanic lithosphere on age: Jour. Geophys. Research, v. 84, p.7572-7576.

Chapple, W.M., and Forsyth, D.W., 1979, Earthquakes and bending of plates at trenches: Jour. Geophys. Research, v. 84, p.6729-6749.

Cloetingh, S., and Wisse, G., 1981, Finite element modelling in geodynamics: The state of stress at passive continental margins: Finite Element News, no.3, p.37-40.
Crough, S.T., 1975, Thermal model of oceanic lithosphere: Nature, v. 256, p.388-390.
Curray, J.R., and Moore, D.G., 1974, Sedimentary and tectonic processes in the Bengal deep-sea fan and geosyncline: *in* Burk, C.A., and Drake, C.L., eds., The Geology of continental margins, Springer Verlag, New York, p.617-627.
Dewey, J.F., 1969, Continental margins: A model for conversion of Atlantic-type to Andean-type: Earth and Planetary Sci. Letters, v. 6, p.189-197.
Dewey, J.F., 1975, Finite plate evolution: Some implications for the evolution of rock masses at plate margins: Am.Jour.Sci., v. 275A, p.260-284.
Dickinson, W.R., and Seely, D.R., 1979, Structure and stratigraphy of forearc regions: AAPG Bull., v. 63, p.2-31.
England, P., and Wortel, R., 1980, Some consequences of the subduction of young slabs: Earth and Planetary Sci.Letters, v. 47, p.403-415.
Evans, B., and Goetze, C., 1979, The temperature variation of hardness of olivine and its implication for polycrystalline yield stress: Jour.Geophys.Research, v. 84, p.5505-5524.
Forsyth, D.W., and Uyeda, S., 1975, On the relative importance of driving forces of plate motion: Geophys.Jour.Royal Astronom.Soc., v. 43, p.163-200.
Fujita, K., and Sleep, N.H., 1978, Membrane stresses near mid-ocean ridge-transform intersections: Tectonophysics, v. 50, p.207-221.
Haxby, W.F., Turcotte, D.L., and Bird, J.M., 1976, Thermal and mechanical evolution of the Michigan Basin: Tectonophysics, v. 36, p.57-75.
Hoffman, P.F., 1980, Wopmay orogen: A Wilson cycle of early Proterozoic age in the north-west of the Canadian shield, *in* Strangway, D.W., ed., The continental crust and its mineral deposits: Geol.Assoc.Can.Spec. Pap., v. 20, p.523-549.
Hutchinson, D.R., Grow, J.A., Klitgord, K.D., and Swift, B.A., 1981, Deep structure and evolution of the Carolina trough, this volume.
Karig, D.E., Lawrence, M.B., Moore, G.F., and Curray, J.R., 1980, Structural framework of the fore-arc basin, N.W.Sumatra: Jour.Geol.Soc. London, v. 137, p.77-91.
Kirby, S.H., 1980, Tectonic stresses in the lithosphere: constraints provided by the experimental deformation of rocks: Jour.Geophys.Research, p.6353-6368.
Kusznir, N.J., and Bott, M.H.P., 1977, Stress concentration in the upper lithosphere caused by underlying visco-elastic creep: Tectonophysics, v. 43, p.247-256.
Lister, C.R.B., 1975, Gravitational drive on oceanic plates caused by thermal contraction: Nature, v. 257, p.663-665.
McAdoo, D.C., Caldwell, J.G., and Turcotte, D.L., 1978, On the elastic-perfectly plastic bending of the lithosphere under generalized loading with application to the Kuril Trench: Geophys.Jour.Royal Astronom.Soc., v. 54, p.11-26.
McKenzie, D.P., 1977, The initiation of trenches: a finite amplitude instability, *in* Talwani, M., and Pitman III, W., eds., Island arcs, deep sea trenches and back-arc basins: Am.Geophys.Union, Maurice Ewing Series, v. 1, p.57-62.

MARC Analysis Research Corporation, 1980, Marc general purpose finite element program: User manual, Volume A-E, Palo Alto.
Mercier, J.-C.C., Anderson, D.A., and Carter, N.L., 1977, Stress in the lithosphere: inferences from steady state flow of rocks: Pure and Appl.Geophysics, v. 115, p.199-226.
Neugebauer, H.J., and Spohn, T., 1978, Late stage development of mature Atlantic-type continental margins: Tectonophysics, v. 50, p.275-305.
Oxburgh, E.R., and Parmentier, E.M., 1977, Compositional and density stratification in oceanic lithosphere-causes and consequences: Jour.Geol.Soc.London, v. 133, p.343-355.
Parsons, B., and McKenzie, D., 1978, Mantle convection and the thermal structure of the plates: Jour.Geophys.Research, v. 83, p.4485-4496.
Parsons,B., and Sclater, J.G., 1977, An analysis of the variation of ocean floor heat flow and bathymetry with age: Jour.Geophys.Research, v. 82, p.803-827.
Paterson, M.S., 1979, The mechanical behaviour of rocks under crustal and mantle conditions, *in* McElhinny, M.N., ed., The earth, its origin, structure and evolution: New York, Academic Press, p.469-489.
Pollack, H.N., and Chapman, D.S., 1977, On the regional variation of heat flow, geotherms and lithospheric thickness: Tectonophysics, v. 38, p.279-296.
Richter, F.M., and McKenzie, D., 1978, Simple plate models of mantle convection: Jour. of Geophysics, v. 44, p.441-471.
Sheridan, R.E., Grow, J.A., Behrendt, J.C., and Bayer, K.C., 1979, Seismic refraction study of the continental edge of the eastern United States, *in* Keen, C.E., ed., Crustal properties across passive margins: Amsterdam, Elsevier, p.1-26.
Solomon, S.C., Sleep, N.H., and Richardson, R.M., 1977, Implications of absolute plate motions and intraplate stress for mantle rheology: Tectonophysics, v. 37, p.219-231.
Speed, R.C., 1982, Passive paleozoic continental margin in the western U.S. and its modification by collisions, accretion, and truncation, this volume.
Speed, R.C., and Sleep, N.H., 1982, Antler orogeny: a model: submitted to Geol.Soc.America Bull.
Turcotte, D.L., 1974, Are transform faults thermal contraction cracks: Jour.Geophys.Research, v. 79, p.2573-2577.
Turcotte, D.L., and Ahern, J.L., 1977, On the thermal and subsidence history of sedimentary basins: Jour.Geophys.Research, v. 82, p.3762-3766.
Turcotte, D.L., Haxby, W.F., and Ockendon, J.R., 1977a, Lithospheric instabilities, *in* Talwani, M., and Pitman III, W., eds., Island arcs, deep-sea trenches and back-arc basins: Am.Geophys.Union, Maurice Ewing Series, v. 1, p.63-69.
Turcotte, D.L., Ahern, J.L., and Bird, J.M., 1977b, The state of stress at continental margins: Tectonophysics, v. 42, p.1-28.
Uyeda, S., and Ben-Avraham, Z., 1972, Origin and development of the Philippine sea: Nature, v. 240, p.176-178.
Uyeda, S., and Miyashiro, A., 1974, Plate tectonics and the Japanese Islands, a synthesis: Geol.Soc.America Bull., v. 85, p.1159-1170.
Vlaar, N.J., and Wortel, M.J.R., 1976, Lithospheric aging, instability and subduction: Tectonophysics, v. 32, p.331-351.
Walcott, R.I., 1972, Gravity, flexure and the growth of sedimentary basins at a continental edge: Geol.Soc.America Bull., v. 83, p.1845-1848.

Watts, A.B., and Steckler, M.S., 1979, Subsidence and eustasy at the continental margin of eastern North America, *in* Talwani, M., and others, eds., Deep drilling results in the Atlantic ocean: Continental margins and paleoenvironment: Am.Geophys.Union, Maurice Ewing Series, v. 3, p.218-234.

Watts, A.B., Bodine, J.H., and Steckler, M.S., 1980, Observations of flexure and the state of stress in the oceanic lithosphere: Jour.Geophys.Research, v. 85, p.6369-6376.

Watts, A.B., and Cochran, J.R., 1974, Gravity anomalies and flexure of the lithosphere along the Hawaiian-Emperor seamount chain: Geophys.Jour.Royal Astronom.Soc., v. 38, p.119-141.

Weissel, J.K., Anderson, R.N., and Geller, C.A., 1980, Deformation of the Indo-Australian plate: Nature, v. 287, p.284-291.

Williams, H., 1979, Appalachian orogen in Canada: Canadian Jour.Earth Sci., v. 16, p.792-807.

Wortel, R., 1980, Age-dependent subduction of oceanic lithosphere (Ph.D.dissert.): Utrecht, The Netherlands, Utrecht University, 147 p.

Evolution of passive continental margins and initiation of subduction zones

S. A. P. L. Cloetingh, M. J. R. Wortel & N. J. Vlaar

reprinted from
nature

Reprinted from Nature, Vol. 297, No. 5862, pp. 139-142, 13 May 1982

Evolution of passive continental margins and initiation of subduction zones

S. A. P. L. Cloetingh, M. J. R. Wortel & N. J. Vlaar

Vening Meinesz Laboratory, Instituut voor Aardwetenschappen, University of Utrecht, Budapestlaan, 4, 3584 CD Utrecht, The Netherlands

Although the initiation of subduction is a key element in plate tectonic schemes for evolution of lithospheric plates, the underlying mechanisms are not well understood. Plate rupture is an important aspect of the process of creating a new subduction zone, as stresses of the order of kilobars are required to fracture oceanic lithosphere[1]. Therefore initiation of subduction could take place preferentially at pre-existing weakness zones or in regions where the lithosphere is prestressed. As such, transform faults[2,3] and passive margins[4,5] where the lithosphere is downflexed under the influence of sediment loading have been suggested. From a model study of passive margin evolution we found that ageing of passive margins alone does not make them more suitable sites for initiation of subduction. However, extensive sediment loading on young lithosphere might be an effective mechanism for closure of small ocean basins.

The state of stress at a passive margin is determined by its local geometrical and rheological lithospheric properties and by the system of forces acting on the lithosphere. Of these features the thickness of the oceanic lithosphere[6], its rheological stratification[7], the push exerted by the elevation of the oceanic ridge[8,9] and the forces associated with the (negative) buoyancy of the lithosphere[10] are a function of the age of the oceanic lithosphere. The sediment loading capacity of oceanic lithosphere increases with age, through its continued cooling and densification. One might therefore expect a coupling between the height of the sedimentary column deposited at the passive margin and the age-dependent thermal subsidence of the underlying oceanic lithosphere[11]. In previous studies of the state of stress at passive margins[12-14] the possible implications of age-dependent properties of the oceanic lithosphere were not taken into account. We have studied the interrelations between age-dependent forces, geometry and rheology, to decipher their net effect on the state of stress at passive margins. We have constructed finite element models for a passive continental margin in different stages of evolution at ages of 20, 30, 60, 100 and 200 Myr. For all models a half spreading rate of 1 cm yr^{-1} is taken, characteristic of oceanic lithosphere without downgoing slabs attached to it[15]. The model features are summarized in Fig. 1. As a model for sedimentary loading we adopt triangular wedges at the continental shelf and rise. As our reference we assume that the maximum thickness of the sediments at the margin corresponds with the thickness that results if the sedimentation has been keeping up with the subsidence of a boundary layer model of the cooling oceanic lithosphere[11,16]. This implies for the maximum height of the sedimentary triangular wedge an increase from 3.6 km at 20 Myr to 9.4 km at 200 Myr, following roughly a square root of age relation. Observational data on thicknesses of post-rift sedimentary sequences are now available from geophysical surveys carried out on passive margins during the past few years[17]. From these data it follows that the reference model is representative of most of the sediment loading histories and resulting thicknesses observed at passive margins. The huge sediment accumulations at deltas, however, clearly exceed the thicknesses as given by the reference model. Therefore, a second class of models was constructed in which the full loading capacity of oceanic lithosphere was taken up by sediments with the sedimentary thicknesses ranging from 10 to 15.8 km. The width of the sedimentary wedges varies between 150 km for very young margins to 250 km for mature margins, based on data compilations[17]. As the sediments replace water we consider only excess densities ($\Delta\rho = 2.4$ $1 = 1.4$ g cm^{-3}).

Studies on seismicity and flexure of oceanic lithosphere bending at trenches[18,19] and analysis of flexure of the oceanic lithosphere under the influence of seamount loading[20] have demonstrated that the lithosphere is capable of supporting stresses of the order of some kilobars on geological time scales. The experimental work of Goetze and co-workers[21,22] shows that the strength of the lithosphere first increases with depth and then decreases rapidly to a level of a few hundred bars in the lower part of the plate, where temperature effects become dominant and the maximum stress achievable is limited by thermally activated ductile flow. Deriving temperature profiles from Crough's[23] model for the oceanic lithosphere, which model combines the merits of the boundary layer model and the plate model, we have constructed lithospheric strength envelopes for a wide range of ages. These are based on Goetze's ductile flow laws in olivine for power-law and Dorn-creep rheologies, assuming a strain-rate of $\dot{e} = 10^{-18}\ s^{-1}$. For the sediments we assume a zero strength. A similar approach was followed by Bodine and co-workers[24]. Yield envelopes for lithospheric ages of 30 and 100 Myr are given in Fig. 2 which shows that both the thickness H of the 'mechanical plate' (given by the depth below which the strength of the plate is <0.5 kbar) and the maximum strength increase strongly with age. The flexure of the lithosphere is counteracted by isostasy. Isostatic forces proportional to the deflection due to loading are included in the model. Of the plate tectonic forces implemented in the models those associated with the ridge push and the negative buoyancy of the oceanic lithosphere are calculated on the basis of Oxburgh and Parmentier's[25] model for the formation of oceanic crust and Crough's[23] model for the thermal evolution of oceanic lithosphere. We ignore drag at the base of the lithosphere. Zero horizontal displacements are prescribed for the right-hand boundary of the model to simulate a ridge push transmitted through the continent from an adjacent oceanic plate.

The deformation of the lithosphere at passive margins and the resulting stress field (order of magnitude of a few kilobars) are dominated by sediment loading[26]. The contribution of the plate tectonic forces to the stress field is an order of magnitude smaller. Differential stresses are largest at the points of maximum flexure. These are located under the rise in the oceanic plate close to the transition of oceanic and rift-stage lithosphere. Figure 2*a*, *b* shows the stress maxima for 100 and 30 Myr for the reference load. The lowermost part of the mechanical plate is in yield due to the tensile stresses developed at the base. The main part of the plate remains in the elastic state. The effect of the rheological stratification of the lithosphere is twofold: stress relaxation in the lowermost part and stress concentration in the mechanically stronger upper part. This effect is particularly important if the full loading capacity of the lithosphere is taken up by sediments. This can even result in complete failure of the lithosphere as demonstrated in Fig. 2*c*.

Figure 2 also shows that the state of stress depends on the age of the margin. To illustrate this dependence more clearly we have plotted in Fig. 3*a* the maximum differential (tensional)

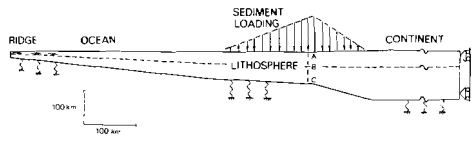

Fig. 1 Model features: geometry, rheology, system of forces and boundary conditions. Mechanical thickness indicated by broken horizontal line. Young's modulus $E = 7 \times 10^{10}$ N m^{-2} and Poisson's ratio $\nu = 0.25$

stresses as a function of age. The age dependence is strongest for ages below 100 Myr. From 30 to 100 Myr—an interval in which the sedimentary loading, the mechanical thickness and the strength increase—the differential stress maxima increase with age. From 100 to 200 Myr the mechanical thickness and the strength of the plate show only a small increase. For ages

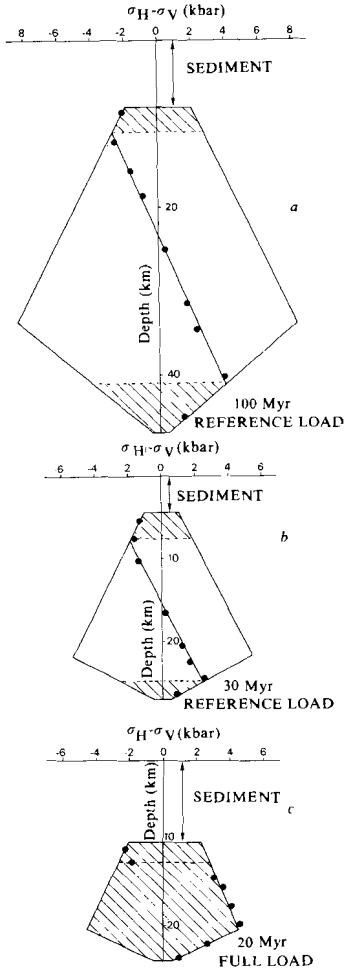

Fig. 2 Strength envelope and results of model calculations (●) at cross-section through the upper part of the lithosphere at the point of maximum flexure (AB of cross-section ABC in Fig. 1). The line inside strength envelope connecting the solid dots is the stress distribution. Differential stresses ($\sigma_H - \sigma_V$) are plotted versus depth. Sign convention for the stresses: tension positive, compression negative. Zero-strength has been assumed for the sediments. Hatched areas in the upper and lower part of the mechanical layer denote failure by brittle fracture and ductile flow respectively. *a*, *b*, The results for the reference model of sediment loading for ages of 100 and 30 Myr. *c*, The results for the full load model for 20 Myr. The horizontal dashed line indicates the neutral surfaee just before complete failure of 20-Myr old lithosphere takes place.

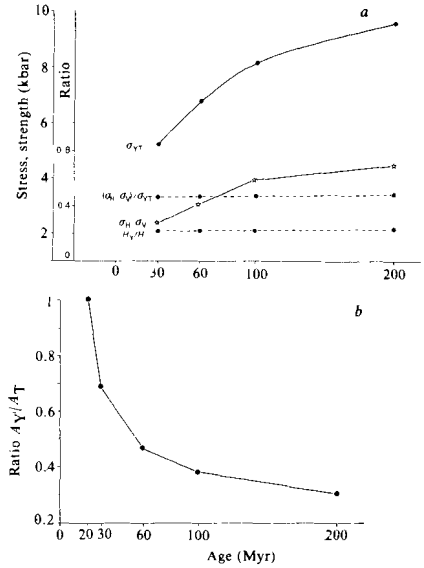

Fig. 3 *a*, Model results for reference load: maximum differential stresses ($\sigma_H - \sigma_V$), tensile strength σ_{YT}, their ratio and the relative thickness of the mechanical layer in failure (H_Y/H) plotted as a function of lithospheric age. *b*, Results full load model: ratio of A_Y (the hatched area inside the strength envelope, see Fig. 2) and A_T (total area of the envelope) as a function of lithospheric age. For ages below 20 Myr complete lithospheric failure is induced.

above 100 Myr the increase in sediment loading according to our reference model results in only a minor increase of the stresses. Interesting quantities are the ratio of the maximum stress generated and the maximum strength, and the ratio of A_Y, corresponding with the hatched area (inside the strength envelope (Fig. 2)) and the total area A_T of the envelope. For the reference model of sediment loading these quantities prove to be essentially independent of age because load, strength and plate thickness all exhibit the same square root of age behaviour due to the thermal evolution of the plate. The situation changes drastically if the full loading capacity is taken up. The surplus load of sediments added to the reference load is most effective in creating high stresses when deposited on a young margin. Figure 3*b* and results of numerical calculations made for ages below 20 Myr (not shown here) demonstrate that full loading on a young passive margin (age below 20 Myr) leads to complete failure of the lithosphere. Owing to the stabilizing affect of the density changes accompanying the formation of oceanic crust[25] oceanic lithosphere is gravitationally stable for ages <20–40 Myr (ref. 16). As a result of its further cooling and thermal contraction the lithosphere becomes unstable for ages above 20–40 Myr (refs 16, 25). Taking into account only the lithospheric instability it was reasonable to expect that chances for initiation of subduction of oceanic lithosphere would increase with the age of the margin[10]. Our work shows that if after a short evolution of the plate, subduction has not yet started, continued ageing of the passive margin alone does not result in conditions more favourable for plate rupture and initiation of subduction.

Although most of the present deltas of the world are deposited on old oceanic lithosphere[27] and very few examples of modern thick sedimentary cones on young lithosphere are known, extensive sedimentary loading might have been an effective mechanism for closure of small ocean basins in geological history. Closure of small oceanic basins has an important

role in the process of mountain building. In this context, note that in a comprehensive account of the evolution of the central Alps, Frisch[28] presents evidence for closure of oceanic basins within the first 100 Myr after opening.

For older margins in general, however, it seems that the stresses generated are insufficient to induce lithospheric failure and initiation of subduction. Therefore, pre-existing weakness zones in oceanic lithosphere might be more suitable sites for initiation of subduction than passive margins. This view is consistent with the results of a survey of recently initiated subduction zones in the Pacific[29] showing that zones initiated in the Neogene are either at the sites of transform faults or rejuvenated pre-existing subduction zones. Many of the present circum-Pacific zones are in fact the successors of subduction zones already present in the configuration before the breakup of Gondwanaland. Further back in geological time different plate configurations and a different thermal regime might have provided conditions more suitable for initiation of subduction. As an extreme example one might consider the Archaean where, due to the much steeper temperature profiles[30], the lithosphere must have been considerably weaker than nowadays. In such a situation plate rupture requires a considerable lower stress level. This suggestion is corroborated by geological data on Precambrian orogenic belts[31], showing extensive activation of passive margins bordering small oceanic basins.

In the present lithospheric system special circumstances may arise in the process of global plate reorganization, when plate tectonic forces may be concentrated locally. This can be important in an oceanic plate attached to a subduction zone where the pull acting on the subducting slab can be concentrated to a high level (order of magnitude of several kilobars)[32]. In particular Wortel and Cloetingh[32] have shown that lateral variations in the age of the slab descending in a subduction zone might provide a mechanism for fragmentation of oceanic plates and the formation of spreading centres. In an opening oceanic basin, however, the only plate tectonic force to be concentrated is the ridge push, inducing stresses with an order of magnitude of only a few hundred bars. Although the concentration factor might be quite high[33] the level of the concentrated stresses due to ridge push is by no means comparable with the stresses resulting from sediment loading. Therefore, plate reorganization might take place predominantly by the formation of new spreading ridges. In such a process new subduction zones might be subsequently created at the sites of transform faults already present in the plate, when the new spreading direction has a component perpendicular to the direction of the transform fault.

We thank Gerald Wisse (Delft University of Technology) for support with the finite element calculations, and Joel S. Watkins and Rob van der Voo for critically reading an earlier version of the manuscript.

Received 19 January; accepted 8 March 1982.

1. Kirby, S. H. *J. geophys. Res.* **85**, 6353 (1980).
2. Uyeda, S. & Ben-Avraham, Z. *Nature* **240**, 176 (1972).
3. Dewey, J. F. *Am. J. Sci.* **275A**, 260 (1975).
4. Dietz, R. S. *J. Geol.* **71**, 314 (1963).
5. Dewey, J. F. *Earth planet. Sci. Lett.* **6**, 189 (1969).
6. Parsons, B. & Sclater, J. G. *J. geophys. Res.* **82**, 803 (1977).
7. Caldwell, J. G. & Turcotte, D. L. *J. geophys. Res.* **84**, 7572 (1979)
8. Richter, F. & McKenzie, D. *J. Geophys.* **44**, 441 (1978).
9. England, P. & Wortel, R. *Earth planet. Sci. Lett.* **47**, 403 (1980).
10. Vlaar, N. J. & Wortel, M. J. R. *Tectonophysics* **32**, 331 (1976).
11. Turcotte, D. L. & Ahern, J. L. *J. geophys. Res.* **82**, 3762 (1977).
12. Walcott, R. I. *Bull. geol. Soc. Am.* **83**, 1845 (1972).
13. Bott, M. H. P. & Dean, D. S. *Nature phys. Sci.* **235**, 23 (1972).
14. Turcotte, D. L., Ahern, J. L. & Bird, J. M. *Tectonophysics* **42**, 1 (1977).
15. Forsyth, D. W. & Uyeda, S. *Geophys. J. R. astr Soc.* **43**, 163 (1975)
16. Wortel, M. J. R. Thesis, Utrecht Univ. (1980).
17. Watkins, J. S., Montadert, L. & Dickerson, P. W. *Am. Ass. petrol. Geol. Mem.* **29** (1979)
18. Chapple, W. M. & Forsyth, D. W. *J. geophys. Res.* **84**, 6729 (1979).
19. McAdoo, D. C., Caldwell, J. G. & Turcotte, D. L. *Geophys. J. R. astr. Soc.* **54**, 11 (1978).
20. Watts, A. B., Bodine, J. H. & Steckler, M. S. *J. geophys. Res.* **85**, 6369 (1980).
21. Goetze, C. *Phil. Trans. R. Soc.* A**288**, 99 (1978)
22. Goetze, C. & Evans, B. *Geophys. J.R. astr. Soc.* **59**, 463 (1979)
23. Crough, S. T. *Nature* **256**, 388 (1975).
24. Bodine, J. H., Steckler, M. S. & Watts, A. B. *J. geophys. Res* **86**, 3695 (1981)
25. Oxburgh, E. R. & Parmentier, E. M. *J. geol. Soc. Lond.* **133**, 343 (1977)
26. Cloetingh, S. A. P. L., Wortel, M. J. R. & Vlaar, N. J. *Am. Ass. petrol. Geol. Mem* (in the press).
27. Kinsman, D. J. J. in *Petroleum and Global Tectonics* (eds Fischer, A. G. & Judson, S.) 83 (Princeton University Press, 1975).
28. Frisch, W. *Tectonophysics* **60**, 121 (1979)
29. Karig, D. Preprint, Cornell Univ.
30. Sharpe, H. N. & Peltier, W. R. *Geophys. J.R. astr. Soc* **59**, 171 (1979)
31. Kröner, A. in *Precambrium Plate Tectonics* (ed. Kröner, A.) 56 (Elsevier, Amsterdam, 1981).
32. Wortel, R. & Cloetingh, S. *Geology* **9**, 425 (1981)
33. Kato, T., Shimazaki, K. & Yamashina, K. *Geophys. J.R. astr. Soc.* **60**, 377 (1980)

CURRICULUM VITAE

De schrijver van dit proefschrift behaalde in 1968 het diploma HBS-B aan het Heymans Lyceum (thans Heymans College) te Groningen. In hetzelfde jaar werd begonnen met de studie in de geologie aan de Rijksuniversiteit te Groningen. Nadat in 1972 het kandidaatsexamen G3 werd afgelegd, werd in 1977 het doctoraalexamen Geofysica met hoofdrichting Fysica van de vaste aarde en bijvakken numerieke wiskunde en structurele geologie aan de Rijksuniversiteit te Utrecht cum laude behaald. Sinds 1977 is hij als wetenschappelijk medewerker verbonden aan de afdeling Theoretische Geofysica van het Instituut voor Aardwetenschappen van de Rijksuniversiteit Utrecht.